UNIVERSITA' DEGLI STUDI DI TRIESTE

XXX CICLO DEL DOTTORATO DI RICERCA IN
BIOMEDICINA MOLECOLARE

Regulation of autophagy by Ubiquitin Specific Peptidase 1 (USP1)

Settore scientifico-disciplinare: BIO11

DOTTORANDA
Marzia Raimondi

COORDINATORE
Prof.ssa Germana Meroni

SUPERVISORE DI TESI
Prof. Claudio Schneider

CO-SUPERVISORE DI TESI
Dott. Francesca Demarchi

ANNO ACCADEMICO 2016 / 2017

ABSTRACT 2
ACKNOWLEDGEMENTS 4
LIST OF ABBREVIATIONS 5

1. INTRODUCTION 7

1.1 AUTOPHAGY 7
1.1.1 WHAT IS AUTOPHAGY? 7
1.1.2 THE PROCESS OF AUTOPHAGY 8
1.1.3 REGULATION OF AUTOPHAGY BY SIGNALING PATHWAYS 13
1.1.4 PHYSIOLOGICAL ROLES OF AUTOPHAGY 14
1.1.4.1 Immunity, starvation and cell death 15
1.1.4.2 Housekeeping and aggregates removal 16
1.1.5 AUTOPHAGY AND DISEASE 17
1.1.5.1 Autophagy and Alzheimer's diseases (AD) 17
1.1.5.2 Autophagy and Parkinson's diseases (PD) 18
1.1.5.3 Autophagy and Huntington's disease (HD) 18
1.1.5.4 Autophagy and cancer 18

1.2 UBIQUITINATION AND DEUBIQUITINATING ENZYMES 21
1.2.1 THE UBIQUITINATION PATHWAY 21
1.2.2 THE DEUBIQUITINATING ENZYMES 23
1.2.3 THE UBIQUITIN SPECIFIC PROTEASE 1 (USP1) ENZYME 27
1.2.3.1 Regulation of USP1 function 29
1.2.3.2 USP1-regulated pathways 33
1.2.1 THE ROLE OF UBIQUITIN MODIFICATIONS IN AUTOPHAGY REGULATION 36
1.2.2 THE ROLE OF DEUBIQUITINATING ENZYMES IN AUTOPHAGY REGULATION 37

2. AIM OF THE THESIS 39

3. MATERIALS AND METHODS 40

3.1 CHEMICALS AND REAGENTS 40

3.2 CELL CULTURE 40

3.3 TRANSIENT PLASMID DNA TRANSFECTION 41

3.4 TRANSIENT SIRNA KNOCKDOWN OF MAMMALIAN CELLS 41

3.5 PROTEIN EXPRESSION ANALYSIS 42

3.5.1 CELL LYSIS AND PROTEIN EXTRACTION 42

3.5.2 PROTEIN QUANTIFICATION 43

3.5.3 ELECTROPHORESIS (SDS/PAGE) 43

3.5.4 MEMBRANE TRANSFER AND IMMUNOLABELLING 43

3.6 IMMUNOPRECIPITATION 45

3.7 TRITON-SOLUBLE AND -INSOLUBLE FRACTIONATION 46

3.8 CONFOCAL MICROSCOPY ANALYSIS 46

3.9 IMMUNOHISTOCHEMISTRY 47

3.10 COLONY FORMATION ASSAY 48

3.11 CELL VIABILITY ASSAYS 49

3.12 WST-1 CELL PROLIFERATION ASSAYS 49

3.13 11STATISTICAL ANALYSIS 50

4. RESULTS AND DISCUSSION 51

4.1 USP1 STABILIZES ULK1 IN MAMMALIAN CELLS 51

4.2 USP1 MODULATES ULK1 COMPARTMENTALIZATION IN MAMMALIAN CELLS 54

4.3 INHIBITION OF USP1 ACTIVITY BY PIMOZIDE MODULATES ULK1 COMPARTMENTALIZATION 58

4.4 USP1 DEPLETION INCREASES P62/ULK1 COLOCALIZATION 60

4.5 USP1 DOWNREGULATION FACILITATES THE RECRUITMENT OF ULK1 TO AGGRESOMES AND RETAINS ITS KINASE ACTIVITY. 62

4.6 USP1 INTERACTS WITH ULK1 IN VIVO 68

4.7 ULK1 LOCALIZES TO THE NUCLEUS AND INTERACTS WITH USP1 69

4.8 USP1 REMOVES THE K63-LINKED UBIQUITIN CHAINS OF ULK1 ERRORE. IL SEGNALIBRO NON È DEFINITO.

4.9 USP1 DEPLETION IMPAIRES CANONICAL AUTOPHAGY 73
4.10 USP1 DEPLETION INHIBITS THE AUTOPHAGIC FLUX 76
4.11 TARGETING USP1 TO KILL AUTOPHAGY COMPETENT CANCER CELLS. 77

5. CONCLUSION 88

LIST OF PUBBLICATIONS 90

REFERENCES 91

"Humanity also needs dreamers, for whom the disinterested development of an enterprise is so captivating that it becomes impossible for them to devote their care to their own material profit. Without doubt, these dreamers do not deserve wealth, because they do not desire it. Even so, a well-organized society should assure to such workers the efficient means of accomplishing their task, in a life freed from material care and freely consecrated to research" Marie Curie

.

ABSTRACT

Ubiquitination is a post-translation modification of cellular proteins that occurs through a coordinated enzymatic cascade ending in the attachment of ubiquitin's C-terminal glycine (Gly76) to an acceptor lysine residue, via an isopeptide bond. In opposition to ubiquitination lies deubiquitination, the hydrolysis of the isopeptide bond and subsequent release of ubiquitin from its substrate. This is achieved by a ~100-membered group of enzymes termed deubiquitinases, or DUBs. They are further divided into five families and they contribute to regulate levels, activity and localization of many cellular proteins and maintain the pool of free ubiquitin.

The ubiquitin specific proteases (USP) family is the largest family of DUBs in humans and Ubiquitin specific peptidase1 (USP1) is one of the best-characterized. USP1 is the main player in the cellular response to DNA damage and it is deregulated in several types of human cancer, suggesting that this enzyme could represent a favourable therapeutic target for cancer treatment. Autophagy is a cellular mechanism for the degradation of cytoplasmic material, damaged organelles and protein aggregates in the lysosomes. Autophagy has a complex role in tumorigenesis and cancer treatment, since it has a role in both tumor prevention and in tumor survival and in resistance to treatment. The serine/threonine kinase ULK1, is one of the most upstream autophagy-related factors. It forms a complex with ATG13, FIP200 and ATG101, commonly considered as an initiator of the autophagic cascade. However, how the deubiquitinases may be involved in the regulation of autophagy is still unclear.

In the present work, we show that ULK1, critical for autophagy initiation, is a target of USP1. To understand what is the biological effect exerted by USP1 upon ULK1, we depleted USP1 in several cell lines and followed the fate of endogenous ULK1.

We transfected USP1 specific siRNA, or treated cells with pimozide, a chemical inhibitor of USP1, and we observed a sharp reduction of ULK1 in Triton X-100 soluble cellular lysate and its redist ribution in a 5M urea soluble fraction. Additionally, in USP1-depleted cells this fraction shows an enrichment of p62/SQSTM1 protein and HDAC6, an aggresome marker.

Furthermore, by both immunofluorescence and co-immunoprecipitation assays, we confirmed that in USP1 depleted cells, ULK1 aggresomes contain p62/SQSTM1. Moreover, we observed that ULK1 redistribution did not affect ULK1 kinase activity. Notably, depletion of USP1 impairs the autophagic flux.
In breast tumors, it is still a matter of debate whether autophagy suppresses or promotes tumor progression. In this study, we describe the existence of a collection of breast tumors co-expressing USP1 and LC3 proteins, suggesting that USP1-autophagy axis represents a promising tool for the treatment of tumors relying on this axis for survival.

ACKNOWLEDGEMENTS

I would like to thank my Supervisor Prof. Claudio Schneider for giving me the possibility to work in his laboratory during the years of my PhD course. I am extremely grateful to my co-supervisor Dr. Francesca Demarchi, whose enormous support and insightful comments were invaluable during my study. I am especially thankful for provinding me your exceptional scientific knowledge in a very interesting field of research and given the independence to develop myself as a scientist.

I thank also all the people of LNCIB that help me and make nice the lab life. A special acknowledge to Dr. Leticia Peche for her technical support and for all the helpful discussions. I would also like to thank Miss Annie Zappone and Dr. Valentina Buemi for making me smile every morning, even on the rainy days, for being the best colleagues and friends I could have ever wished for.

I am very appreciative to my past colleagues Dr. Elena Marcassa end Dr. Francesca Cataldo for all the important things that I have learned from them.

To my two examiners: Prof. Alessandro Marcello and Prof. Carmine Settembre, whose careful proofreading and suggestions have led to an improvement of the quality of this thesis.

Finally, I would also like to express my gratitude to my parents for their moral support and warm encouragements, backing me for all the decisions I have made.

LIST OF ABBREVIATIONS

AD Alzheimer's disease

AMPK: AMP-activated protein kinase

APC/C: anaphase-promoting complex/cyclosome

ATG: autophagy-related gene

BACH1/BRIP1: BRCA1-associated C-terminal helicase 1, BRCA1-interacting protein 1

bHLH: basic-helix-loop-helix

Bcl2: B-cell lymphoma 2

BRCA1: breast cancer type 1

CAPN1: calpain 1 or micro-μ-calpain

CAPN2: calpain 2 or milli-m-calpain

CAPNS1: calpain small subunit 1

Cdk5: cyclin-dependent kinase 5

CMA: chaperon-mediated autophagy

CUL3: Cullin 3

CUL4: Cullin 4

CUL5: Cullin 5

DUB: deubiquitinating enzyme

FA: Fanconi anemia

FAK: focal adhesion kinase

FAN1: FANCD2/FANCI-associated nuclease 1

FANCD2: Fanconi anemia complementation group D2 protein

FIP200: focal adhesion kinase family-interacting protein of 200kd

GABARAP: GABA Type A Receptor-Associated Protein

HD: Huntington's disease

HDAC6: histone deacetylase 6

HSC70: heat shock cognate protein of 70 KDa

ID: inhibitors of DNA binding

JAMM: JAB1/MPN/Mov34 metallo-enzyme

KLHL20: Kelch Like Family Member 20

LAMP: lysosome-associated membrane protein

LC3: microtubule-associated protein light chain 3

MEF: mouse embryonic fibroblast

MMC: mitomycin C

mTOR: mammalian target of rapamycin

NEDD4: Neural Precursor Cell Expressed, Developmentally Down-Regulated 4, E3 Ubiquitin Protein Ligase)

NRF2: Nuclear factor (erythroid-derived 2)-like 2

OTU: ovarian tumour protease

PCNA: proliferating cell nuclear antigen

PD: Parkinson's disease

PE: phosphatidylethanolamine

PI3K: Phosphoinositide 3-kinase

PIP2: phosphatidylinositol-4,5-bisphosphate

PIP3: phosphatidylinositol (3,4,5)-trisphosphate

PTM: post-translation modification

SCF: Skp1-Cullin-F-box protein complex

TLS: translesion synthesis

TNF: tumour necrosis factor

TRAF6: TNF receptor associated factor

TSC2: Tuberous Sclerosis Complex 2

UAF1: USP1-associated factor 1

Ub: ubiquitin

UBA: ubiquitin-associated domain

UBC: ubiquitin-conjugating enzyme

UBD: ubiquitin-binding domain

UCH: ubiquitin C-terminal hydrolase

ULK1: Unc-51-like kinase 1

ULK2: Unc-51-like kinase 2

USP: ubiquitin-specific protease

USP1: ubiquitin-specific peptidase 1

UV: ultraviolet

ZnF-UBP: zinc finger ubiquitin-specific protease domain

1. INTRODUCTION

1.1 Autophagy

1.1.1 What is autophagy?

In 1963, Christian de Duve introduced the term autophagy from the Greek words αυτό (self) and φαγία (eating). Autophagy is well conserved a catabolic process from yeast to higher eukaryotic cells. It's a self-digestive mechanism where metabolites are recycled within the cells. During the process, organelles (e.g. mitochondria and endoplasmic reticulum membranes), cellular proteins and cytoplasm are enclosed and degraded in the lysosomes[1,2,3].

In mammalian cells, it appears to be constitutively activated and can be further regulated up or down, depending on environmental conditions, e.g. starvation, hypoxia and DNA damage. In addition, autophagy has different functions and levels of activity in different cell types. Normally, autophagy performs the role of housekeeper, recycling proteins regularly before they denature. In the event that proteins are mutated and form aggregates, autophagy can help the cell avoid the toxic effects of this accumulation. In addition, autophagy has a major role in multiple cellular mechanisms such as inflammation, innate and acquired immunity, lifespan extension and cell death as well as differentiation and development[4,5,6,7,8]. Alterations of autophagy lead to several human disorders including cancer, cardiomyopathy, diabetes, neurodegeneration, liver disease, autoimmune disease and infections[9]. There are three forms of autophagy: chaperon-mediated autophagy (CMA), microautophagy and macroautophagy. The three processes share common molecular machinery and their cargo is degraded in the lysosomes for all three types. Chaperone-mediated autophagy degrades cytosolic proteins selectively. Proteins targeted for this pathway contain a specific peptide motif (KFERQ) recognized by the hsc70 chaperone in the cytoplasm, which is responsible for targeted proteins transportation to the lysosome where they are unfolded and degradated. Microautophagy occurs directly at the lysosomal or vacuolar membrane. Cytosolic components are engulfed in the lysosome through invagination of the lysosomal membrane. The adjacent cytoplasm is being fused to form a vescicle already contains within the

lytic compartment. The third type of autophagy is macroautophagy. It is the most characterized autophagic clearance mechanism and hereafter it will be referred to as "autophagy" for semplicity. Macro-autophagy releases cytoplasmic cargo to the lysosome for degradation after inclusion in a double-membrane vesicle, termed autophagosome. This vescicle first fuses with endosome forming a hybrid organelle termed amphisome and then it fuses with lysosome, forming the autophagolysosome. Inside the autophagolysosome the cargo is degraded into free nucleotides, amino acids and fatty acids by hydrolytic enzymes and then recycled[10] (Figure 1.1).

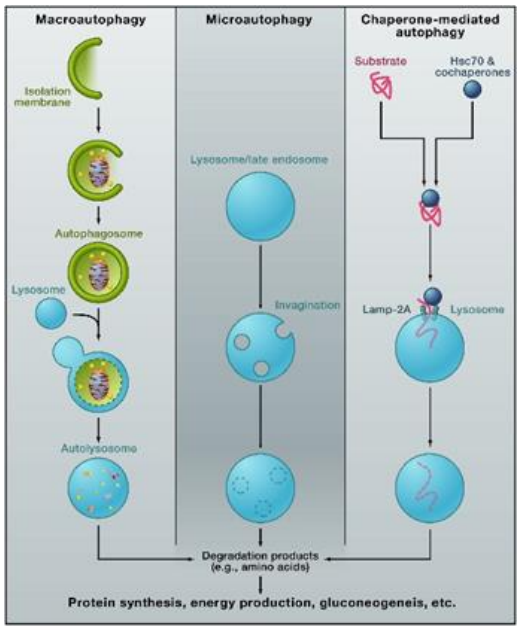

Figure 1.1. **Different type of autophagy**. Macroautophagy, microautophagy and chaperone-mediated autophagy are three types of autophagy in mammals. Here, the main steps in these processes as well as the most important characteristic structures and the related mediators are presented. Figure adapted from[10].

1.1.2 The process of autophagy

Autophagy is controlled by the autophagy-related genes (*Atg*) that have been identified in *S. cerevisiae* and they are highly conserved between yeast and

human. To date, 32 Atg genes have been identified in mammals and they can be grouped in six group, according to their function: 1) the ULK1-Atg13-FIP200 kinase complex; 2) the PI3K class III complex including the core proteins Vps34, p150 and Beclin1; 3) the PI3P-binding Atg2/Atg18 complex; 4) the multi-spanning transmembrane protin Atg9; 5) the ubiquitin-like Atg5/Atg12 system and 6) the ubiquitin-like LC3 conjugation system[11,12,13]. These proteins are involved in different steps of autophagy: initiation, autophagosome formation, fusion and degradation (Figure 1.2).

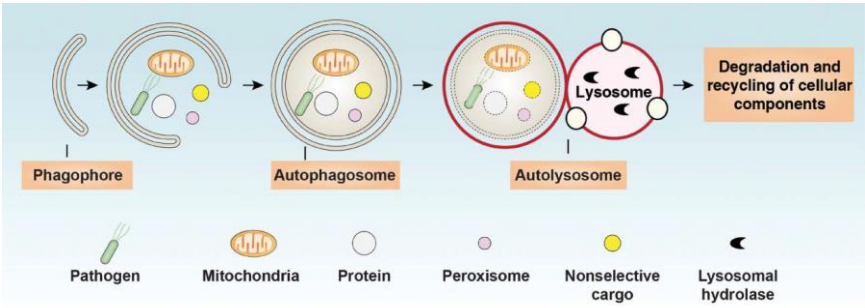

Figure 1.2 The autophagic process in mammalian cells. General overview of the principal steps of the autophagy: vesicle nucleation (formation of phagophore), vesicle expansion (autophagosome formation), maturation (fusion of autophagosome with lysosome), degradation (acidification). Figure adapted from[14].

Initiation: The induction of autophagy in yeast cells is controlled by the Atg1-Atg13-Atg17 complex, whereas in mammals, the Unc-51-like kinase 1 (ULK1) sits on the top of the autophagy initiation cascade and along with the Unc-51-like kinase 2 (ULK2), represents the Atg1 yeast homologs. ULK1 and ULK2 form a complex with mammalian ATG13 (Atg13 homolog), the focal adhesion kinase family-interacting protein of 200Kd (FIP200) (Atg17 homolog) and AT[1]G101 which does not have any obvious ortholog in *S. cerevisiae*[15,16,17].

mTORC1 is a molecular trigger for autophagy in response to glucose, amino acids and growt

factors. Under nutrient rich conditions, the ULK complex interacts with mTORC1 and remains inactivated by mTORC1-mediated phosphorylation of all members of the Atg13-ULK-FIP200-Atg101 complex[18]. The initiation of autophagy is constitutively kept at low levels. During starvation, mTORC1 dissociates from the complex causing de-phosphorylation and activation of ULK1 and ULK2, which can then phosphorylate and activate ATG13 and FIP200, leading to a subsequent localization of the activated ULK complex to the phagophore[19,20]. Nonetheless, mTOR has been also suggested to directly phosphorylate and inactivate ATG13 under nutrient rich conditions[21]. Hence, the phosphorylation status of ATG13 depends on both ULKs and mTOR activity, it occurs in different sites, excerting opposite effects.

Autophagosome formation: The first step of this process refers to the nucleation of the phagophore. The formation of new autophagosomes requires the activity of several protein. Beclin1 protein is the mammalian ortholog of yeast Atg6 and it is an interacting partner of anti-apoptotic protein Bcl-2. During starvation Beclin1 is released from the Bcl-2 complex and forms a complex with Vps34 and Vps15, two proteins involved in vacuolar sorting pathways. Vps34 is a class III phosphoinositide-3-kinase (PI3K) and Vps15 is a non-catalytic regulatory unit in the complex[22]. Anhoter interactor of the Vps34-Vps15-Beclin1 complex is the BECLIN1-associated autophagy-related key regulator (BARKOR), also known as autophagy-related protein 14-like (ATG14L) protein for its high homology with yeast Atg14)[23]. ATG14L targets the protein complex to sites of phagophore nucleation. Others two proteins associated with the PI3K complex are: the activating molecule in BECLIN1-regulated autophagy protein 1 (AMBRA1) and UVRAG (UVirradiation-resistance-associated gene). The former, upon autophagy induction, is activated by ULK1 phosphorylation and releases the PI3K core complex to sites of phagophore nucleation[24]. The latter is a positive regulator of autophagosome formation[25]. The origin of the autophagosomal membrane is still unclear. Some studies suggest that either the ER or the Golgi

are the source, while others propose both ER and mitochondria, or a *de novo* membrane generation[26,27,28].

Elongation of autophagosomes: The expansion of the phagophore and, ultimately the formation of the autophagosome, depend on two ubiquitin-like conjugation systems: the Atg12-Atg5-Atg16 complex and the LC3-phosphatidylethanolamine (PE) complex. Autophagy conjugation systems share structural and functional similarities to ubiquitin conjugation pathway during proteasomal degradation. As illustrated in Figure 1.3, Atg12 is first activated in an ATPdependent manner by Atg7 (it functions like an ubiquitin-activating enzyme, E1), leading to the formation of a thioester bond between the C-terminal glycine in Atg12 and a cysteine residue in Atg7. Atg12 is then transferred to Atg10 (an E2-like enzyme) and then conjugated to the target protein Atg5. The ATG12-ATG5 complex associates then to ATG16-like (ATG16L; Atg16 yeast homolog) forming a multimeric Atg5–Atg12–Atg16L complex that associates with the extending phagophore[29,30,31]. The second ubiquitin-like system requires the protein microtuble-associated protein 1 light chain (MAP1-LC3). In human, have been identified three LC3 isoforms (LC3A, B and C) and four additional Atg8 yeast homologs (GABARAP, GEC1/GABARAPL1, GATE16/GABARAPL2 and GABARAPL3)[32]. Upon autophagy induction, LC3 is first precessed by cysteine protease Atg4, which removes 22 amino acids from the C-terminal of LC3 and generates the cytosolic form (LC3-I)[33]. The carboxyterminal glycine exposed by Atg4-dependent cleavage, is then activated by the E1-like Atg7. Activated LC3-I is then transferred to Atg3 and finally, Atg12-Atg5 covalently binds PE to LC3-I generating the lipidated form, LC3-II. Autophagosomes have double membrane and a different composition between the inner and the outer membranes. LC3 is presents both in the inner and outer membrane where it plays a role in selecting cargo for degradation. Thus, LC3 is the only credible marker of the autophagosome in mammalian cells[34]. LC3-II interacts with 'adaptor' molecules on the target (e.g. protein aggregates, mitochondria), thus contributing to their selective uptake and degradation. In this regard, p62/SQSTM1 is an adaptor

molecule that promotes turnover of polyubiquitinated protein aggregates. p62 contains a C-terminal ubiquitin-associated (UBA) domain that binds ubiquitin, and a LC3-interacting region (LIR), important for direct binding to human LC3 family members[35]. NBR1 is another autophagy receptor that acts similarly to p62/SQSTM1 in promoting turnover of ubiquitinated proteins[36].

Fusion and degradation: Completed autophagosome moves towards endosome and lysosome along actin microfilaments and microtubules. LAMP-2, the small GTPase RAB7 and UVRAG are essential for the fusion of auophagosome with the lysosome[37,38]. Inside the autolysosome, the cargo is lysed mainly by cathepsins and the macromolecules are being digested to their monomeric units and released to the cytosol for their reuse. One of the main autophagy regulators, mTORC1, is localised to the surface of lysosomes in response to amino acid release and therefore, inhibits the autophagy thus preventing an over-activation of autophagy[39,40].

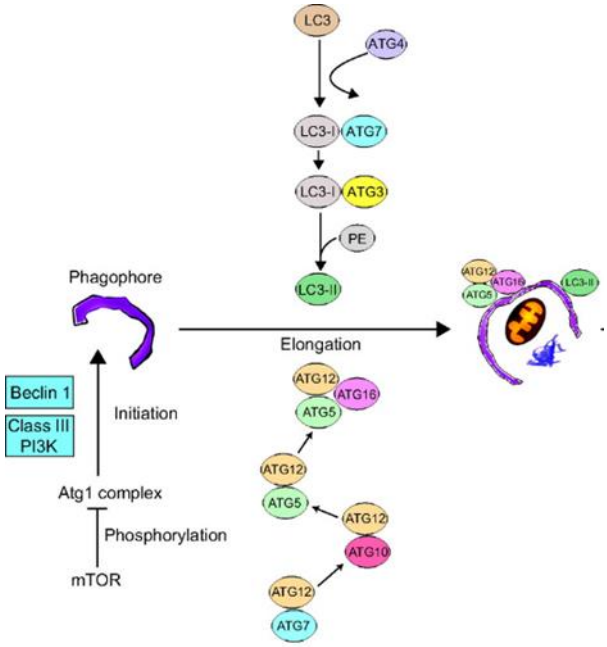

Figure 1.3 Two essential ubiquitin-like conjugation systems in autophagy. The first conjugating system includes Atg8, -4, -7, and -3 and PE. This system conjugates a single PE molecule to the COOH terminus of Atg8/LC3. The second conjugation system includes Atg12, -7, -10, -5, and 16.

This conjugation leads to the covalent attachment of the COOH-terminal glycine of Atg12 to Atg5 through an internal lysine residue. Figure adapted from[41].

1.1.3 Regulation of autophagy by signaling pathways

Owing to its energy sensing functions, mTOR (the mammalian target of rapamycin) is considered the master regulator of autophagy in response to a spectrum of signals including growth factors (e.g. insulin-like factors, PDGF, VEGF and EGF), nutrients (e.g. amino acids and glucose), energy (ATP) and oxygen. Several studies suggest that when nutrients are abundant, active mTORC1 inhibits autophagosome formation by associating with the ULK-ATG13-FIP200-ATG101 complex and phosphorylating ULK1 and Atg13[42]. Inhibition of mTORC1 by rapamycin or starvation results in dephosphorylation of ULK1 and initiation of autophagy.

Glucose is the primary energy source for mammalian cells and when energy depletion occurs in cells, autophagy is activated to restore ATP from cellular components[43]. Another important cellular energy sensor is AMPK, which positively regulates autophagy[44,45]. AMPK is activated when the cells are under conditions of glucose starvation and it promotes autophagy through two mechanisms: it activates the ULK1 complex through phosphorylation and inactivates mTORC1 by phosphorylating Raptor and TSC2 (tuberous sclerosis 2)[46,47]. Since ULK1 is free from mTOR, it interacts with AMPK, which phosphorylates and activates ULK1. The activation of the ULK1 complex marks the initiation of autophagy, which promotes cell survival in the presence of energy stress[42]. Varius groups have sequenced the phosphorylation sites of ULK1 releted to AMPK and mTOR.

Growth factors are molecules secreted by cells and can stimulate the proliferation and/or differentiation of the secreting cells by autocrine signalling, or stimulate neighbouring cells by paracrine interactions. Growth factors bind to receptor tyrosine kinases (RTKs) on the cell surface and in turn PI(3)K is recruited to the cell membrane and activated generating PIP3

(phosphatidylinositol-3,4,5 trisphosphate). This leads to a signalling cascade at the membrane. Akt, Rheb and mTORC1 complex are in turn activated[48].

The concentration of amino acids is the dominating signals for the activation of the multi-protein complex mTORC1. Studies have proved that mTORC1 is also located to the outer surfaces of lysosomes[49] where interacts with TFEB and through this interaction, it senses the lysosomal content[50]. The pathway is regulated by Rag GTPases, GATOR1 and GATOR2 complexes[51] and it is conserved from yeast to mammalian cells.

Autophagy can also be up-regulated by genotoxic stress such as DNA damage and reactive oxygen species (ROS)[52]. The p53 tumour suppressor plays important roles in cell cycle regulation, DNA damage response and programmed cell death. Cytosolic and nuclear p53 play opposing roles in autophagy regulation. In the nucleus, p53 plays the role of a transcription factor[53] and, in the presence of genotoxic stress, p53 actives a number of autophagy genes including AMPK, ULK1 and ULK2[54,55]. In contrast, cytoplasmic p53 mainly inhibits autophagy[53].

Other autophagy-modulating molecules include Bcl-2[22] and BNIP3 (Bcl-2/adenovirus E1B 19-kDa interacting protein 3)[56]. Bcl-2 is an important regulator of programmed cell death, which interacts with Beclin-1 through BH3 (Bcl-2 homology 3) domains and indirectly inhibits autophagy[22]. Autophagy is also activated in response to hypoxia. BNIP3 and BNIP3L are two essential elements for hypoxia-induced autophagy. Through their BH3 domains, disrupt the interactions between Beclin1 and Bcl-2[56]. Hypoxia induced autophagy is thought to be a pro-survival mechanism utilized by cancer cells[57].

To summarise as shown in Figure 1.4, autophagy is constitutively kept at low levels and can be activated by energy stress or genotoxic stress.

1.1.4 Physiological roles of autophagy

Considering the important role of autophagy in maintaining cellular homeostasis and integrity, it is not surprising that loss of autophagy would perturb this balance and cause human diseases. Autophagy plays a role in

several physiological aspects and also it has been implicated in a spectrum of pathological conditions including neurodegenerative disorders, infections, autoimmune diseases, diabetes, muscular diseases and cancer[9].

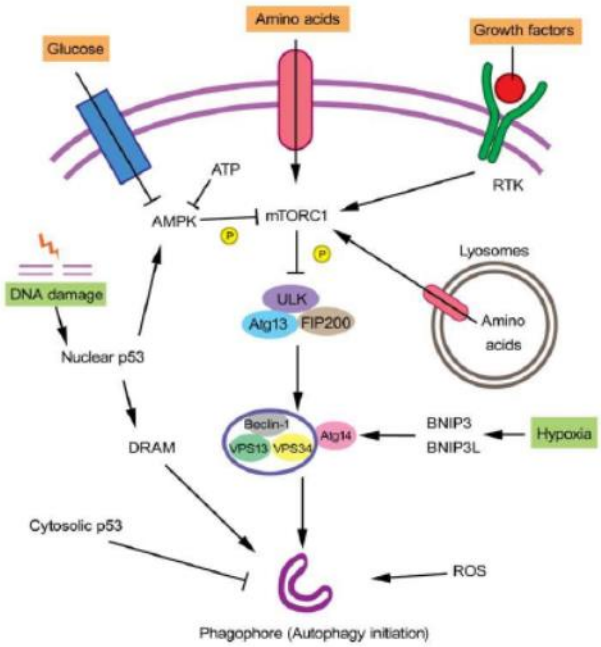

Figure 1.4 Autophagy levels are modulated in response to a variety of stimuli in mammalian cells. The major signaling pathways of autophagy regulation under conditions of nutrients (amino acids, growth factors) deprivation, energetic stress, endoplasmic reticulum (ER) stress, energetic stress, are depicted.

1.1.4.1 Immunity, starvation and cell death

Autophagy can protect cells from invasion by pathogens through a process termed xenophagy. Autophagy has been found to be up-regulated during infections. *Micobacterium tuberculosis* (MTB) and other pathogens (e.g. *Listeria, Salmonella, Shigella,* and viral capsids) can be cleared via autophagy, through recognition by a specific autophagy adaptor protein p62/SQSTM1[58,59]. However, under selective pressure, certain bacteria and viruses have developed strategies to antagonize autophagy functions. The Bacterium *Shigella flexneri*

avoids recognition by autophagic pathway by expressing modified surface proteins[60]. Some microbes have even evolved mechanisms that utilize components of the autophagic machinery to facilitate viral maturation[61]. Autophagy also participates in programmed cell death, expecially for growing tissues. Indeed, in some cases the same proteins control both autophagy and apoptosis. Apoptotic signaling can regulate autophagy and conversely autophagy can regulate apoptosis. Indeed, it has been suggested that the p53 regulation of autophagy depends on its localisation; indeed nuclear p53 appears to induce autophagy at transcriptional level, whereas cytosolic p53 suppresses autophagy[53]. In addition, few years ago, the interaction between ATG7 and p53 has been proposed (Figure 1.5). During starvation, ATG7 is essential for initiation of cell cycle arrest by binding to p53 and inducing expression of the cell cycle inhibitor p21. During starvation conditions, absence of ATG7 results in increased DNA damage, the production of reactive oxygen species (ROS), transcriptional increase of the proapoptotic genes PUMA, NOXA, BAX and ultimately, in the p53-dependent apoptosis[62]. Another autophagy gene connected with apoptosis is the ATG5, which is regarded like the "molecular switch" between autophagy and apoptosis. Under stress factors, the calpains, a family of proteases, cleaves ATG5 which triggers the release of mitochondrial cytochrome c and leads to an autophagosome-independent cell death (Figure 1.5). The essential role of autophagy in preserving cell viability upon deficiency of nutrients, was first read up in yeast. Few years later a similar cytoprotective role of autophagy was also illustrated in mammalian cells[19].

1.1.4.2 Housekeeping and aggregates removal

Autophagy is also instrumental for housekeeping within the cell, therefore is involved in removing damaged or over-activated and potentially dangerous organelles (mitochondria, endoplasmatic reticulum, peroxisomes and lysosomes)[63,64]. In addition, autophagy together with proteasome degradation, is important to remove misfolded or damaged proteins. In general, proteasome degrades smaller proteins which are specifically recognised by E3 ligases. On

the other hand, autophagy degrades proteins and aggregates that can not access inside the proteasome structures because unwieldy. Misfolded proteins exist in neuronal inclusions or plaques in the brain, which are responsible for several neurodegenerative conditions. Therefore, autophagy is a crucial factor for neuronal development and homeostasis. Autophagy pathways have been linked to Alzheimer's disease, Huntington's disease, Parkinson's disease[65]. These conditions often result from inheritable mutations, which lead to protein misfolding and aggregate formation. Autophagy plays a protective role against these disorders.

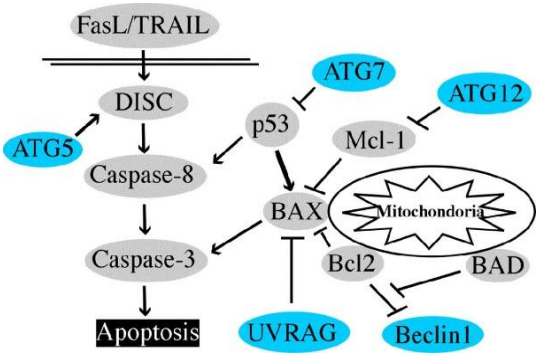

Figure 1.5 Crosstalk between autophagy and apoptosis regulators. Examples of interaction between autophagy regulators (blue) and apoptosis regulators (gray). Figure adapted from[66].

1.1.5 Autophagy and disease

1.1.5.1 Autophagy and Alzheimer's diseases (AD)

The accumulation of extracellular plaques including aggregated amyloid-ß (Aß) peptide and intracellular tangles, is associated with the pathogenesis of AD. Autophagy has a role in both the clearance of Aß plaques and the generation of them. Since Aß is generated in the endo-lysosomal pathway, normally it is found in autophagosomes and lysosomes. However, in the case of impaired autophagosome/lysosome fusion, Aß plaque-rich autophagosomes build up within the cell, as demonstrated in the brains of patients[67].

1.1.5.2 Autophagy and Parkinson's diseases (PD)

Parkinson's (PD) is the second most common neurodegenerative disease. It is generated by proteins accumulation in clump called Lewy Bodies, but the main protein of those clump is α-synuclein. Several evidences indicate that autophagy defects are involved in PD disease. As per its function in aggregate removal, autophagy induction decreases the accumulation of α-synuclein. Mutations in key autophagy proteins such as PINK-1 or parkin, are implicated in PD disease. The former is a serine-threonine kinase that interact with Beclin-1 to induce autophagy, the latter is an E3 ubiquitin ligase which localizes to damaged mitochondria and then assists in mitophagy. Mitophagy is disrupted in cells that have mutated parkin and PINK-1[68].

1.1.5.3 Autophagy and Huntington's disease (HD)

Huntington's disease is an inherited CAG–polyglutamine repeat disorder, causing accumulation of misfoldedhuntingtin (Htt) protein. HD shares many features with common neurodegenerative disorders, such as Alzheimer's disease (AD) and Parkinson's disease (PD). Autophagy plays a protective role in HD disease by removing PolyQ and PolyA aggregates from cells. Although autophagy can degrade Htt and protect cells, it seems that Htt might have a negative effect on autophagy. Htt forms aggregates around some autophagy regulator proteins, causing an alteration of the process. Whilst Htt sequesters mTORC1 and turn on autophagy[68], on the other side, it can sequester Beclin1 and reduces autophagy levels[69].

1.1.5.4 Autophagy and cancer

The functions and outcome of autophagy in cancer are highly context specific. Several reports have referred to autophagy as "a double edged sword" or "janus-faced"[70,71], infact it can promote cancer cell survival or cancer cell death[72] (Figure 1.6). In general, cancer can be divided into three critical stages: initiation, promotion and progression. To become neoplastic, normal cells acquire insensitivity to growth suppressors and they undergo uncontrolled over-

growth. Tumour cells are able to break out programmed cell death and attain replicative immortality. Primary tumours can migrate from the site of origination and invade into a secondary part of the body. Metastatic cancer can establish itself by recruiting blood supply and modify surrounding cells to form a tumour microenvironment[73]. Before tumorigeneis, autophagy is able to suppress tumor initiation by protecting normal cells and inhibiting inflammation and necrosis, but in contrast, in estabilished tumors, autophagy can be a pro-survival mechanism for cancer cells and provides oxygen and nutrients[74]. In 1999, the tumor suppressive role of autophagy was fixed from Beclin1 studies[75]. Following, it was demostated that mice with heterozygous disruption of Beclin1 were capable to develop tumors[76]. Therefore, when Beclin1 was stably transfected into MCF-7 cells, inhibiton of tumor development was promoted. In addition, down regulation of ATG5 encouraged tumorigenesis[77]. These data support the idea that autophagy, through its role in homeostasis and quality control, acts as a tumour suppressor mechanism. Indeed, alterations of autophagy, lead to an accumulation of protein aggregates, damaged mitochondria and misfolded proteins which in turn leads to increased ROS production and DNA damage, promoting tumorigenesis.

Autophagy regulates p62 levels in the cells and suppression of autophagy is related to p62 accumulation and tumorigenesis[78]. p62 is an autophagy receptor important for selective autophagy. It recognises and sequesters specific ubiquitinated cargoes (e.g. misfolded proteins) destined to be degraded by autophagy[79]. p62 is itself degradated through autophagy and alterations of autophagy lead to accumulation of p62 in the cells. On the contrary, p62 loses its useful role when in the cells there are elevated levels of it. Indeed, high intracellular levels of p62 are responsible for the formation of protein aggregates, which are tighly linked with neurodegeneration, liver injury and hepatocellular carcinoma[80]. Autophagy suppression leads to an increase of p62 levels and overexpression, activation and translocation of Nrf2 to the nucleus, followed by transcription of the Nrf2 gene targets and tumourigenesis. NRF2 has been suggested to have a dual role in cancer: although it protects from

oxidative stress, its overexpression promotes survival and growth of tumour cells[81]. However, p62 is often up-regulated in human cancer and can promote tumorigenesis. One of the hallmarks of cancer is its ability to escape recognition by immune cells and it is generally proved that in more tumours, inflammation and immune responses are pro-tumourigenic[73]. Disruption of BENC1 gene displays an increased inflammation in hepatcarcinoma[76] .

In addition, in cancer framework, autophagy contributes to induce senescence. Senescence can be activated by DNA damage or by oncogenic signals and autophagy is found to mediate the establishment of oncogene-induced senescence[82].

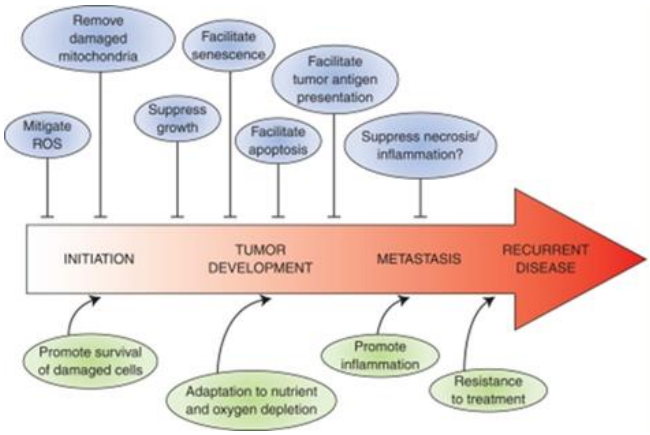

Figure 1.6 The contrasting roles of autophagy in cancer. In healthy cells, autophagy prevents cellular transformation by removing ROS and damaged mitochondria. However, following transformation, activation of autophagy can promote and suppress cancer progression, depending on the timing or stage of disease. Autophagy either mediates its effects directly or "communicates" with other cellular pathways such as senescence, apoptosis, necrosis, and inflammation. Figure adapted from[83].

All studies described above give both genetic and mechanistic evidence that autophagy can act as a tumour suppressor, during the initial stages of tumourigenesis. Autophagy can also promote tumor progression. Cells in the core of the tumour have to overcome adverse conditions such as hypoxia and

limited access to nutrients. Unlike normal cells that have low basal autophagy levels, cancer cells seem to be "addicted" to high levels of autophagy under nutrients depletion[84]. The oncogenic role of autophagy is supported by several genetic studies. For example, depletion of FIP200, a gene essential for autophagy, inhibits carcinogenesis[85,86]. Deletion of Atg5 or Atg7 in the liver leads to benign tumours. It should be noted that these tumours do not progress into malignant adenocarcinoma and don't acquire the capacity to metastasize[87]. In summary, autophagy can act as a tumour suppressor by maintaning cellular homeostasis, limiting genetic instability and inflammation; however, it supports the survival of cancer cells in established tumours. Therefore, the role of autophagy in cancer development is complex and seems to depend on cell type, stage and genetic context.

1.2 Ubiquitination and deubiquitinating enzymes

1.2.1 The ubiquitination pathway

Post-translational modifications (PTMs) are essential mechanisms used by eukaryotic cells to expand the functional diversity of the proteome. This mechanism, together with RNA splicing, increases the number of protein variants in the cell and is important to coordinate proteins interaction, to modulating enzymatic activity, or altering cellular localization and half-life. Post-translational modifications are caused by a variety of stimuli and upstream signaling events. Here, we discuss the covalent modification of proteins with ubiquitin. Ubiquitin is a 76-amino acid protein (~ 8.5 kDa) constitutively expressed in all eukaryotic cells. Ubiquitination occurs through a sequential cascade of enzymatic reactions by which an isopeptide bond links the C-terminal glycine (Gly 76) of ubiquitin to lysine on the target proteins. This is achieved through sequential ubiquitin activation (E1 enzymes), conjugation (E2 enzymes), and ligation (E3 enzymes)[88]. The major function of ubiquitinetion is tagging proteins for proteasomal degradation, although not exclusively. Ubiquitinetion is necessary for cell cycle progression, transcriptional regulation,

DNA repair, apoptosis, protein trafficking, endocytosis, and signal transduction[89]. Alterations of ubiquitination are involved neurodegenerative disorders and pathologies of the inflammatory immune response[90]. The E1 enzyme binds both ubiquitin and ATP-Mg2+ forming an adenylated ubiquitin intermediate. Then, its catalytic cysteine, attacks this adenylated ubiquitin to form a ubiquitin-charged E1, connected by a high energy thioester bond. Ubiquitin is then transferred to one of about 40 E2 enzymes via a trans-thio esterification reaction. Subsequently, the charged E2 binds to one of hundreds of E3 enzymes which function as the substrate recognition molecules of the system. E3 enzymes are capable to interact with both E2 and substrate and create an isopeptide bond between a lysine of the target protein and the C-terminal glycine of ubiquitin (Figure 1.7).

Proteins that are linked to a single ubiquitin monomer are referred to as monoubiquitinated. Similarly, addition of ubiquitin monomers on multiple lysine residues of the target protein, leads to its multi-ubiquitination or multi-monoubiquitination. Monoubiquitination has several regulatory roles for the targeted protein, such as inducing changes in subcellular localization, conformation, activity and protein interactions. However, this type of ubiquitination does not control active protein turnover or degradation.

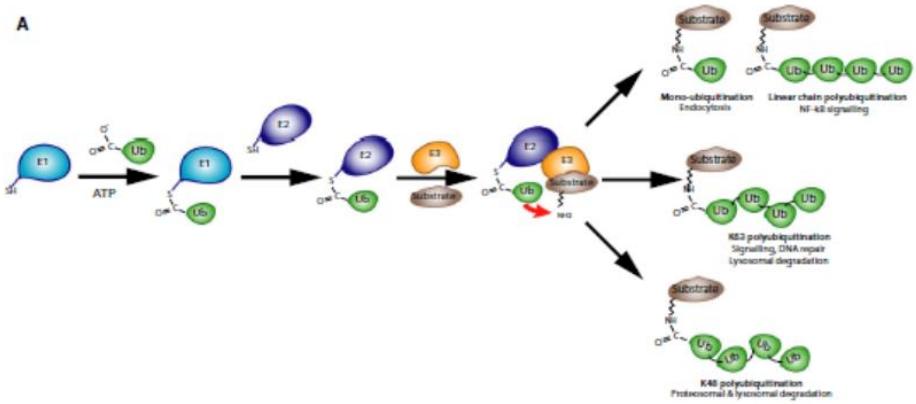

Figure 1.7 Steps of the ubiquitination process. E1 enzyme activates ubiquitin in an ATP dependent manner. The ubiquitin is passed to the E2 enzyme before being covalently attached to its substrate via E3 ligase. Figure adapted from[91].

The sequential addition of many ubiquitin monomers to the same protein, is termed polyubiquitination. Ubiquitin has 7 lysine residues, (K6, K11, K27-, K29-, K33-, K48- and K63) that may serve as points of ubiquitination. These different linkages are responsible for a variety of cellular events. The most well-studied polyubiquitin chain, K48-linked, tag mutated or damaged proteins for degradation via the proteasome[92], as well as, K11 and K29-linked ubiquitin chains[93]. Moreover, K11 and K29-linked ubiquitin chains are also crucial for cell cycle progression through degradation of cell cycle regulators[94,95]. K6-linked ubiquitin chain is discovered to be of importance in the BRCA1/BARD1-dependent localisation of conjugated ubiquitin to DNA damage foci[96]. Recently, K6 linkages have been identified in ubiquitylated mitochondrial outer membrane (MOM) proteins upon depolarization of the organelle[97]. K63-linked ubiquitination regulates cellular responses to DNA damage[98], NF-kB activation[99] and lysosomal trafficking[100].

1.2.2 The deubiquitinating enzymes

Deubiquitinase enzymes (DUBs) play an important regulatory role in the ubiquitin pathway, by removing ubiquitin from target proteins or modifying polyubiquitin chains on target proteins. Deubiquitinating enzymes are mainly cysteine proteases that act oppositely to E3 ligases. Over 100 proteins with DUB like activity have been identified[101]. DUBs regulate and maintain the homeostasis of free ubiquitin pools in the cell. Apart from their active domains, most DUBs also contain additional domains that regulate substrate recognition and protein-protein interactions[102]. They are classified into five subfamilies based on sequence, structure and mechanistic properties. The first four subfamilies are cysteine (Cys) proteases; namely the ubiquitin-specific proteases (USP), the ubiquitin carboxyl-terminal hydrolases (UCH), the ovarian tumour

related proteases (OTU-related) and Josephine domain DUBs. The fifth subfamily consists of zinc-dependent metalloproteases containing the JAMM/MPN+ domain. Cysteine DUBs hydrolyze isopeptide bonds utilizing a catalytic triad Cys, His and Asp; metallo DUBs have two zinc ions responsible for catalysis by an active site-bond water molecule[103]. DUBs can hydrolyse both isopeptide bond between ubiquitin and a substrate protein's lysin residue and between two ubiquitin monomers[104]. Some DUBs are specific for one chain type, other DUBs have specificity for the ubiquitinated substrate. They can remove whole ubiquitin chain from the substrate, cleave in the middle of a chain or they eliminate the furthest end of the chain and remove monomers sequentially. In addition to their DUB domains, they contain ubiquitin binding domains (UBDs) which bind monoubiquitin, sometimes polyubiquitin, with weak affinity in the high micromolar range.

Ubiquitin-specific processing proteases (USPs) The ubiquitin specific proteases or USP family is the largest family of DUBs containing about 60 members[105]. Their catalytic triad contains cysteine (Cys), histidine (His) and aspartic acid or asparagine (Asp or Asn) residues, which allows nucleophilic attack on the isopeptide bond, between the C-terminal of ubiquitin and the lysine residue of the protein target, by forming an acyl intermediate between the catalytic Cys and the carboxyl group of ubiquitin, which is further hydrolysed[103].

Ubiquitin carboxy-terminal hydrolases (UCHs) The ubiquitin carboxy-terminal hydrolases or UCHs exert their activity towards small amides and esters at the C-terminus of the ubiquitin molecule. This family of DUBs such as a classical cysteine proteases contains a catalytic triad residues and a three-dimensional structure like the USPs and also share with them a similar mechanism of catalysis.

Ovarian tumour related proteases (OTUs) The ovarian tumour related (OTU-related) proteases are almost 14 in human. The OTU core domain consists of 5 stranded ß-sheet surrounded by helical domains that differ between family members[102].

Josephin domain proteases This class of DUBs has a catalytic triad and its catalytic core structure is similar to the USP and UCHs.

JAMM/MPN+ proteases This subfamily includes metalloproteases that bind two zinc ions in order to proteolytically cleave ubiquitin and are distinct from the Cys proteases USPs, UCHs, OTUs and Josephin domain DUB enzymes[103]. JAMM/MPN+ DUBs have been found in association with the 26S proteasome.

Like ubiquitination, DUB enzymes have been implicated in numerous cellular process, such as growth regulation, gene transcription, cell cycle control, stem cell maintenance and differentiation, DNA damage response and repair[102,106,107]. DUB activity can be grouped in three categories: ubiquitin precursor processing, ubiquitin deconjugation and editing of ubiquitin (Figure 1.8). First ubiquitin is transcribed from several genes as a multimeric 4 and 9 tandem repeat pro-protein and it is tied to ribosomal proteins. In order to be used in the ubiquitin-proteasome system, ubiquitin need be processed into single ubiquitin molecules, thus DUBs activity is required for the generation of free ubiquitin molecules[108]. Second, DUBs can remove ubiquitin from post-translationally modified proteins, saving proteins from proteasomal or lysosomal degradation. On the other hand, once a protein is targeted to proteasomal degradation DUBs can act by recycling ubiquitin molecules, contributing to ubiquitin homeostasis. Third, DUBs can trim ubiquitin chain of a protein target and edit the type of ubiquitin signal[103]. A20 is an exemple of this categorie, since it changes receptor-interacting serine-threonine kinase 1 (RIPK1) ubiquitination status from Lys63- to Lys48-linked polyubiquitination and promotes its proteasome degradation[109]. Therefore, if the accumulation of a target protein results dangerous for the cell, it might be interesting impair DUBs activity through a specific pharmaceutical treatment. This is the case of USP28 that stabilizes the proto-oncogene MYC[110], or USP7 that stabilizes p53 and its E3 ubiquitin ligase MDM2[111].

There are three protesome-associated DUBs whose task is to remove ubiquitin from proteins: UCHL5, USP14 and PHO1. POH1 is a member of 19S proteasome lid, that recognizes proteasomal substrates and allows their access into the proteolytic centre of 26S complex. POH1 cleaves the Lys63-linked

polyubiquitin chain, but can also break the first isopeptide bond that links the substrate and the proximal ubiquitin[112].

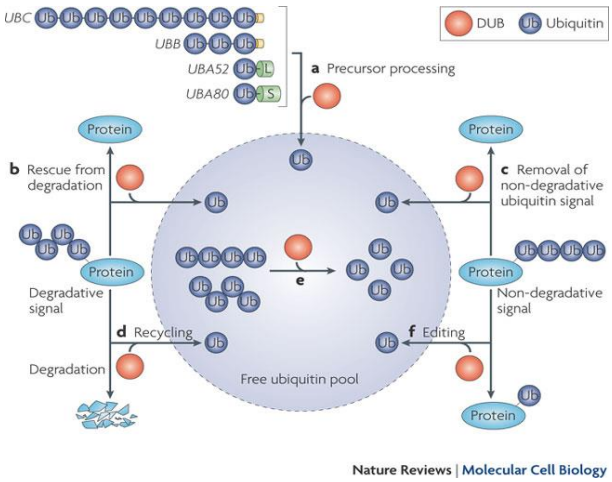

Figure 1.8. General roles of DuBs. a Ubiquitin is encoded by four genes (*UBC*, *UBB, UBA52* and *UBA80*) and is transcribed and translated as a linear fusion consisting of multiple copies of ubiquitin or ubiquitin fused to the amino terminus of two ribosomal proteins, 40S ribosomal protein L40 (L) and 60S ribosomal protein S27a (S). Note that the polyubiquitin genes encode an extension one or several amino acids long at their carboxyl terminus (shown in yellow). Generation of free ubiquitin from these precursors is a key function of deubiquitinases (DUBs; also known as deubiquitylating or deubiquitinating enzymes). **B** Deubiquitylation can rescue proteins from degradation. **C** Alternatively, deubiquitylation can remove a non-degradative ubiquitin signal. **d** DUBs have a crucial role in maintaining ubiquitin homeostasis and preventing degradation of ubiquitin together with substrates of the 26S proteasome and lysosomal pathways (recycling of ubiquitin). **e** Disassembly of ubiquitin chains generated by *en bloc* removal from substrates ensures that recycled ubiquitin re-enters the free ubiquitin pool. **f** Some DUBs might function to edit ubiquitin chains and thereby help to exchange one type of ubiquitin signal for another. Figure adapted from[103].

To avoid errant protease activity of DUBs towards cellular proteins they are tightly regulated by multiple mechanisms such as substrate-induced conformational changes, binding to adaptor proteins, proteolytic cleavage, and post-translational modifications. Certain DUBs require ubiquitin binding to reach their active conformation[113]. In addition, DUBs can undergo allosteric conformational changes upon interaction with ubiquitin or other proteins and increasing their catalytic activity. Several DUBs have low affinity for ubiquitin

and require additional interactors for binding their substrates[105]. An example is USP1, whose activation is facilitated by binding the adaptor molecule WDR48[114]. In the same way, other DUBs need to be embedded within large macromolecular complexes to become active. Another way of DUBs regulation is through a proteolytic cleavage of their own. This is symbolized, for instance, by USP1, which just after undergoes autoproteolysis it gets inactive[115]. Post-translational modification is another way to control catalytic activity of DUBs, thus phosphorylation can turn on or off their activity. For example, phosphorylation of A20, USP7, USP15, USP16, USP19, USP28, USP34 and USP37, stimulates their activation[116,117], while phosphorylation of CYLD inibhits its activity. Finally, their subcellular localization has been shown to be important for enhance DUBs activity [118].

Several DUBs show a relationship with different diseases. Mutations of CYLD were found in patients with familial cylindromatosis which develop skin tumours of the head and neck[119]. CYLD depletion, is associated with aberrant activity of NF-$_K$B pathway and promotes cell survival, providing a possible mechanism for tumour formation. USP6 was the first DUB to be identified as an oncogene and its over-espression leads closer to a transformed phenotype[120]. Moreover, UCHL1 is implicated in many malignancies including lung, breast and colon[121, 122]. Alterations of several DUBs occurs in a variety of neurodegenerative diseases. Indeed, mutations that impair the catalytic activity of UCHL1, are linked to Parkinson's disease (PD)[123]. UCHL1 is located in Lewy body protein aggregates associated with PD. These Lewy bodies collect normal and abnormal proteins, many of which are ubiquitylated. Low levels of functional UCHL1 are inversely proportional to accumulation of amyloid protein aggregates in Alzheimer's disease[124].

1.2.3 The ubiquitin specific protease 1 (USP1) enzyme

Among the human DUBs, the ubiquitin specific protease represents the largest DUB family with about to 60 members. USPs are large enzymes with a conserved catalytic core which presents a peculiar structure consisting of the

palm, thumb, and finger domains (Figure 1.9). The C-terminus of ubiquitin sits in a slot located between the thumb and the palm subdomains, while the globular portion of ubiquitin interacts with the finger.

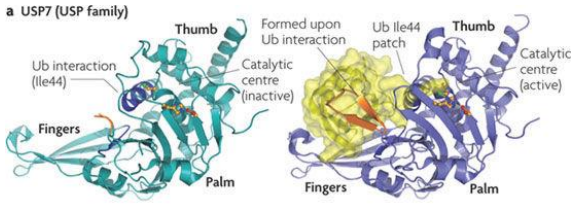

Figure 1.9 Structures of USPs enzyme. Inactive (green) and active (blue) structures of the catalytic domains of of ubiquitin-specific protease 7 (USP7), with ubiquitin (Ub) shown in yellow. The thumb, palm and fingers subdomains of the USP domain are indicated. Figure adapted from[103].

When USP domains are not bound to any substrate they display an inactive catalytic configuration and they undergo conformational changes, when bind ubiquitin [103].

The USP1 gene was cloned in Tanaka's lab, in 1998[125]. USP1 belongs to the USP family and conserves the domain that characterizes this DUB family, with an amino-terminal Cys box motif and a carboxy-terminal His box motif where siting the catalytic residues (Cys90, His593 and Asp751) (Figure 1.10) [114]

Figure 1.10 USP1 domain and structure Schematic representation of USP1 protein showing the position of its amino-terminal Cys box and carboxy-terminal His box domains. The catalytic residues Cys90, His593 and Asp751 are indicated by arrowheads. Figure adapted from[114].

USP1 has been identified as a key regulator of multiple important steps in the DNA repair processes, mainly in the Fanconi anemia (FA) pathway, by deubiquitinating the main effector proteins of this pathway, FANCD2 and FANCI and in the process of translesion synthesis (TLS) by deubiquitinating PCNA and preventing the recruitment of low fidelity DNA polymerases in the absence of damage. Moreover, recent study has shown that USP1 may also stabilize differentiation in specific cellular contexts, inhibiting proteins of the ID (inhibitors of DNA binding) family and helping to retain the undifferentiated state of osteosercoma cells[115,126,127].

1.2.3.1 Regulation of USP1 function

There are several mechanisms that regulate the expression levels and the catalytic activity of USP1. Indeed, cell cycle, protein-protein interaction, autocleavage, degradation and phosphorylation work together to control USP1 function (Figure 1.11). Growing evidence suggests that the activity of USPs is tightly regulated through their interaction with other proteins. The enzymatic activity of USP1 alone is very low and is greatly increased upon interaction with USP1-associated factor 1 (UAF1)[128]. UAF1 contains 677 aminoacids and harbors eight potential WD40 repeats in the N-terminal region and a predicted coiled-coil domain in the C-terminal portion. UAF1 binding induces a conformation change of USP1, raising its activity by stabilizing it and leading to an increment in the monoubiquitinated form of FANCD2 and PCNA[129]. Other two DUBs, USP12 and USP46 are able to bind UAF1 and they are governed by this interaction[130]. Another way to control USP1 activity is to expose cells to genotoxic agent, such as UV light. As a result, USP1 is auto-cleaved at an internal diglycine motif (Gly670-Gly671)[115]. The upshot of the autocleavage is the generation of an amino-terminal fragment (USP1NT) and a shorter carboxy-terminal fragment (USP1CT). Unexpectedly USP1 autocleavage is still enzymatically active despite is destroyed its His box catalytic motif; this could be explained because $USP1_{NT}$ and $USP1_{CT}$ fragments may be held together by UAF1 forming a catalytically competent ternary complex[128]. In addition,

reactive oxigen species (ROS) induce a reversible inactivation of USP1, that is because inactivation of DUBs by ROS results from the oxidation of their catalytic cysteine residue[131].

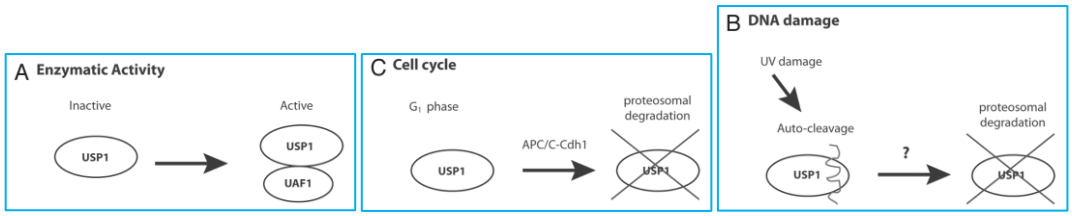

Figure 1.11 Multiple mechanisms regulate USP1 activity. (A) USP1 requires the association of UAF1 for its full enzymatic activity and protein stability. **(B)** Upon UV DNA damage, USP1 is auto-cleaved and degraded by the proteasome. **(C)** APC/CCdh1 binds to and degrades USP1 during the G1 phase of the cell cycle. Figure adapted from[132].

Phosphorylation at Ser313 by cyclin-dependent kinases (CDKs) is anhoter regulatory mechanism of USP1. Ser313 is placed whitin USP1 dragon motif and its phosphorylation is important to regulate cell cycle dependent degradation of USP1. Therefore, during M phase CDK1 phosphoryletes Ser313 enhancing USP1 stability and preventing its degradation by the anaphase-promoting complex/cyclosome[132]. On the other hand, Villami and his group has reported that Ser313 phosphorylation in USP1 is essential for its interaction with UAF1 and for the stimulation of its activity. In this study they mapped a domain of UAF1 interaction (amino acid 235-408) and this interaction is mediated by Ser313 phosphorylation[133]. In contrast with this work, Garcia-Santisteban and his team has mapped a different UAF1-binding site in USP1 which not contains the Ser313[134]. USP1 is also regulated in a cell-cycle-dependent manner. Two ubiquitin E3-ligase complexes, SCF (Skp1/CUL1/F-box protein) and APC/C (Anaphase Promoting Complex/Cyclosome), control the timely transitions of cell cycle phases by promoting the degradation of many key cell cycle regulators. SCF complex mainly functions in G1, S and early M phases, whereas APC/C

regulates mitosis including metaphase-anaphase transition and mitotic exit and maintains G1 phase. APC/C is a large complex (1,5 MDa complex) regulated by the binding of one of its activators: Cdc20 and Cdh1. The former is required for metaphase to anaphase transition, the latter is liable of the degradation of positive regulators of mitosis and S phase and it is the main player of the G_1 phase. In a study of Huang's group has been explored the levels of USP1 protein during cell cycle progression. It revealed that during G1 phase, USP1 is targeted for degradation by APC/C-Cdh1 to assure that USP1 levels are kept in check before S phase entry, otherwise, the levels of USP1 co-factor UAF1/WDR48 that remain stable for the whole. In fact, silence of Cdh1 expression in both synchronized T98G and U2OS cells induces an accumulation of USP1 due to its stabilization. Moreover, Huang's group have shown that G1-stabilized USP1 is still catalytically active. Low levels of USP1 define a permissive environment and enable a robust PCNA monoubiquitination during G1 phase, if required. During M phase Cdk1 is active and phosphorylates USP1 on Ser313. Since this residue is placed whith in the region of interaction with Cdh1, its phosphorylation prevents the interaction with Cdh1 and its degradation. In addition, this phosphorylation, as reported before, can serve for interact with its co-factor UAF1. Therefore, phosphorylation performes both a protective and an activation function, because protects USP1 from degradation and enhances the binding with UAF1. During mitosis Cdh1 is inhibited by Cdk phosphorylation, thus it can not promote degradation of its substrates. In the later mitotic stages, Cdh1 is de-phosphorylated and becomes active. Once cells enter the G1 phase, Cdk activity is low if not absent, therefore USP1 dephosphorylated is then exposed to degradation by APC/C^{Cdh1}. In conclusion, the USP1 regulation during cell cycle progression has two concequences: it allows PCNA mono-ubiquitination and TLS polymerase recruitment, thus promoting DNA repair; further, low levels of USP1 during the G_1 lead to degradation of ID proteins by APC/C^{Cdh1} and an accumulation of p21. In the absence of DNA damage, p21 is able to inhibit PCNA during the G_1 phase by controlling PCNA-interacting TLS polymerases. At the G_1/S, APC/C^{Cdh1} activity

is inhibited and promotes the accumulation of APC/C substrates including USP1 and perhaps, ID proteins. As a concequence, in the absence of DNA damage and during S phase, USP1 stabilizes ID proteins and represses p21 which is no longer able to suppress TLS activity. Therefore, USP1 prevents aberrant error-prone TLS polymerase usage in the absence or presence of DNA damage (Figure 1.12).

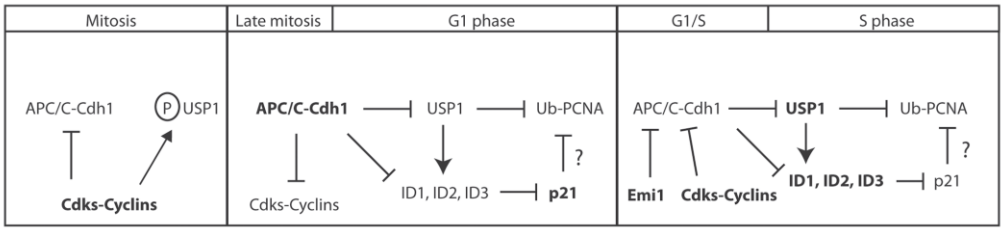

Figure 1.12 Model showing how USP1-mediated events are regulated during normal cell cycle progression. Schematic diagram of the proposed model of how different cell cycle stages can affect USP1 protein stability, regulation of ID proteins and PCNA-directed DNA repair. Briefly, in M phase, both USP1 and APC/C^{Cdh1} are phosphorylated by Cdks, which prevents USP1 from being prematurely targeted for degradation by the APC/C^{Cdh1}. In late M and early G_1, USP1 and APC/C^{Cdh1} become dephosphorylated, leading to the degradation of both USP1 and cyclins. USP1 normally protects ID proteins from ubiquitin-mediated degradation. However, without USP1, ID proteins become subsequently degraded. Loss of ID proteins prevents transcriptional repression of p21, leading to p21 protein accumulation and possible inhibition of TLS activity on PCNA. During the G_1-S or S-phase entry, levels of cyclins rise to inhibit APC/C^{Cdh1}, which lead to the accumulation of USP1 and presumed stabilization of ID proteins. Figure adapted from[132].

Finally, another way to stabilized USP1 is through Calpain activity. Calpain is an intracellular Ca^{2+}-dependent cysteine protease. Ubiquitous microcalpain (μ-calpain) and millicalpain (m-calpain) are heterodimers composed of catalytic subunits (CAPN1 and CAPN2*)* and a regulatory subunit (CAPNS1). A proteomic approach was necessary to identify USP1 deubiquitinase as a CAPNS1-interacting protein by supporting a role of CAPNS1 in maintaining USP1 protein stability expcially in late G_1 phase in a cdh1- and Cdk5/p25-dependent manner[135]. In CAPNS1 depleted cells, the engagement of USP1 in APC/ C^{cdh1} complex is enhanced, in fact in U20S cells this binding was efficiently

demonstrated[135]. However, another way to stabilized USP1 is through a Calpain cleavage at the very N terminus. In the absence of the stabilizing cleavage exerted by calpain, USP1 interacts with cdh1 and is more subjected to ubiquitination by APC/C^{cdh1} (Figure 1.13).

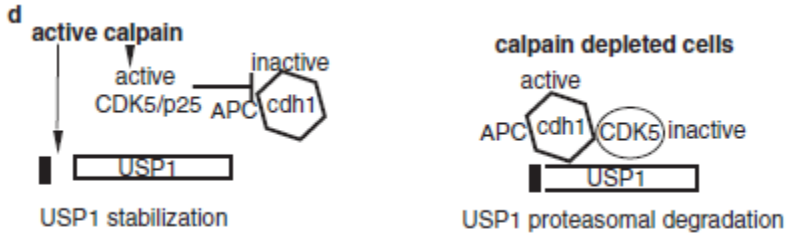

Figure 1.13. Calpain acts as a brake against APC/C$_{cdh1}$-dependent proteasomal degradation of USP1. Working model: Active Calpain cleaves USP1 at very N terminus. generating a product less susceptible to APC/Ccdh1 interaction or ubiquitination. In addition, Calpain actives Cdk5/p25, which in turn inhibits APC/Ccdh1, preserving USP1 stability. When calpain is off, Cdk5 is inactive and USP1 is ubiquitinated by APC/Ccdh1 and degradated by the proteasome. Figure adapted from[135].

1.2.3.2 USP1-regulated pathways

Various studies emphasised the role of USP1 in several important steps of the DNA damage response, mainly in the Fanconi anemia (FA) pathway[128, 136] and in the process of translesion synthesis (TLS)[137]. In addition, USP1 plays a part in cellular differentiation[126] (Figure 1.14).

The Fanconi Anemia pathway Fanconi anemia (FA) is a rare autosomal or X-linked recessive disease characterized by hypersensitivity to DNA crosslinking agents, chromosomal instability and cancer susceptibility. Clinically, FA is characterized by childhood onset aplastic anemia, increased cancer/leukemia susceptibility and developmental defects. To date, 15 genes governing FA pathway and active in the DNA repair have been identified[138]. In response to genomic damage, eight FA proteins form a nuclear complex (the FA core complex) which appears ubiquitin E3 ligase activity and monoubiquitinates

FANCD2 and FANCI that form foci at the presumed sites of DNA damage. Cell cycle synchronization studies indicate that FANCD2 is monoubiquitinated at the G1/S phase, remains monoubiquitinated throughout S phase, and becomes deubiquitinated at the end of S phase when the synchronized cell population enters G2[139]. During DNA replication, in the S phase of the cell cycle, DNA polymerases copy the DNA at the level of several replication forks, whereas in presence of lesions in the chromatin structure, DNA polymerases suppresses its activity. In front of this condition, the FA pathway is activated and colocalizes with replication foci containing BRCA1, RAD51 and PCNA proteins. These foci are believed to represent sites of homologous repair. Replication fork stands still and facilitates a DNA repair response[140].

Deubiquitination takes a crucial role in FA pathway regulation. Relevant studies have revealed that upon silencing of USP1, the monoubiquitinated form of FANCD2 increases similarly after mytomicin C (MMC) treatment[141]. Additionally, *Usp1* -/- mice present a strong similarity to FA mice (small size, infertility, mitomycin C hypersensitivity, and chromosome instability)[142]. These results confirme that USP1 has a regulatory role in the FA pathway.

PCNA and the translesion synthesis Proliferating Cell Nuclear Antigen (PCNA) is a homotrimeric protein complex that forms a ring around double-stranded DNA. Its activity has a central role in orchestrating the association of replication factors during DNA replication and, repair of DNA damage[143]. During normal replication, PCNA operates as a processivity factor to help the replicative DNA polymerases tying the DNA template. In presence of a lesion, the DNA replication machinery stands still and the DNA damage responses is being activated. This allows the DNA replication through an "error prone pathway" termed translesion DNA synthesis (TLS) where alternative low fidelity DNA polymerases are utilized to replicate the damaged DNA template. Unlike the high-fidelity DNA polymerases, TLS polymerases (Polη, Polκ, Polι and Rev1) are non-processive, lack any proofreading capability and are capable to cause damage-induced mutations[144]. During DNA damage, RAD6/RAD18 or $CLR4^{Cdt2}$ can directly monoubiquitinate PCNA recruiting Polη to interact with

the monoubiquitinated form of PCNA and once synthesis through the lesion has been completed, Polη is removed from the replication fork through a degradation mechanism. After DNA damage is overcome, PCNA is deubiquitinated. The work of $CRL4^{Cdt2}$ is constitutively antagonized by the deubiquitinating enzyme USP1[145]. In absence of DNA damage, USP1 limits the accumulation of monoubiquitinated PCNA avoiding mutagenesis. On the contrary, upon DNA damage that determines a downregulation of USP1, monoubiquitinated PCNA accumulates [115]. Moreover, another DUB(s) USP7 plays a part in the suppression of monoubiquitinated PCNA mainly in the repair of H_2O_2-induced DNA lesions and throughout interphase[146]. Notably, USP7 regulates PCNA ubiquitination in two modes: one is stabilizing RAD18 and the other is downregulating PCNA. This suggest that cells are able to choose the appropriate DUB(s) depending on the type of DNA lesion and cell cycle.

USP1 deubiquitinates ID proteins Basic-helix-loop-helix (bHLH) transcription factors are essential regulators of development and differentiation. DNA binding of bHLH proteins is restricted by interaction with inhibitor of DNA-binding proteins named IDs proteins. This family of protein includes four members, ID1, ID2, IID3 and ID4 and have a key role for mammalian development[147]. Proliferative tissues contain high levels of IDs proteins, otherwise they are low in differentiated tissues, suggesting that IDs protein might maintain "stemness"[148]. A large numer of tumors display elevated ID protein levels[149]. The stability and the abundance of IDs depend on to the activity of APC/C-^{Cdh1} complex[150]. A study led by Dixit and colleagues have proved that ID1, ID2 and ID3 are deubiquitinated by USP1 and therefore USP1 protects ID proteins from proteasome degradation. Accordingly, ID proteins and USP1 are overexpressed in human osteosarcomas suggesting that USP1 overexpression is necessary for the proliferation of several osteosarcoma cell lines, but it is also sufficient to prevent normal mesenchymal cell. Mainly ID2 or USP1 overexpression in mesenchymal stem cells inhibit differentiation and preserves mesenchymal stem cell features[126].

1.2.1 The role of ubiquitin modifications in autophagy regulation

Post-translation modifications play a multiple role in autophagy regulation. In fact ubiquitination of the autophagy-related-proteins (Atg) occurs during different stage of autophagy[14].

Several ubiquitination enzyme act by modifying the initiators of autophagy, for example TRAF6 catalyzes K63-linked polyubiquitination of mTOR complex 1 and hence its activation[151]. Moreover, TRAF6 promotes K63-linked polyubiquitination of ULK1 through Ambra1 and thus autophagy induction[18]. Antonioli et al. have demonstrated that under normal conditions, the mTOR inhibitor DEPTOR is ubiquitinated by CUL5, causing its degradation and mTOR activation[152,153].

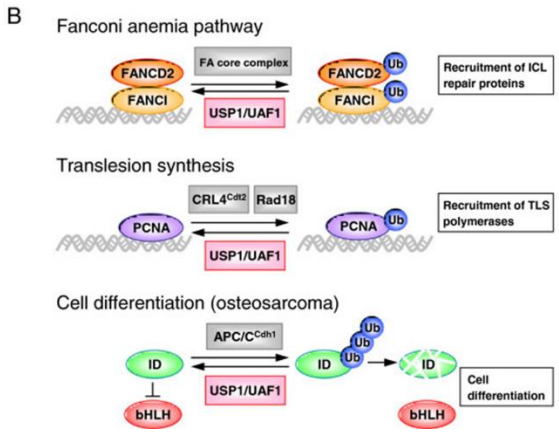

Figure 1.14 Models illustrating the role of the USP1/UAF1 complex as regulator of three different cellular processes. In the Fanconi anemia (FA) pathway (upper panel), the FA core complex monoubiquitinates FANCD2 and FANCI, which mediate the recruitment of other proteins that repair DNA interstrand crosslink (ICL) lesions. USP1/UAF1 antagonizes the FA core complex deubiquitinating FANCD2 and FANCI. In the process of translesion synthesis (TLS) (middle panel), monoubiquitinated PCNA recruits specific TLS DNA polymerases that may bypass DNA lesions but have lower fidelity than replicative polymerases. USP1/UAF1 may prevent unscheduled recruitment of low fidelity TLS polymerases by deubiquitinating PCNA. Finally (lower panel), USP1/UAF1 contributes to the maintaince of the undifferentiated state of osteosarcoma cells by promoting deubiquitination and stability of ID proteins, which, in turn, negatively regulate differentiation-inducing bHLH transcription factors. Figure adapted from [132].

Beclin1 is an autophagic protein important for the nucleation step of the process and its activity can be regulated by ubiquitination. For instance, TRF6 can encourage the separation of Beclin1 and Bcl2 through K63-linked polyubiquitination of Beclin1 and consequently activates autophagy[154]. On the contrary, Nedd4 works as a negative regulator of autophagy by promoting Beclin 1 degradetion via K11-linked polyubiquitination[155]. The termination of autophagy is also governed by many ubiquitination events. Lately, it has been shown that KLHL20/CUL3 function has a key function in autophagy termination since it leads to ULK1 ubiquitination and then its degradation. In addition, KLHL20/CUL3 regulates the turnover of VPS34 and Beclin1, promoting their degragation[156]. Additional to CUL3, others Cullin proteins are crucial for autophagy regulation. DDB1/CUL4, in normal conditions, keeps Ambra1 at low level by promoting its degradation. Otherwise, upon starvation, CUL4 frees Ambra1 which inhibits CUL5 that can not control DEPTOR degradation[152]. Ubiquitination is a degradation signal for selective autophagy processes in fact, ubiquitinated cargo is recognised by adaptor proteins such as p62, NRB1, NDP52, HDAC6 and OPTN, which lead the cargo to the lysosomal degradation[157].

1.2.2 The role of deubiquitinating enzymes in autophagy regulation

Several examples show that deubiquitinating enzymes participate to autophagy regulation and can act at different steps of the process. The deubiquitinase A20, is involved in autophagy regulation by controlling the stability of Beclin 1. Indeed A20 antagonized the activity of TRAF6 and hydrolysed the bond between ubiquitin and Beclin 1, thus allowing the dissociation of its inhibitory factor Bcl2 and enhancing autophagy[154]. USP13 and USP10 are others two DUBs essential to regulate the early events of autophagy process through the deubiquitination of Beclin1-Vps34 complex[158]. An additional possible link between USP10 and autophagy is its role in p53 stabilization, because USP10 is known to stabilyze cytosolic p53. Few years ago, Tripathi et al. discovered an important relationship between the apoptotic and autophagy pathways,

permitted by p53 and Beclin 1 interaction[159]. Recently, USP19 has been proposed as a positive regulator of autophagy because it stabilizes Beclin1 by removing the K11-linked ubiquitin chain[160]. In the contest of mitophagy, USP8 supports mithopagy by stabilizing the E3 ligase Parkin. Parkin ubiqutinates proteins of the outer mitochondrial membrane, which tie the autophagy-receptor p62 in order to be engulfed by autophagosomes and transported to the lysosome[161,162]. Athers three DUBs, USP15, USP30 and USP35 contribute to regular mitophagy through deubiquitination of mitochondrial targets of Parkin, thus preventing the uptake into autophagosome. Knockdown of USP15 can restore the mitophagy defects of PD patient fiboblasts[163] and the reduction of USP30 activity can anhances mitophagy in neurons[164], suggesting that both DUBs could represent a possible target for a therapeutic strategy for Parkinson's disease. Finally, USP36 has a role in the regulation of selective autophagic degradation of protein aggregates[165].

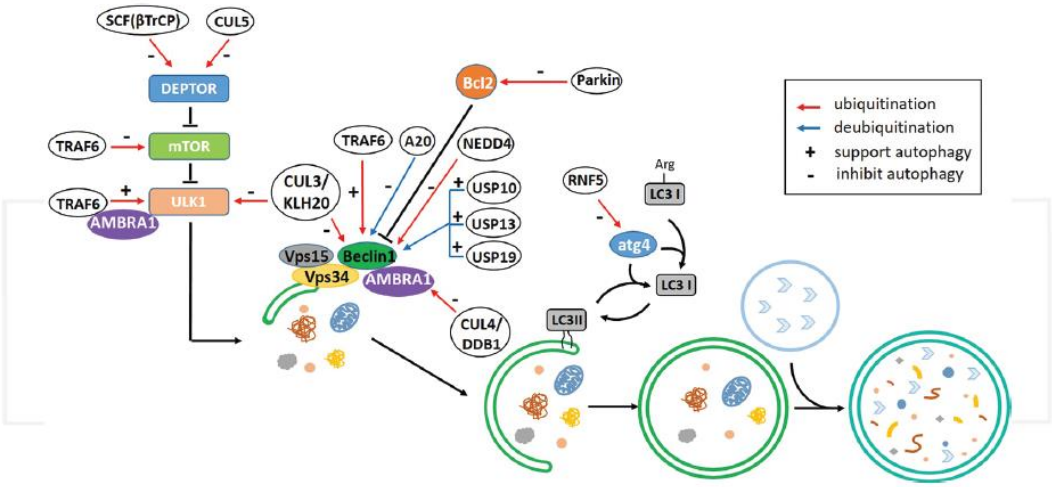

Figure 1.14 Functional role of ubiquitin-related enzymes (E3 ligases and DUBs) in autophagy regulation. An overview shows the involvement of the ubiquitination events during different steps of autophagy. Ubiquitination modifications by E3 ligases are shown in red arrows, and deubiquitination by DUBs are shown in blue arrows. "+" indicates that enzymes play positive regulatory roles (USP10, USP13, and USP19), and "–" indicates those thought to play negative roles ($SCF_{\beta TrCP}$, CUL5, CUL3/KLH20, A20, NEDD4, CUL4/DDB1, Parkin, and RNF5) in autophagy. TRAF6 can function as positive or negative regulator in autophagy via ubiquitination modification of different substrates.

2. AIM OF THE THESIS

The interplay between DUB enzymes and autophagy has not been fully explored. Only recently, a certain number of DUB enzymes have been identified as playing a role in this process. Stork and colleagues, using a selective DUB inhibitor (WP1130), discovered that this compound leads to the recruitment of ULK1 to aggresomes. This relocalization is coupled to an increased ubiquitination status of ULK1[166]. The human genome encodes 79 DUBs which are subdivided into 5 subfamilies. One or more WP1130 targets exhibited a sharp effect on the regulation of ULK1 and autophagy. The purpose of this project is to look at the functions of USP1 (a major topic of interest in our laboratory) within the autophagic pathway and to investigate whether its inhibition may represent a strategy against cancer cells that require autophagy for survival.

Based on the literature mentioned above, the following hypotheses were verified in the study:

- USP1 is an upstream player of autophagy. We planned to analyze the effect of USP1 silencing on autophagic induction and degradation.
- USP1 allows the transfer of ULK1 to aggresome similar to WP1130 by both immunoblotting and by immunofluorescence followed by confocal microscopy.
- The investigation of the role of USP1 in the regulation of ULK1 kinase activity. We sought to explore the phosphorylation status of ATG13 by immunoblotting.

The results present in this work are reported in the following manuscript:

"Raimondi M, Cesselli D, Di Loreto C, La Marra F, Schneider C and Demarchi F. *Ubiquitin specific peptidase 1 targets ULK1 and regulates its cellular compartmentalization and autophagy"*. Manuscript submitted for publication.

3. MATERIALS AND METHODS

3.1 Chemicals and reagents

Bortezomib was purchased from Cell Signaling Technology, Rapamycin, Pepstatin A, E64D, Leptomycin B and Pimozide were bought from Sigma-Aldrich. Lipofectamine RNAiMAX was bought from Invitrogen and Mirus *Trans*IT- LT1 was purchased from MirusBio. *USP1*-specific small interfering RNA (siRNA) was purchased from Eurofins MWG Operon.

All drugs were made up fresh for each experiment and diluted to the appropriate concentration with appropriate medium prior to use.

3.2 Cell culture

U2OS cells were obtained from ATCC and recently authenticated. They were grown in DMEM low glucose (Lonza), supplemented with 10% foetal calf serum (FCS), 1% penicillin/streptomycin (Lonza) and L-glutamine. HEK293 and MEF cells were cultured in DMEM high glucose supplemented with 10% FCS, 1% penicillin/streptomycin. MCF10AT cells were cultured in DMEM (high glucose): Ham's F12 media (1:1) supplemented with 10mg/ml Insulin (Sigma), 20ng/ml EGF (PEPROTECH), 500ng/ml hydrocortisone (Sigma), 5% horse serum, 1% penicillin/streptomycin and 1% HEPES (Gibco). MDA-MB231 and MDA-MB468 were grown in DMEM (high glucose) supplemented with 10% FBS, 1% Penicillin/Streptomycin. BT459 cells were grown in RPMI supplemented with 10% FBS and 1% Penicillin/Streptomycin. All cells were grown in 5% CO_2 at 37^0 C in a humidified incubator. Cells were passaged at a frequency of every 2-3 days. After media was aspirated from the flask or culture dishes, 10ml of PBS were added to the cells to wash them and it was then aspirated. 1% trypsin was added to the flask/dish for approximately 5 minutes at 37°C to detach the cells. Following trypsinisation pre-warmed fresh media was immediately added to the dissociated cells to neutralise trypsin reaction. The cell suspension was then centrifuged at 1000 rpm for 5 minutes at room temperature. After discarding the supernatant, the cells were resuspended in pre-warmed culturing medium

and after their counting, a certain volume with the desired cell number was seeded into new flask/dish.

Cryo-freezing was routinely used for long term deposit of cell lines. Cells were trypsinised and centrifuged at 1000 rpm for 5 minutes at room temperature. The medium/trypsin solution was removed and the cell pellet was resuspended in a solution consisting of 90% FCS and 10% dimethylsulphoxide (DMSO). Cells were aliquoted into cryo-tubes and frozen at -80°C. For longer term storage, the cryotubs were placed in liquid Nitrogen at -180°C.

3.3 Transient plasmid DNA transfection

U2OS and HEK293 cells at 60-80% confluency, were transiently transfected using TransIT-LT1 transfection reagent (Mirus) according to the manufacturer's instructions. All transfections were balanced with empty p3Xflag vector or with empty pEGFP-N1 vector. Plasmids were aliquoted into 300 µl Opti-MEM (gibco) and transfection reagent was added at a ratio of 1µg DNA: 3 µl transfection reagent. Complexes were left to equilibrate at room temperature for 20 minutes and then added onto the cells.

Plasmids encoding for tagged USP1 (Flag-USP1 and GFP-USP1) and encoding for mutated form of USP1 (GFP-USP1 C90A), together with Flag-UAF1/WR48 were kindly provided by Dr. T. Huang. Plasmid encoding for wild type ULK1-HA was generously provided by S. A. Tooze (Crick Institute, London).

3.4 Transient siRNA knockdown of mammalian cells

U2OS and HEK293 cells were subject to RNA interference using small interfering RNA (siRNA), by reverse transfection using Lipofectamine™ RNAiMax (Invitrogen) in according to the manufacturer's protocol. All siRNAs were used at a final concentration of 20 nM (Table 3.1). As a negative control, a siRNA which does not affect gene expression within the cells was used and termed scrambled siRNA.

Briefly, scrambled siRNA. and siRNA against each proteins target were transferred into 300 µl of basal media Opti-MEM, mixed with Lipofectamine™

RNAiMax and left 30 minutes for equilibration, prior to plating onto 6-well plates. About 1.5 x 10^5 cells were then seeded onto each well of the plates containing the transfection mixtures in 2 ml steroid-depleted media. Non-transfected (NT) controls were included containing only basal media and Lipofectamine™ RNAiMax.

Target	siRNA sequence
USP 1 a	5'AACCCUAUGUAUGAAGGAUAU3'
USP 1 b	5'ATGTGGCAGAATTACCTACTA3'
USP 1 c	5'CTGGGACCCATGAATCTGATA3'
ULK 1	5' CGCAUGGACUUCGAUGAGUUU3'

Table 3.1 Sequence of siRNAs used to knockdown target genes.

3.5 Protein expression analysis

3.5.1 Cell lysis and protein extraction

In order to analyse the proteins of interest, the cells need to be lysed. Therefore, a buffer containing 50 mM Tris-HCl pH 7.5, 150 mM NaCl, 5 mM EDTA, 1% Triton X-100, 0.5 mM NaF, 1 mM Sodium orthovanadate was prepared immediately prior to use and samples were processed keeping them on ice. Protease and phosphatase inhibitor cocktails were added immediately prior to use. When specified, nuclear and cytoplasmic extracts were prepared using nuclear and cytoplasmic extraction reagents (ThermoScientific), according to manufacturer instructions. Equal cell number ciming from different treatment conditions was washed twice with ice cold PBS and lysis buffer was added directly onto the cells and incubated for a few minutes. Using a cell scraper, cells were scraped from the culture flask, collected from plates and then transferred to 1.5mL eppendorf tubes and leave for 15mins in rocking at 4^0C. Subsequently, lysates were centrifuged at maximum speed for 15 minutes at

4^0C and supernatants containing total protein were transferred to new microcentrifuge tubes, mixed with 6X electrophoresis loading buffer (120 mM Tris-HCl pH 6.8, containing 4% SDS, 50% glycerol, 0.1% bromophenol blue, 10% mercaptoethanol), boiled for 5 min. and stored at -80°C until use.

3.5.2 Protein quantification

Protein concentration was measured using the Bradford protein assay. The Bradford assay is very fast. Briefly, the principle of this assay is that the binding of protein to Coomassie dye under acidic conditions, results in a color change from brown to blue. This method measures the presence of the basic amino acid residues, arginine, lysine and histidine, which contributes to the formation of the protein-dye complex. The protein concentration was calculated by interpolating absorbance values on a standard curve built by measuring known amount of bovine serum albumin. Absorbance was then measured at 595 nm.

3.5.3 Electrophoresis (SDS/PAGE)

Protein samples and marker were first thawed on ice. Based on the concentrations calculated from the Bradford protein assay, 30 µg of the protein samples were diluted using 6X loading buffer. Samples were vortexed and then heated at 95 ^{0} C for 5 mins to denature the proteins.

3.5.4 Membrane transfer and Immunolabelling

After SDS-PAGE separation, the proteins were transferred from the gel to on a nitrocellulose membrane by applying an electric field. In this way, a copy of the protein pattern that was originally in the polyacrylamide gel is obtained. To verify the efficiency of the proteins, transfer onto the membrane, the transfer membrane was stained with 0.1% Ponceau S for few minutes and then washed with distilled water to visualize the blot. Subsequently the membrane was first blocked with 5% non-fat milk in 1x PBS-T or 5% BSA solution in 1x TBS-T, (depending on the antibody of interest), for 1 hour at room temperature. Primary antibodies were prepared in non-fat milk or BSA solution in 1x TBS-T.

The final concentration depended on the individual antibody as indicated in the table 3.2. The membrane was incubated with the primary antibody at 4°C overnight in a cold room on a level shaker. Then the membrane was washed 3 times for 5 minutes each in 1x PBS-T or 1xTBS-T. The secondary antibody was prepared using non-fat milk or BSA solution in 1x TBS-T. The secondary antibodies used for western blot were labeled with the enzyme horseradish peroxidase (HRP). After on incubation of 45 minutes wiith the secondary antibody, the membrane was washed 3 times for 5 minutes each in 1x TBS-T or 1x PBS-T and analyzed by enhanced chemiluminescence.

Antibody	Host	Manufacturer	Catalugue number	Clone number	Western dilution
α-SH3GLB1	Mouse	Novus Biologicals	NBP2-24733	30A882.1.1	1:1000
α-Flag	Mouse	Sigma	F3165	M2	1:1000
α-ACT	Rabbit	Sigma	A2066		1:10000
α-WDR48 1	Rabbit	Sigma	HPA038421		1:1000
α-VIM	Mouse	BD Transduction Laboratories	550513	RV202	1:1000
α-SQSTM1	Mouse	BD Transduction Laboratories	610832	3	1:1000
α-pULK1 Ser555	Rabbit	Cell Signaling Technology	5869	D1H4	1:1000
α-Ubiquitin	Mouse	Cell Signaling Technology	3936	P4D1	1:1000
α-USP1	Mouse	Bethyl Laboratories	A301-699A		1:1000
α-Myc-Tag	Mouse	Cell Signaling Technology	2276	9B11	1:1000
α-ULK1	Rabbit	Santa Cruz	sc-33182	H-240	1:1000

		Biotechnology			
α-HDAC6	Rabbit	Santa Cruz Biotechnology	Sc-11420	H-300	1:1000
α-BECN1	Rabbit	Santa Cruz Biotechnology	sc-11427	H-300	1:1000
α-HA-Tag	Mouse	Santa Cruz Biotechnology	sc-805	Y11	1:1000
α-Hsp90	Mouse	Santa Cruz Biotechnology	Sc-13119	F-8	1:10000
α-FANCD2	Mouse	Santa Cruz Biotechnology	sc-20022	FI17	1:1000
α-TUB	Mouse	Merck Millipore	05829	DM1A	1:10000
α-GFP	Rabbit	home made			1:1000
α-MAP1LC3A	Rabbit	home made			1:1000
α-Ubiquitin K63	Rabbit	Merck Millipore	05-1308	Apu3	1:1000

Table 3.2 Details of antibodies used in Western blotting studies.

3.6 Immunoprecipitation

Immunoprecipitation was performed to examine interactions between proteins of interest in mammalian cells. Whole-cell extracts were prepared after transfection or treatment with appropriate drugs. Briefly, cells were grown to approximately 60% confluency on 90 mm dishes in serum-containing media prior to collection by scraping into IP lysis buffer (50 mM Tris-HCl pH 7.5, 150 mM NaCl, 5 mM EDTA, 1% Triton X-100, 0.5 mM NaF, 1 mM Sodium orthovanadate and Protease and phosphatase inhibitor cocktails were added immediately prior to use). Cells were incubated at 4^0 C with gentle agitation for 30 minutes. Following lysis, samples were centrifuged for 10 minutes at 13000 rpm to pellet cell debris. Resultanting supernatants were then separated into a 100 µl input and 400 µl extract. The input sample was stored at -80^0 C until and

used to examine expression levels of proteins of interest in the whole cell extract, after IP procedure completation. Samples and extracts were precleared by incubation with Protein G/A Sepharose (PGS; GE Healthcare Life Sciences) for 30 minutes at 4^0 C with gentle agitation and centrifuged for 5 minutes at 5000 rpm to remove PGS. Abuot 2 μg of specific antibody were added to each of the sample tubes and incubated overnight at 4^0 C with agitation. Subsequently an appropriate amount of PGS was added to the samples and incubated for 2 hours at 4^0 C. Beads were then washed three times with lysis buffer, and immunoprecipitates were eluted with 2× SDS Loading Buffer (62.5 mM Tris-HCl pH 6.8, 2% SDS, 10% glycerol, 5% β- mercaptoethanol, 0.05% bromophenol blue) and resolved by SDS–PAGE.

3.7 Triton-soluble and -insoluble fractionation

Cells were lysed on ice in the above-mentioned lysis buffer. After centrifugation at maximum speed for 15 minutes at 4°C, the supernatant was collected and it was considered the Triton X- 100–soluble fraction. After the first extraction, the pellets were solubilized in the same volume of SDS sample buffer (62.5 mM Tris-HCl pH 6.8, 2% SDS, 10% glycerol, 5% β- mercaptoethanol, 0.05% bromophenol blue) and heated to 95^0 C for 5 min, or in the above-mentioned lysis buffer supplemented with 5M urea. Equal amount of protein from soluble fractions, and the corresponding volume of insoluble fractions were processed as described above.

3.8 Confocal microscopy analysis

Immunofluorescence (IF) is a common laboratory technique that allows the visualization of a specific protein or antigen in cells or tissue sections, by its binding to a specific antibody chemically conjugated with a fluorescent dye. Immunofluorescence stained samples were examined under a fluorescence microscope or confocal microscope. Cells were plated on sterile coverslips,

cultured under the conditions indicated and fixed with 3% paraformaldehyde for 20 min. For immunofluorescent staining of endogenous ULK1, SQSTM1/p62, LAMP2 and MAP1LC3A, BECN1 and HDAC6, after fixation, the cells were permeabilized with digitonin (50 µg/µl) for 10 min and blocked by incubation with 5% bovine serum albumin in PBS for 1 hour at room temperature, followed by incubation with the primary antibodies for 2 hours at 37°C. Cells were then incubated with the secondary antibody for 1 hour at 37°C. Then, the slides were washed 3 times with 1X PBS and nuclei were stained with 1 mg/ml Hoechst. After the Hoechst staining, cells were washed again with 1x PBS and coverslips were embedded in Mowiol 4-88. Images were acquired with LSM510 confocal microscope (Zeiss), and processed using ImageJ software, freely available on the net. The quantitative colocalization analysis was performed using JACoP (Just Another Co-localization Plugin) plugin in ImageJ program (NIH Image). For analysis, images of approximately 50 cells were taken in each experiment and 3 experiments were analyzed, bringing the total number of cells to 150 per determination. The value shown represents Pearson's coefficient. A linear equation describing the relationship between the intensities in two images is calculated by linear regression. The Pearson's coefficient provides an estimate of the goodness of this approximation. Its value can range from 1 to –1, with 1 representing complete positive correlation and –1 a negative correlation; zero represents no correlation.

3.9 Immunohistochemistry

Eight tissue microarrays (TMA) have been constructed by incorporating 95 formalin-fixed paraffin embedded (FFPE) breast cancer tumors (24 Luminal A, 24 Luminal B, 23 HER2 and 24 Triple Negative) that were retrieved from the archives of the Department of Pathology of the University Hospital of Udine. The novo diagnosed, non-metastatic and not previously chemo-treated tumors were included in the TMA after revision, by two expert pathologists (CDL and FLM) of: tumor histotype, Elston-Ellis grading, tumor size (pT), lymph node involvement (pN), and molecular subtype. In this regard, on the basis of both

the expression of estrogen receptors (ER, clone SP1, Neomarkers), progesterone receptors (PR, clone PgR 636, Dako) and ki67 (clone Mib1, Dako), as assessed by immunohistochemistry, and of HER2 amplification, as evaluated by immunohistochemistry (HercepTest, Dako) and fluorescence in situ hybridization (PathVysion kit, Vysis, Abbott), breast cancers were classified as: Luminal A (ER+ and/or PR+, HER2-, Ki67<15%), Luminal B (ER+ and/or PR+, HER2-, Ki67≥15%), HER2 (ER-, PR-, HER2+) and Triple Negative (ER-, PR-, HER2-). TMA were constructed by GALILEO CK4500 instrument. Specifically, 3 cores of 1 mm representative of the lesion were collected from each block. 4µm-thick FFPE sections were stained by immunohistochemistry for USP1 (rabbit polyclonal, Bethyl, 1:200) and homemade MAP1LC3A (rabbit polyclonal, 1:300). After heat induced epitope retrieval using EnVision™ FLEX Target Retrieval Solution, either low pH (LC3) or high pH (USP1), in PT Link (Dako). Dako EnVision+ Dual Link System-HRP (DAB+) detected primary antibodies and nuclei were stained by Gill Hematoxylin. For each tumor, USP1 and MAP1LC3A expression was quantified by two expert pathologists (CDL and FLM) adopting a semiquantitative approach (Histoscore method). Specifically, for each core it has been defined a score, ranging from 0 to 300, obtained by multiplying the percentage of labelled cells by the staining intensity (1=weak, 2=moderate, or 3=strong). For each tumor, the average value of the three respective cores was calculated.

3.10 Colony formation assay

U2OS cells ($1x10^3$) and MCF10AT cells ($5x10^2$) were seeded in 35 mm^2 dishes and incubate at 37^0 C in a humidified, 5% CO_2 atmosphere. Drug or solvent as a control were added 24 hours after seeding and after ten days in selective medium the plates were fixed with 3% paraformaldehyde for 20 minutes at room temperature and stained with 0.5% Crystal violet. Excess stain was removed by washing repeatedly with PBS and colonies were counted. For quantification, the colonies were analyzed using ImageJ software. Three reduplicate dishes were used from each condition.

3.11 Cell Viability Assays

The CellTiter-Glo® luminescent cell viability assay (Promega) determines the number of viable cells in culture based on quantitation of the ATP present, which is directly proportional to the number of cells present in culture. U2OS, MCF10A and MCF10AT were counted and 5000 cells for aech condition were resuspended in 100Ml of medium. The suspension was transferred to an opaque-walled 96 well plate and then, exposed to appropriate treatments of Bortezomib (50nM, Cell Signaling Technology) or Pimozide (2,5μM, Sigma-Aldrich) for 24 and 48 hours. Medium containing no cells was used as a background control. After the time indicated, cell viability was measured using the CellTiter-Glo® reagent. The plate weas equilibrated at room temperature for 30 mins and following 100μL of reagent (prepared according to the manufacturer's guidelines) was added to each well. The content of the plate was mixed for 2 mins on an orbital shaker and incubated at room temperature for 10mins. Following incubation, the signal was recorded by a luminometer.

3.12 WST-1 Cell Proliferation Assays

The stable tetrazolium salt WST-1 is cleaved to a soluble formazan by a complex cellular mechanism that occurs primarily at the cell surface. This bioreduction is largely dependent on the glycolytic production of NAD(P)H in viable cells. Therefore, the amount of formazan dye formed directly correlates to the number of metabolically active cells in the culture. MEF *Ulk1*$^{+/+}$ MEF *Ulk1*$^{-/-}$, MEF *Atg13*$^{+/+}$ MEF *Atg13*$^{-/-}$, were counted and 5000 cells for aech condition were resuspended in 100μL medium. The suspension was transferred to a 96 well plate and then, exposed to appropriate treatments of Bortezomib (50nM, Cell Signaling Technology) or Pimozide (2,5μM, Sigma-Aldrich) for 24 and 48 hours. Medium containing no cells was used as a background control. After the time indicated, cell proliferation was measured using the colorimetric Cell proliferation WST-1 reagent (SIGMA-ALDRICH). Cells were incubated with the WST-1 reagent for 4 hours. After this incubation period, the formazan dye

formed is quantitated with a scanning multi-well spectrophotometer (ELISA reader). The measured absorbance directly correlates to the number of viable cells.

3.13 11Statistical analysis

Quantification of immunofluorescence, cellular growth, viability and colony formation experiments are expressed as means ± standard deviations of at least three independent experiments. Indicated p values were calculated using two-tailed Student's t test or two-way ANOVA using Graphpad Prism software. For analysis of immunohistochemistry data, Fisher's exact test and Spearman's Rho were applied using Graphpad Prism software.

4. RESULTS AND DISCUSSION

4.1 USP1 stabilizes ULK1 in mammalian cells

The mammalian ULK1-ATG13-RB1CC1-ATG101 complex plays a central role in the initiating steps of autophagy. In recent years, several groups have sought to clarify the molecular regulation of this complex. To date, several papers have reported that ubiquitination plays an important role for ULK1 regulation[18,167]. Few years ago, Stork's group has shown that the treatment of cells with the DUB inhibitor WP1130 determines a reduction of ULK1 in the Triton X 100 soluble fraction in mammalian cells [166]. In order to investigate the functions of ubiquitin modification in ULK1 regulation, we depleted *USP1* using siRNAs, targeting three different regions of *USP1*. Both siRNAs efficiently inhibited the expression of endogenous USP1 in U2-OS cells (Figure 4.1A). Under basal condition, depletion of *USP1* remarkably reduced the total ULK1 protein level in the soluble fraction. Several groups have investigated the regulatory phosphorylation of ULK1 by upstream kinases[168,169]. Various studies demonstated that phosphor-Ser555 represent a major site for AMPK-dependent binding. Kim et al reported that AMPK-dependent phosphorylation and activation of ULK1 is stimulated by starvation[170]. Since the analysis of ULK1 phosphorylation is a suitable approach to investigate ULK1 activation, we next monitored the level of ULK1 p-Ser555 and we confirmed its reduction in the soluble fraction of *USP1* depleted cells (Figure 4.1A). This result was reproducible in various cell lines, such as U2-OS osteosarcoma cells, the human embryonic kidney cells (HEK293) and Ras-transformed human breast epithelial cells (MCF10AT) (Figure 4.1 A-F). Since the result on ULK1 was similar with all the *USP1* specific siRnas, we used *USP1a* siRNA for the remainder of the study. To further confirm the role of USP1 in ULK1 regulation, we overexpressed USP1 in U2-0S cell line and found that overexpression of USP1 significantly enhanced the amount of ULK1 and ULK1 p-Ser-555 in the soluble fraction, thus pointing to a potential stabilizing role of USP1 toward ULK1 (Figure 4.2A). To elucidate whether the catalytic activity of USP1 is essential

for its function in ULK1 regulation, we next transfected U2-0S cells with plasmid encoding wild-type or catalytically inactive USP1 mutant (C90S). As shown in Figure 4.2B-D, cells expressing wild-type USP1 display an enhanced accumulation of ULK1 and and ULK1 p-Ser-555 protein in the soluble fraction. By contrast, ectopic expression of C90S mutant failed to rescue the reduction of ULK1 and ULK1 p-Ser-555 in the soluble fraction (Figure 4.2B-D). These results suggest that USP1-mediated effect on ULK1 depends on its catalytic activity.

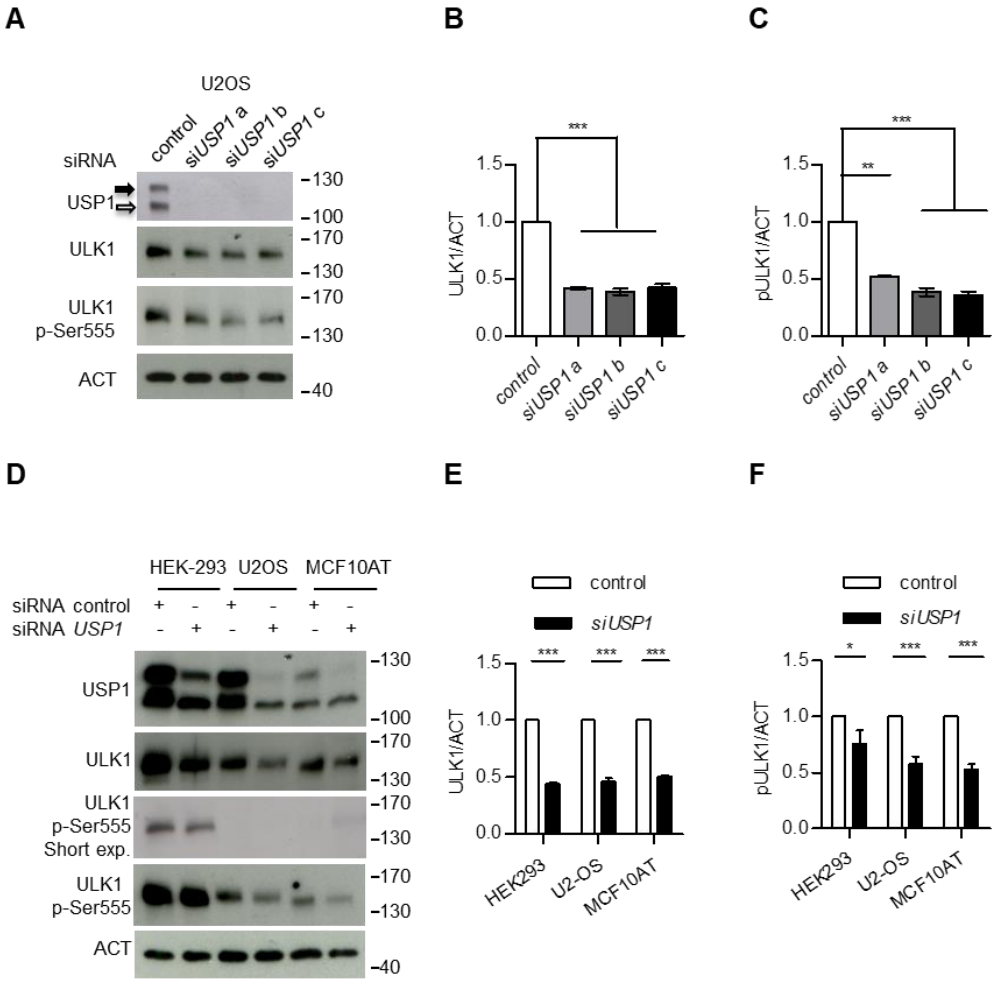

Figure 4.1. USP1 modulates ULK1 in mammalian cells. (A) U2OS cells were transfected with scrambled control siRNA or three different *USP1* specific siRNAs. The relative amounts of each protein were quantified using ImageJ. The ratio of p-ULK1/ACT and ULK1/ACT was calculated and indicated in the graphs **(B)** and **(C)**. **(D)** HEK293, U2-OS and MCF10AT cells were

transfected with scrambled control or *USP1*-specific siRNA. 72 hours later, samples were lysed in 1% Triton X-100 containing buffer and, the cleared lysates utilized to monitor endogenous ULK1 and ULK1 p-Ser555 protein levels by Western Blot. The relative amounts of each protein were quantified using ImageJ. The ratio of p-ULK1/ACT and ULK1/ACT was calculated and indicated in the graphs **(E)** and **(F).** Filled arrow indicates full length USP1; empty arrow indicates its autocleaved derivative.

Next, we investigated whether the decline of ULK1 protein level was caused by proteasomal degradation, as described for ID2[126]. However, a time course experiment with the proteasome inhibitor bortezomib, in USP1 depleted U2-OS and MCF10AT cells, did not abolish the reduction of ULK1, indicating that USP1 reduces ULK1 levels in the soluble fraction, without the action of the proteasome (Figure 4.2 E-L). Several studies have shown that the proteasome inhibitor bortezomib promotes apoptotic cell death. In other cell types, bortezomib has also been shown to promote autophagy. Interestingly, using this approach, in U2-OS control cells and after 6 hours of treatment, ULK1 protein levels are downregulated. This date, as stated in a recent work of Cecconi's groutp, confermes that autophagy is an oscillatory process. In basal conditions, the ULK1 complex is maintained in an inhibited state by MTOR. During the early phase of autophagy induction, ULK1 is activated by both phosphorylation and regulatory ubiquitination; in enduring starvation, NEDD4L promotes ULK1 degradation by the proteasome, while *ULK1* mRNA is actively transcribed. During prolonged starvation, MTOR is reactivated and *ULK1* mRNA is translated and then inhibited again by MTOR, preventing excessive autophagy. When a new stimulus occurs, the system is thus ready for a new round of autophagy. However, unlike U2-OS cells, in MCF10At cells, after 6 hours of treatment, ULK1 protein levels don't change, suggenting that ULK1 turnover has different time between the two cell lines.

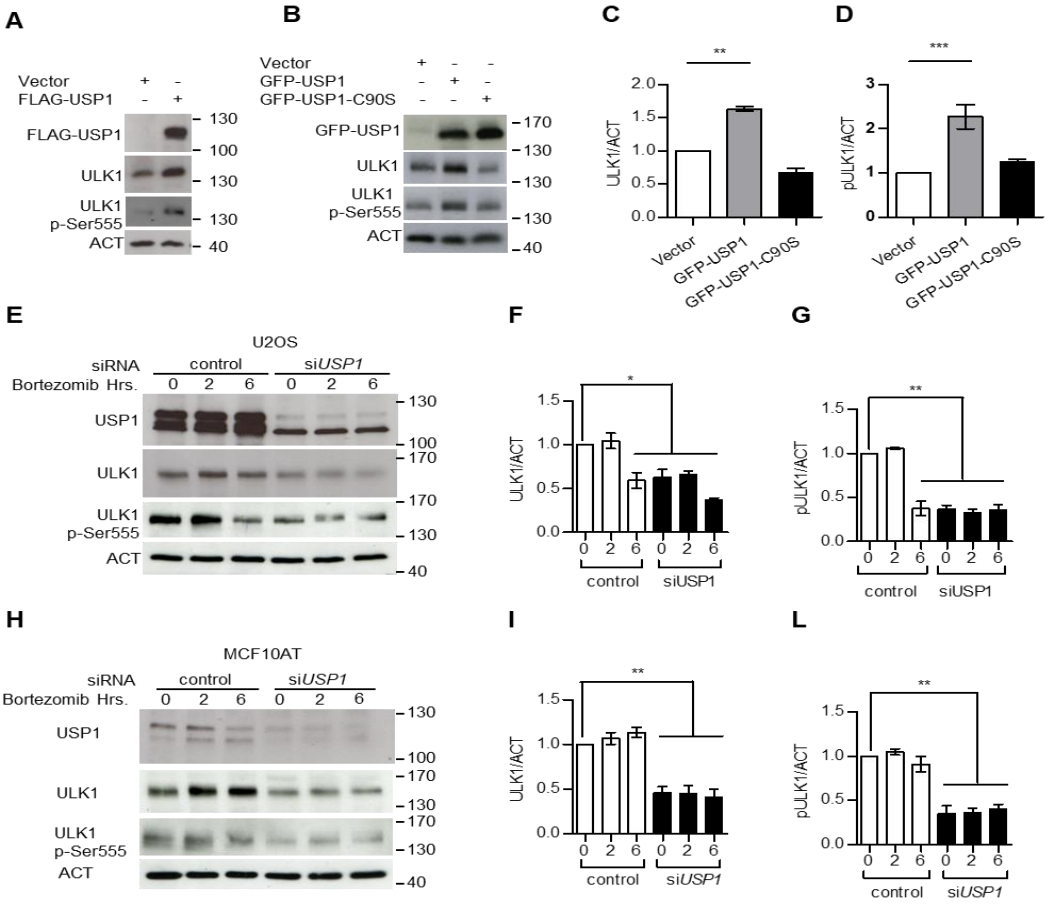

Figure 4.2 USP1 stabilizes ULK1. (A and B) U2OS cells were transfected with the indicated constructs. 24 hours later the samples were lysed in 1% Triton X-100 containing buffer and, the cleared lysates utilized to monitor endogenous ULK1 and ULK1 p-Ser555 protein levels by Western Blot. The relative amounts of each protein were quantified using ImageJ. The ratio of p-ULK1/ACT and ULK1/ACT was calculated and indicated in the graphs **(C)** and **(D)**. **(E)** U2OS and **(H)** MCF10AT cells were transfected with scrambled or *USP1*-specific siRNA, and 72 hours later were incubated with 100 nM Bortezomib for the indicated time intervals. The cleared lysates were utilized to monitor endogenous ULK1 and ULK1 p-Ser555 by immunoblot. The relative amounts of each protein were quantified using ImageJ and the ratio of p-ULK1/ACT and ULK1/ACT was calculated and indicated in the graphs **(G** and **G)** and **(I** and **L).**

4.2 USP1 modulates ULK1 compartmentalization in mammalian cells

The DUB inhibitor WP1130 induced recruitment of GFP-ULK1 to peripheral aggresome, as showed by microscopy observation and by a biochemical assay of soluble and insoluble fraction upon cells lysis[166]. To determine whether USP1 regulates ULK1 transfer to aggresomes, we examined the localization of ULK1

in USP1 depleted U2-0S cells. Interestingly, as highlighted in Figure 4.3A and in Figure 4.3B, ULK1 aggregates were evident in USP1 depleted cells. Simultaneously, the cells attached to the Petri dishes were lysed in sample buffer and the lysates utilized to check silencing efficiency (Figure 4.3C). To confirm the role of USP1 in ULK1 relocalization, we transfected U2-OS cells with wild type ULK1-HA and as shown in Figure 4.3D and in Figure 4.3E, similar results were obtained with ectopic ULK1.

To investigate whether the solubility of ULK1 was altered after USP1 depletion, cellular lysates were fractionated into Triton X-100 -soluble and -insoluble fractions. We used low concentration of SDS or 5M urea to solubilize aggregated proteins. Although SDS is an efficient solubilizing agent, one problem of this approach is that certain proteins tend to reaggregate, causing streaks or precipitates on the 2-D gel. Therefore, we compare two different procedures for solubilizing ULK1 protein. The level of endogenous ULK1 from USP1 depleted cells, dramatically increased in the urea- soluble fraction (Figure 4.4) suggesting that to keep the extracted proteins in solution, superior results were obtained with urea buffer in comparison to SDS buffer, particularly in the case proteins with high Molecular Weight. Since it was previously shown that HDAC6, a microtubule-associated deacetylase, is a component of the aggresome[171], we looked at the HDAC6 level in our samples. Another

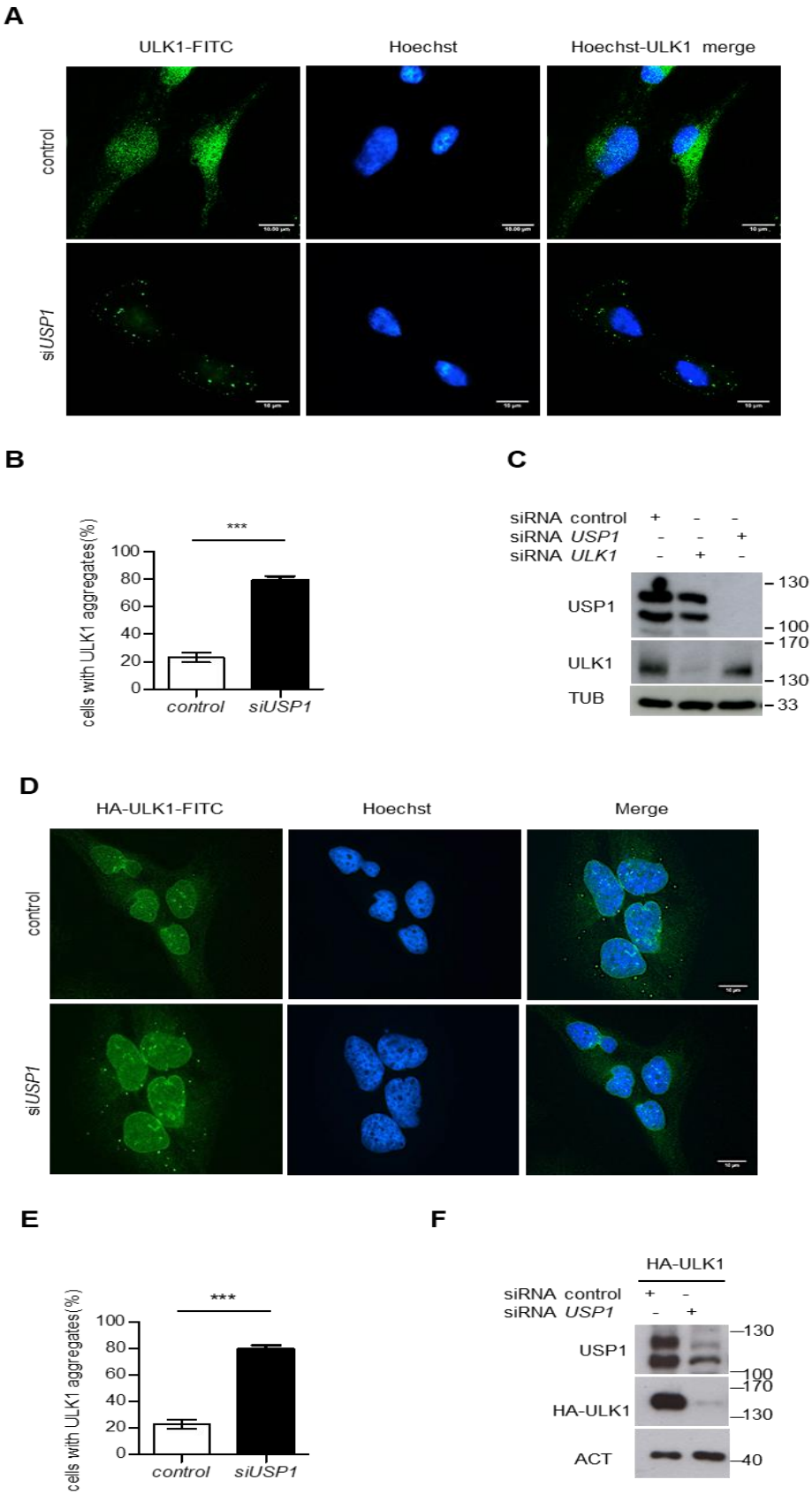
A
ULK1-FITC
Hoechst
Hoechst-ULK1 merge
control
siUSP1
B
cells with ULK1 aggregates(%)
***
100
80
60
40
20
0
control
siUSP1
C
siRNA control + - -
siRNA USP1 - - +
siRNA ULK1 - + -
USP1
ULK1
TUB
130
100
170
130
33
D
HA-ULK1-FITC
Hoechst
Merge
control
siUSP1
E
cells with ULK1 aggregates(%)
***
100
80
60
40
20
0
control
siUSP1
F
HA-ULK1
siRNA control + -
siRNA USP1 - +
USP1
HA-ULK1
ACT
130
100
170
130
40

Figure 4.3 USP1 depletion is coupled to a shift in ULK1 compartmentalization. (A, B and C) U2OS cells were silenced with scrambled or *USP1*-specific siRNA. 72 hours later they were fixed and immunostained with anti ULK1 antibody and analyzed by confocal laser scanning microscopy. **(A)** Representative images. Scale bar: 10 µm. **(B)** Quantification of the percentage of cells containing ULK1 aggregates. Data are means ± SD of three independent experiments ***=P<0.0001. 50 cells per each condition were analyzed **(C)** Control blot. **(D)** Ectopic ULK1 forms aggregates in USP1 depleted cells. 72 hours after transfection with scrambled or *USP1*-specific siRNA, U2-OS cells were transfected with plasmids encoding HA-ULK1. 24 hours later, the cells were fixed and analyzed by confocal laser scanning microscopy. Representative images. Scale bar represents 10 µm. **(E)** Quantification of cells numbers with ULK1 aggregates. The graph reports the mean ± SD of 3 independent experiments; at least 50 cells per group per experiment were counted. ***=*P*<0.0001. **(F)** Control blot.

aggresomes marker is vimentin[171]. Similarly, HDAC6 and vimentin were accumulated in the insoluble fraction, as expected. Notably, while vimentin distribution was independent of USP1, HDAC6 relocalization to the insoluble fraction was sharply enhanced in USP1 depleted cells, as it was the case for ULK1 (Figure 4.4). Interestingly, a similar distribution was observed for FANCD2, the prototype target of USP1 (Figure 4.4).

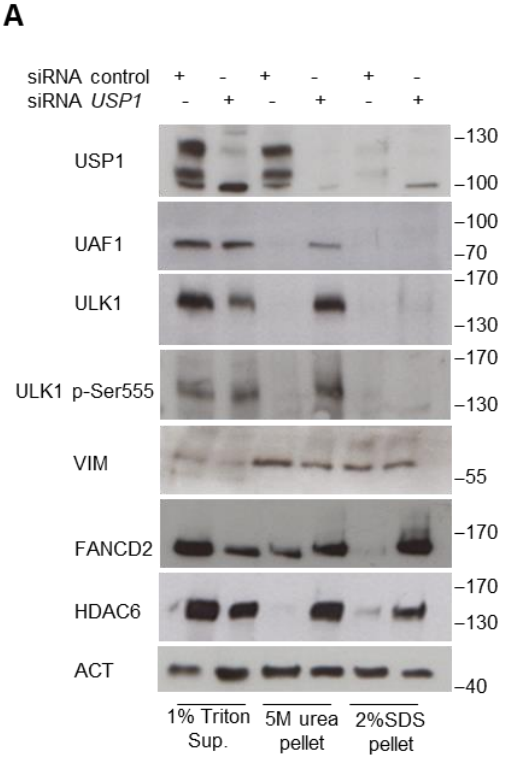

Figure 4.4 ULK1 is recruited to the insoluble proteins fraction in USP1 depleted cells. U2-OS cells were transfected with scrambled or *USP1*-specific siRNA; 72 hours later, 1% Triton soluble and insoluble fractions were separated by centrifugation. Pellets were solubilized alternatively in 5M urea or in 2% SDS containing buffers and analyzed by immunoblot with the indicated antibodies.

4.3 Inhibition of USP1 activity by pimozide modulates ULK1 compartmentalization

Some years ago, through quantitative high-throughput screening, pimozide has been identified as a USP1/UAF1 inhibitor. PCNA and FANCD2 are two prototype targets of USP1. PCNA is ubiquitinated by Rad6/Rad18 upon DNA damage, leading to the recruitment of TLS Polη and subsequently is deubiquitinated by USP1 to reestablish the interaction with high fidelity DNA polymerases[115]. Furthermore, USP1 physically associates with FANCD2 and the proteins colocalize in chromatin after DNA damage. USP1 deubiquitinates FANCD2 when cells exit S phase[141]. USP1 negatively regulates PCNA and FACD2 monoubiquitination, so we expected that the treatment of human cells with pimozide, wuold leads to an increase in PCNA and FANCD2 monoubiqitination, supporting its effect as an USP1/UAF1 inhibitor[172]. To further investigate the implication of USP1 activity in the modulation of ULK1 compartmentalization, we tested wheter treatment with USP1 inhibitor pimozide, has the same effect as the USP1 depletion. For this reason, ULK1 distribution was analysed by immunofluorescence and biochemical analysis. As shown in Figure 4.5A and in Figure 4.5B, pimozide treatment induces an accumulation of ULK1 into aggresomes already after 4 hours.

Accordingly, once again, ULK1 and HDAC6 enrichment was clear in 5M urea soluble pellet (Figure 4.5C). USP1/UAF1 was shown to deubiquitinate both PCNA and FANCD2 in response to DNA damage. In order to demonstrate that pimozide inhibit the USP1/UAF1 activity, we observed the levels of Ub-PCNA or Ub-FANCD2 in cells treated with pimozide. The levels of monoubiquitinated PCNA and FANCD2 can be followed by the appearance of a band at a higher

molecular weight. When U2-OS cells were treated with pimozide, a significant increase of Ub- FANCD2 and Ub-PCNA was detected, confirming that USP1 activity was down-regulated (Figure 4.5C).

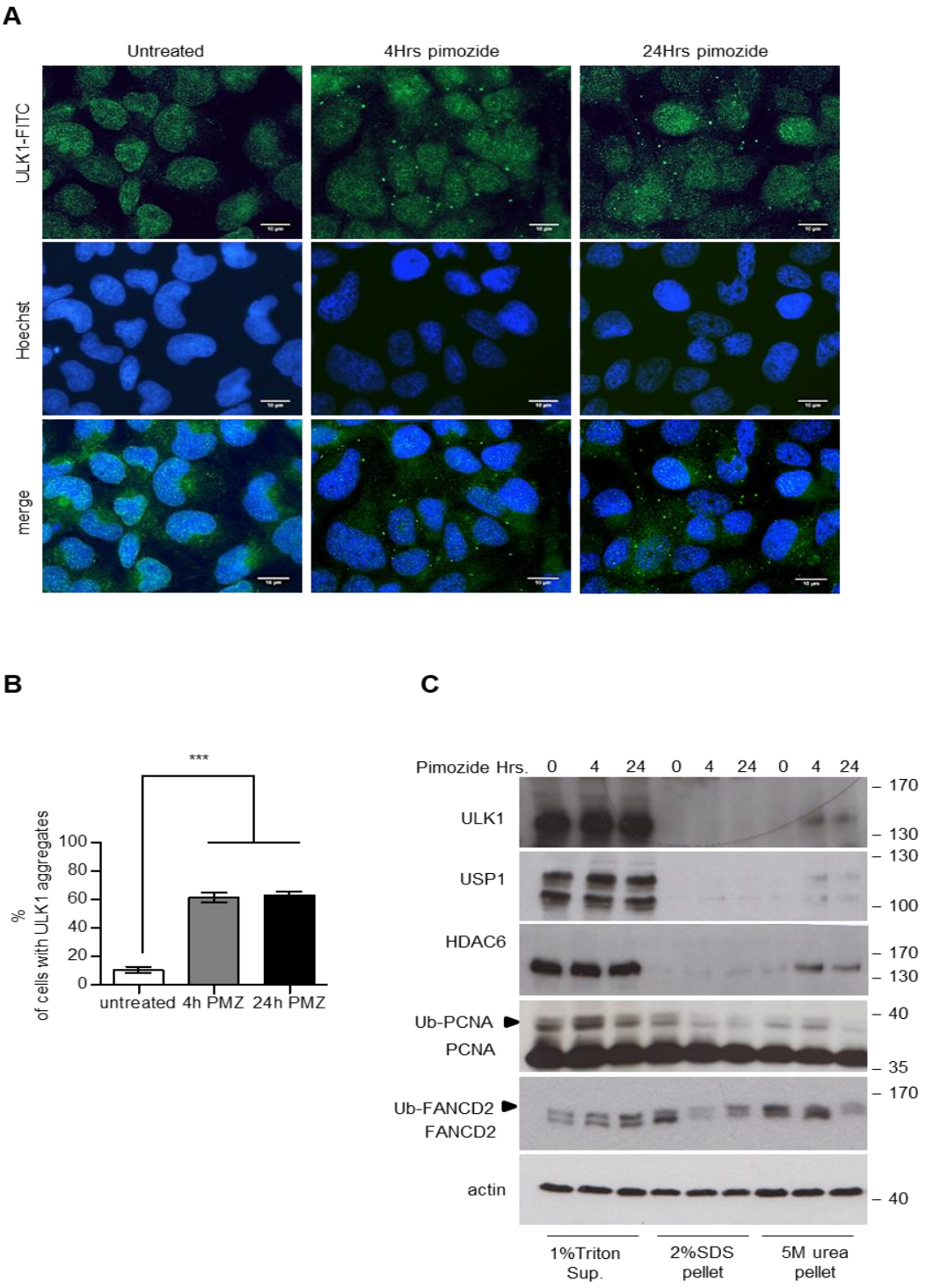

Figure 4.5 USP1 inhibitor pimozide affects ULK1 compartmentalization/solubility. (A, B) U2OS cells were left untreated or incubated with 2,5 μM pimozide for the indicated time points, then fixed for immunofluorescence analysis with anti-ULK1 antibody and analysed by confocal laser scanning microscopy. **(A)** Representative images, scale bar represents 10 μm. **(B)** Quantification of cells with ULK1 aggregates. The graph reports the means ± SD of 3 independent experiments, at least 50 cells per group per experiment were counted. ***=P<0.0001. **(C)** U2OS cells were left untreated or treated with 2,5 μM pimozide for the indicated time intervals. Next, 1% Triton X100 soluble and insoluble fractions were separated by centrifugation. Pellets were solubilized either with 5M urea or 2% SDS containing buffers, and analyzed by immunoblot with the indicated antibodies.

4.4 USP1 depletion increases p62/ULK1 colocalization

Next, we sought to characterize the ULK1 puncta observed in USP1 depleted cells, so we checked wether other proteins were conteined in ULK1 puncta, using immunofluorescence analysis and immunoprecipitation experiments. p62/SQSTM1 is a ubiquitin-binding scaffold protein that is degraded by autophagy and accumulates when autophagy is inhibited. Therefore, p62 was the first candidate protein to be tested. Confocal microscopy analysis using JACoP (Just Another Co-localization Plugin), revealed that endogenous ULK1 and p62/SQSTM1 partly colocalized in the same structure in USP1 depleted cells, whereas both proteins were diffused in control cells, as already shown for WIP130-dependent GFP-ULK1 aggresomes[166] (Figure 4.6A and Figure 4.6C). Furthermore, p62/SQSTM1 is known to be required for aggresome formation in autophagy deficiency condition[80]. Notably, downregulation of USP1 increased the number of p62 dots (Figure 4.6B). Simultaneously, the cells attached to the Petri dishes were lysed in sample buffer and the lysates utilized to check silencing efficiency (Figure 4.6D). In addition, we confirmed the interaction between ULK1 and p62/SQSTM1 with a co-immunoprecipitation experiment of U2-OS cells lysates, using an antibody directed against endogenous ULK1. *ULK1* silencing was used as a negative control. We analyzed the results by Western Blot and we observed that p62/ULK1 interaction was stronger in USP1 depleted cells than in control ones, (Figure 4.6E). Moreover, in accordance with the data shown in Figure 4.1, Figure 4.2 and Figure 4.3, the ULK1 protein level was reduced in the lysates of *USP1* depleted cells, as compared to control ones.

Interesting evidences suggest that HDAC6 plays an important role in autophagy, recognizing polyubiquitinated proteins and controlling the fusion process of autophagosomes to the lysosome[173]. Thus, we wanted to verify the binding of ULK1 to HDAC6 by immunoprecipitation experiments. After depletion of USP1, U2-OS cells lysates were immunoprecipitated using an anti-ULK1 antibody and analysed by Western Blot. As shown in Figure 4.6E, HDAC6 associates with ULK1 in an immunocomplex, but a reduced binding was observed in control cells. Recently it has been demonstrated that the ubiquitin proteasome system controls the protein stability of HDAC6[174], indeed only after bortezominb treatment, HDAC6 interacts with ULK1 even in control cells (Figure 4.6E). Moreover, this interaction is ULK1 dependent. Since p62/ULK1 interaction increased in USP1 depleted cells, we expected to find p62 in the insoluble fraction as with ULK1. To investigate whether the solubility of p62 was altered in USP1 depleted cells, cellular lysates were fractionated into Triton X-100-soluble and -insoluble fractions. As expected, we observed an increase in p62 protein level in cells in which USP1 gene is depleted with respect to cells in which USP1 gene is normally expressed. Furthermore, we found that 5M urea-solubilized pellet, obtained from cellular lysates of USP1 depleted cells, was enriched in p62 (Figure 4.6F). In addition, another interesting observation was that in USP1 depleted cells, the abundance of two other autophagy players, MAP1LC3A (LC3) and BECN1 was decreased in the soluble fraction, compared to control-silenced cells. Conversely, the insoluble fraction was enriched of these proteins. As evidenced by Guan and colleagues, ULK phosphorylates BENC1 and this phosphorylation step is crucial for the function of BECN1 in autophagy [175], therefore it was very interesting to find ULK1 and BECN1 in the same protein fraction. This interaction was also tested by immunoprecipitation (Figure 4.6E) and immunofluorescence experiments (Figure 4.7A-B). Western blot analysis showed that the endogenous association between ULK1 and BECN1 increased considerably in USP1 depleted cells (Figure 4.6E-F). Supporting these data, confocal microscopy examination revealed that in absence of USP1, ULK1 and BECN1 colocalized in the same

structures and additionally, their colocalization was sensitive to autophagy induction by rapamycin treatment (Figure 4.7A and Figure 4.7B). Simultaneously, as shown in Figure 4.7C and in Figure 4.7D, we confirmed the ULK1/HDAC6 interaction even through immunofluorescence experiment. Futhermore, the Endophilin B1, known as BIF1, was also present in 5M urea solubilized pellet obtained from cellular lysates of USP1 depleted cells (Figure 4.6F). Wang and colleagues shown that BIF1, interacts with BECN1 and regulates vesicle nucleation during autophagy[176]. Our results strongly suggest that without USP1 many of autophagic proteins are accumulated into the aggresome to be subsequently re-used.

4.5 USP1 downregulation facilitates the recruitment of ULK1 to aggresomes and retains its kinase activity.

Since we observed that USP1 downregulation leads to the transfer of ULK1 to aggresomes, we next analysed whether this process also affects ULK1 kinase activity. As reported in several works, ULK1 phosphorylates ATG13 on Ser-318, thus phosphorylation of this residue can be used as a read-out of ULK1 kinase activity in cells[177,178]. Thus, we analyzed the phosphorylation status of ATG13 by immunoblotting. As reported by Mizushima and his colleagues[179], we confirmed that ATG13 was downshifted in MEF *Ulk1-/-* (Figure 4.8B), confirming that the interaction with ULK1 is important for ATG13 phosphorylation. Interestingly we noticed that in *USP1* siRNA-treated U2-OS cells, phosphorylation of ATG13 was reduced, as detected by a faster migration of the protein in SDS-PAGE (Figure 4.8A and Figure 4.8C). This downshifted band was not observed in the isoluble fraction of USP1 depleted cells (Figure 4.8C). Additionally, we monitored the phosphorylation of ATG13 at Ser-318 with a specific phospho-antibody. In order to induce ULK1 kinase activity we treated cells with rapamycin and we observed a clear induction of ATG13 phosphorylation. As shown in Figure 4.8C, *USP1* siRNA treatment did not affect ATG13 phopshorylayon at Ser318 in the Triton X-100-soluble fraction.

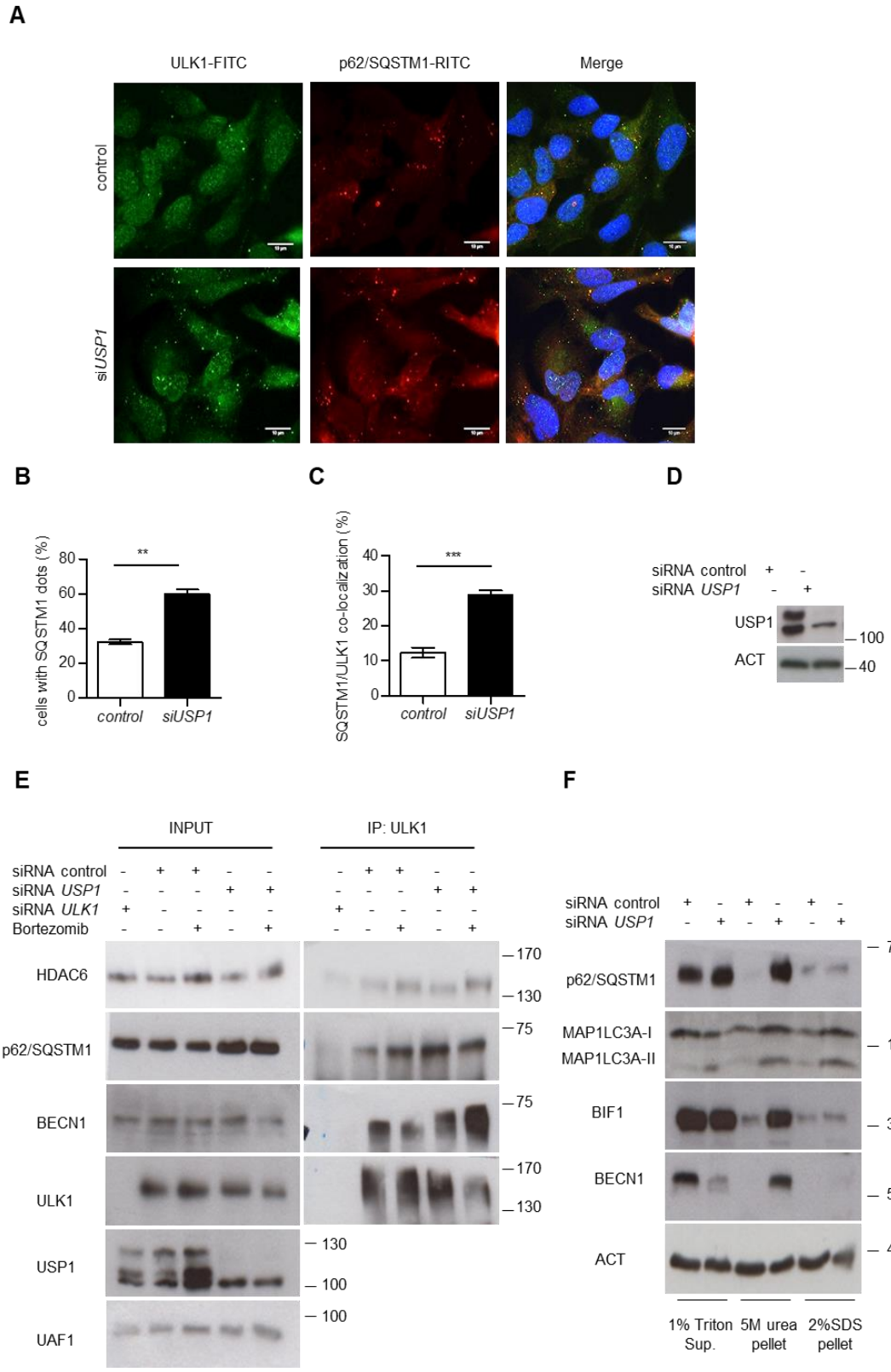

Figure 4.6 USP1 depletion is coupled to an increase in p62/ULK1, Beclin1/ULK1 colocalization and enrichment of autophagic proteins in 5M urea solubilized pellet. (A) U2OS cells were

transfected with scrambled or *USP1*-specific siRNA and then fixed for immunofluorescence analysis with anti p62 and ULK1 specific antibodies. **(A)** Representative images. Scale bar represents 10 µm. **(B)** Percentage of cells containing p62 dots. **(C)** Quantification of p62/ULK1 colocalization. Both graphs (**B** and **C**) report the mean ± SD of n = 3 independent experiments; at least 50 cells per group per experiment were counted. **=P<0.001 and ***=P<0.0001. Colocalization was analyzed by confocal microscopy performed using the JACoP plugin in ImageJ (NIH Image) as described in the Materials and Methods. **(D)** Control blot. **(E)** U2OS cells were transfected with control, *ULK1* or *USP1* specific siRNA. 72 hours later, the cells were left untreated or incubated with 100 nM of Bortezomib for 6 hours. Cleared lysates were immunoprecipitated with anti-ULK1 antibody and analyzed by immunoblotting with the indicated antibodies. **(F)** U2OS cells were transfected with scrambled or *USP1*-specific siRNA and were lysed after 72 hours, in 1% Triton containing buffer. Detergent-soluble and insoluble fractions were separated by centrifugation and the pellets were solubilized either with 5Murea, or 2% SDS based buffers and analyzed by immunoblots with the indicated antibodies.

Vice-versa, in 5M urea solubilized pellet obtained from cellular lysates of USP1 depleted cells, ATG13 phosphorylation at Ser318 was clearly increased. To further establish the validity of these data, we monitored the phosphorylation status of ULK1. Earlier works in both yeast and mammalian systems, suggests that the nutrient and energy signals change the phosphorylation status of ULK1. mTOR has been reported to directly phosphorylate ULK1 weakening its kinase activity[180,179]. Ser757 became dephosphorylated by rapamycin treatment or mTOR knockdown, suggesting that mTOR mediates the phosphorylation of this site[181–183]. To test if there was a correlation between ATG13 (Ser-313) phosphorylation and mTOR signaling to ULK1, we then examined the phosphorylation of ULK1 at Ser-757. Interestingly, ULK1-mediated ATG13 phosphorylation inversely correlated with the inhibitory phosphorylation on ULK1. In fact, in the Triton X-100-soluble fraction, *USP1* siRNA treatment clearly decreased total ULK1 level, whereas increased the phosphorylation of ULK1 (Ser-757, the TORC1 target site). However, in 5M urea or 2%SDS solubilized pellet, ULK1 phosphorylation at Ser757 was not detected neither in control or USP1 depleted cells. Furthermore, in accordance with previous works, rapamycin treatment decreased Ser757 phosphorylation, pointing out that mTORC activity was inhibited by rapamycin (Figure 4.8D). These observations suggest that the USP1-mediated transfer of ULK1 to aggresomes, positively regulates ULK1 activity. Indeed, without USP1, in the soluble

fraction prevails the inactive form of ULK1, indicating an impairment of autophagy. On the contrary, the solubilized pellet gets rich by ULK1 active, by stating that without USP1, ULK1 is not degradated but it builds up in the aggresomes, together with other autophagic protein, as suggest in Figure 4-6 and in Figure 4.7 and they are ready to work. Whereas the previous data might be in line with Stork's[166] work, we observe an increment in ULK1 activity in the solubilized pellet, contrary to what is stated by Stork's group. This observation is not freaky because Stork's results demonstrate that WP1130 negatively regulates ULK1 activity indirectly through ULK1 aggregation; whereas in our work, we observed that USP1, that has not been established as a terget of WP1130, mediates the relocation of ULK1 to aggresomes and influences ULK1-dependent phosphorylation of ATG13.

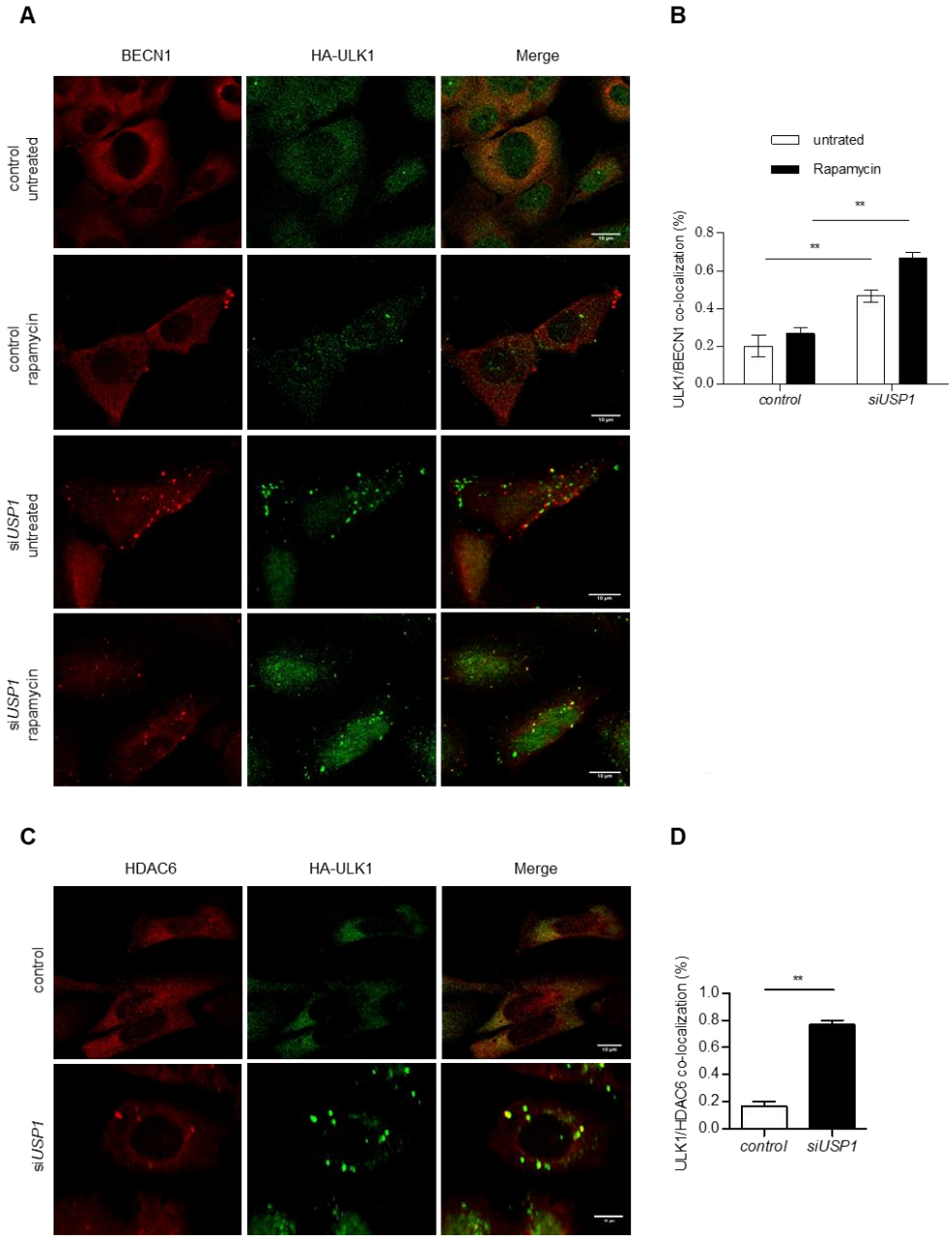

Figure 4.7. USP1 depletion increases BECN1/ULK1 and HDAC6/ULK1 colocalization. (A and **B)** U2OS cells were transfected with scrambled or *USP1*-specific siRNA for 72 hours and transfected with plasmids encoding HA-ULK1. 24 hours later the cells were treated with rapamycin for 3 hours and fixed for immunofluorescence analysis with anti BECN1 and HA specific antibodies. **(A)** Representative images. Scale bar represents 10 µm. **(B)** Quantification of BECN1/ULK1 colocalization. The graph reports the mean ± SD of n = 3 independent experiments; at least 50 cells per group per experiment were counted. **=P<0.001. **(C** and **D)**. Colocalization was analyzed by confocal microscopy performed using the JACoP plugin in ImageJ (NIH Image) as described in the Materials and Methods. U2OS cells were transfected with scrambled or *USP1*-specific siRNA for 72 hours and transfected with plasmids encoding HA-ULK1. 24 hours later the cells were fixed for immunofluorescence analysis with anti HDAC6 and HA specific antibodies. **(C)** Representative images. Scale bar represents 10 µm. **(D)** Quantification of HDAC6/ULK1 colocalization. The graph reports the mean ± SD of n = 3

independent experiments; at least 50 cells per group per experiment were counted. **=P<0.001. Colocalization analysis was performed as described in the Materials and Methods.

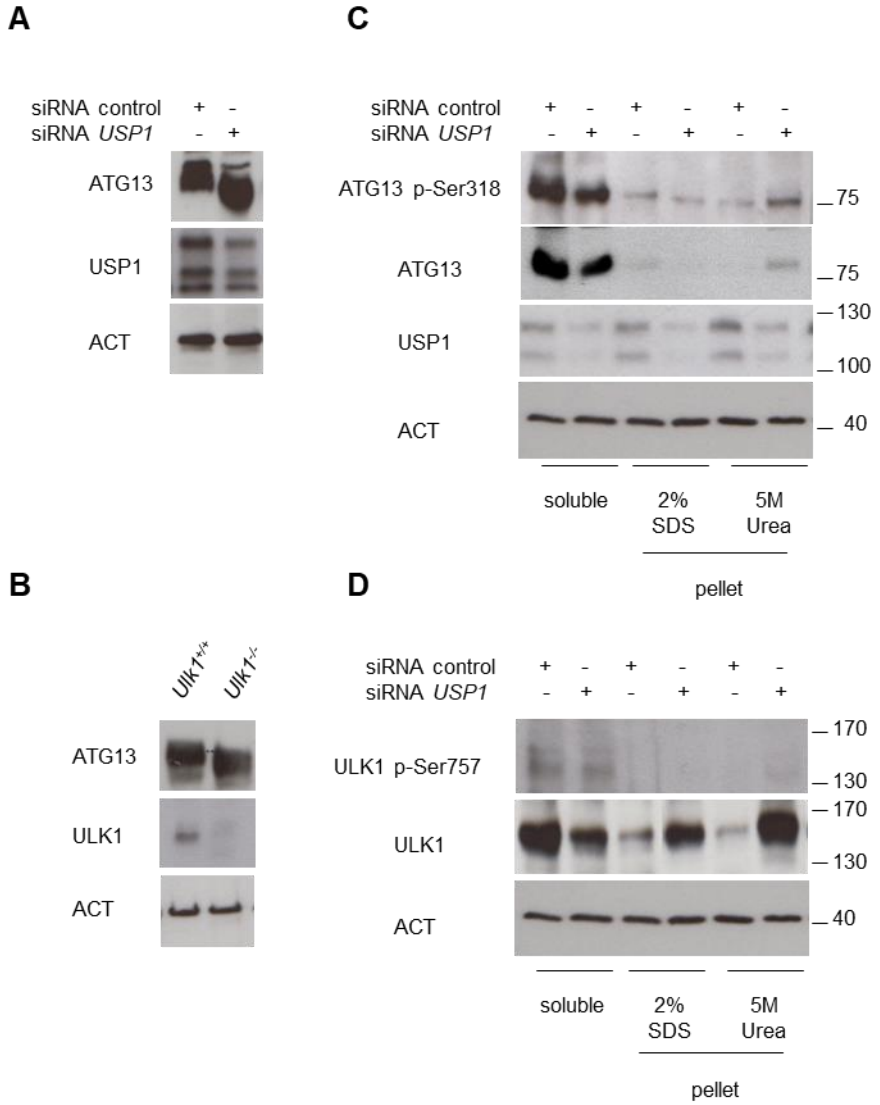

Figure 4.8 USP1 retains ULK1 kinase activity. (A) U2OS cells were transfected with scrambled or *USP1*-specific siRNA, lysed after 72 hours in 1% Triton containing buffer and analyzed by immunoblots with the indicated antibodies. **(B)** MEF cells were lysed in 1% Triton containing buffer and analyzed by immunoblots with the indicated antibodies. **(C)** and **(D)** U2-OS cells were transfected with scrambled or *USP1*-specific siRNA; 72 hours later, 1% Triton soluble and insoluble fractions were separated by centrifugation. Pellets were solubilized alternatively in 5M urea or in 2% SDS containing buffers and analyzed by immunoblot with the indicated antibodies.

4.6 USP1 interacts with ULK1 in vivo

We have demonstrated that USP1 depletion dramatically affects ULK1 compartmentalization. To elucidate whether the effect was direct, we monitored ULK1/USP1 interaction by coimmunoprecipitation analysis. Endogenous USP1 was immunoprecipitated with an anti-USP1 antibody from lysates of HEK293 cells, untreated or treated with rapamycin and we found that the endogenous association between ULK1 and USP1 increased considerably in rapamycin treated cells (Figure 4.9A). This result suggests that USP1 specifically interacts with ULK1 during autophagy. Previous works have reported that the WD-repeat containing protein 48, also known like UAF1, forms a complex with USP1 *in vivo*, regulating its enzymatic activity[130]. Since we have shown that down-regulation of USP1 reduces ULK1 protein level in the Triton X-100-soluble fraction, we decided to check whether we have an equal effect with *UAF1* siRNA treatment. We transfected human osteosarcoma U2OS cells with scrambled siRNA or with *UAF1*-targeting siRNA and *USP1*-targeting siRNA and lysates were collected and used to monitor the ULK1 trend. We followed ULK1 protein levels in Western Blot analysis and in contrast to USP1 depletion, downregulatin of UAF1 didn't have an impact upon ULK1 protein level (Figura 4.9B). As mentioned first, AMPK phosphorylation site Ser555 contributes to ULK1 activation. Then we evaluated ULK1 phosphorylation at Ser555 and as expected we observed that, ULK1 phosphorylation at Ser555 was decreased in UAF1 and USP1 depleted cells (Figura 4.9B). Thus, whilst UAF1 doesn't influence ULK1 stability, it positively regulates autophagy. To assess whether UAF1 can interanct with ULK1, HEK293 cells were transfected with Myc-tagged UAF1 and the whole-cell extracts were immunoprecipitated using an antibody directed against Myc. We analyzed the results by Western Blot and we observed that Myc-tagged UAF1 interacts with ULK1, as shown by the appearance of the specific band, (Figure 4.9C). Altogether these data support the formation of a USP1-UAF1-ULK1 complex.

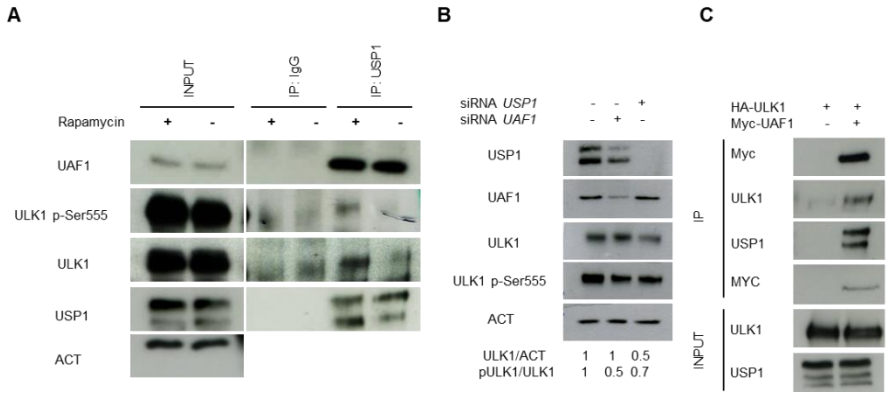

Figure 4.9 USP1 interacts with ULK1 in vivo. (A) HEK293 cells were left, or incubated with 0.5 μM rapamycin for 3 hours, then lysed and immunoprecipitated using IgG or anti USP-1 antibody and analyzed by western blotting using the indicated antibodies. **(B)** U2OS cells were transfected with scrambled or *UAF1* and *USP1*-specific siRNA. 72 hours later, samples were lysed in 1% Triton X-100 containing buffer, and the cleared lysates utilized to monitor endogenous ULK1 and ULK1 p-Ser555 protein levels by Western Blot. The relative amounts of each protein were quantified using ImageJ the ratio of p-ULK1/ULK1 and UL1/ACT were calculated. **(C)** Control vector or Myc-UAF1 (USP1 cofactor) expressing plasmid were transfected in HEK293 cells. Cleared lysates were Immunoprecipitated with anti Myc antibodies and analyzed by immunoblot with the indicated antibodies.

4.7 ULK1 localizes to the nucleus and interacts with USP1

ULK1 functions primarily in the cytosol, whereas USP1 is predominanlty located in the nucleus[134,141]. Therefore, we examined the subcellular distribution of endogenous ULK1 in HE293 and in U2-OS cells. Immunoblot analyses showed that although ULK1 is more abundant in the cytoplasm, it is also present in the nucleus. Likewise, as previously shown by our group[184], USP1 is present also in the cytoplasmic compartment (Figure 4.10A). It has been previously speculated that ULK1 localizes to the nucleus and enhances the activity of PARP1[185]. Since we observed the ULK1-USP1/UAF1 complex interaction, we next immunoprecipitated USP1 from both nuclear and cytoplasmic extracts and assessed the presence of endogenous ULK1. Immunoblot analyses confirmed the ULK1-USP1 interaction mainly in the nuclear extract (Figure 4.10B). Next, to confirm the ULK1-USP1 interaction, we performed immunofluorescence assays by using MEFs deficient in ULK1 to

exclude a non-specific signal. MEF *Ulk1*$^{+/+}$ and MEF *Ulk1*$^{-/-}$ cells were transiently transfected with GFP-USP1 and after 24 hours cells were treated with rapamycin for 3 hours and then fixed and analyzed by immunofluorescence. As expected, USP1 had a predominant nuclear localization and ULK1 was observed also into the nucleus. Interestingly, confocal imaging further demonstrated that USP1 and ULK1 colocalized in a certain percentage of cells expecially after rapamycin treatment (Figure 4.10C and Figure 4.10D). This result reinforces that USP1 specifically interacts with ULK1 during autophagy.

4.8 USP1 removes the K63-linked ubiquitin chains of ULK1

Since USP1 is a deubiquitinating enzyme, we next asked the question whether the ubiquitination status of ULK1 is affected by *USP1* siRNA treatment. The fraction of ubiquitinated ULK1 was analyzed in both control and USP1 depleted cells. Cleared lysates from control and USP1 depleted cells, untreated or treated for 6 hours with bortezomib, were immunoprecipitated with anti ULK1 p-Ser-555 antibody or with IgG as a negative control and analyzed by immunoblot with antibody to total ubiquitin. The immunoprecipitation products were hyperubiquitinated in the samples derived from bortezomib treated cells, as expected. Interestingly, even without bortezomib treatment, silencing of USP1 significantly increased the polyubiquitination of ULK1 p-Ser-555 (Figure 4.11A). Since different types of polyubiquitination processes, including lysine 48 (K48), K11, K63 and K27-linked ubiquitination, have been implicated to regulate protein fate, we also examineted which types of ULK1 ubiquitination

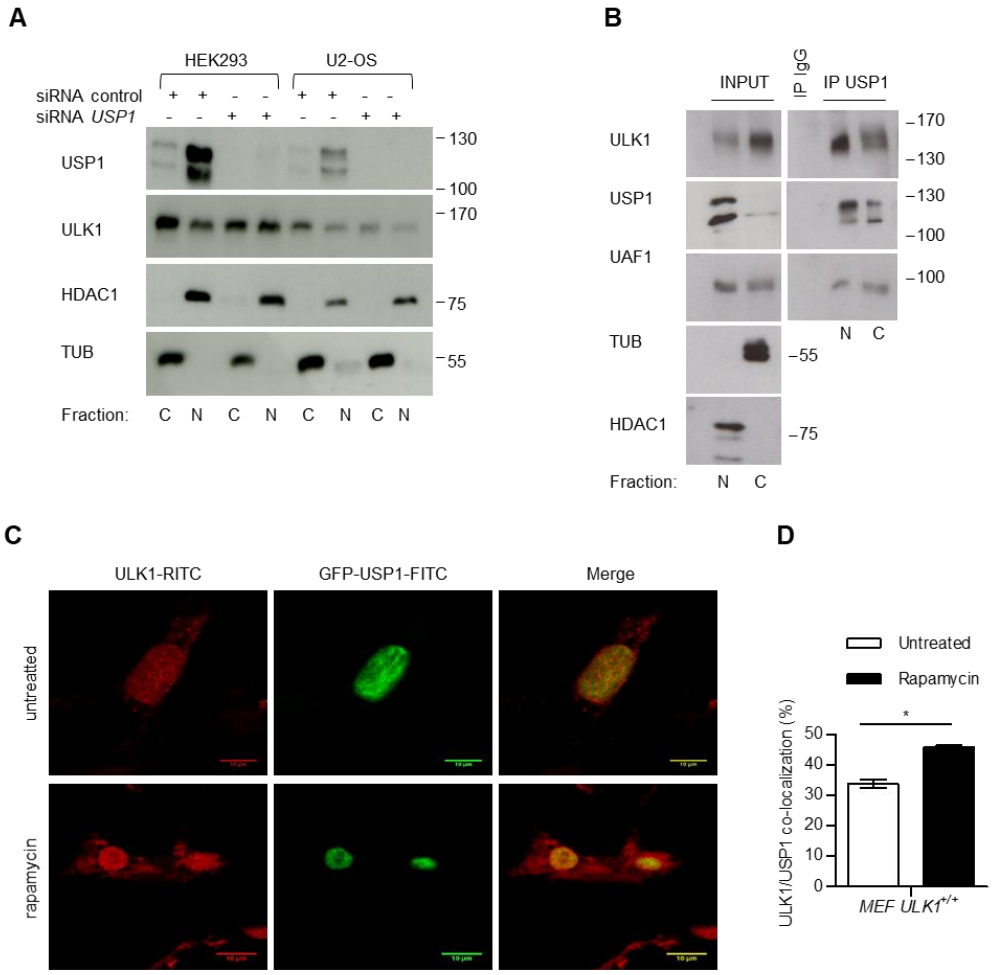

Figure 4.10 ULK1 interacts with USP1/UAF1 complex. (A) Nuclear (N) and cytosolic (C) fractions were prepared from HEK293 and U2-OS cells and subjected to immunoblot analyses using antibodies against USP1, HADAC1, α-TUB and ULK1. The nuclear-enriched fraction shows the presence of ULK1 in the nucleus. **(B)** Nuclear (N) and cytosolic (C) fractions were prepared from HEK293 and were subjected to IP with an anti-USP1 antibody. Endogenous USP1 immunoprecipitates with endogenous ULK1, mainly from nuclear extracts. **(C)** MEF *Ulk1+/+* cells were transiently transfected with GFP-USP1. 24 hours after transfection, cells were treated with 0,5 μM of rapamycin and after 3 hours were fixed for immunofluorescence analysis. Representative images. Scale bar represents 10 μm. **(D)** Quantification of USP1/ULK1 colocalization. The graph reports the mean ± SD of n = 3 independent experiments; at least 50 cells per group per experiment were counted. *=P<0.05.

could be affected by USP1. Previously, Nazio et al. have reported that mTOR controls ULK1 ubiquitination and function through AMBRA1 and the associated E3-ligase TRAF6. In their model, autophagy induction with rapamycin treatment, promoted a net induction of K63-linked ULK1

ubiquitination, mediated by AMBRA1-TRAF6 complex. This change enhanced its kinase activity[18]. To assess whether USP1 may be responsible for K63-linked deubiquitination of ULK1, we analyzed ULK1 ubiquination status in control and USP1 depleted cells, before and after treatment with rapamycin. We confirmed published data on the increase of K63 ubiquitination upon rapamycin treatment. Furthermore, USP1 siRNA treated cells exhibited an increase of mono (and poly)-K63-linked ubiquitination in the ULK1 immunoprecipitates (Figure 4.11B). This piece of data is in line with the increased interaction of USP1/ULK1 upon rapamycin treatment (Figure 4.9A) and sustains our hypothesis that USP1 directly removes K-63-linked ubiquitin from ULK1.

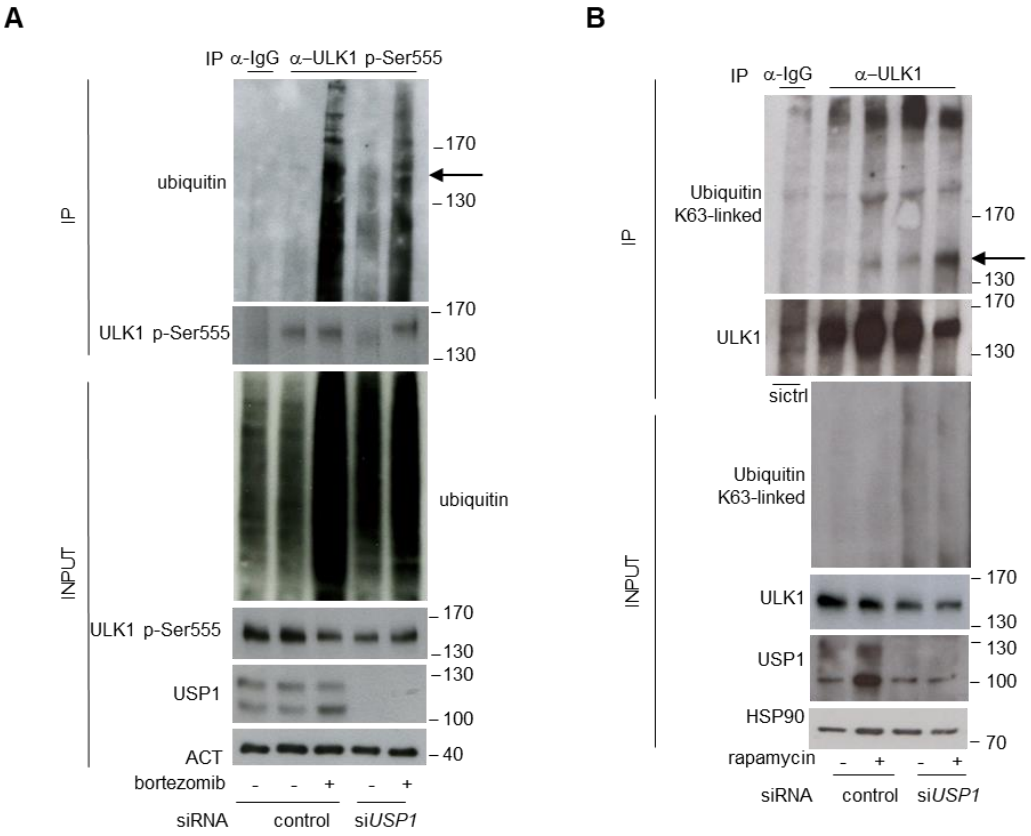

Figure 4.11. USP1 interacts with and deubiquitinates ULK1 in vivo. (A) U2OS cells transfected with scrambled or *USP1*-specific siRNA, were left untreated or incubated with 100 nM of Bortezomib for 6 hours. Cleared lysates were immunoprecipitated using anti-IgG or anti-ULK1 p-Ser555 antibody and analyzed by immunoblot as indicated in the figure. **(B)** U2OS cells transfected with scrambled or *USP1*-specific siRNA were left untreated or incubated with 0.5

μM rapamycin for 3 hours. Cleared lysates were immunoprecipitated with anti- IgG or anti-ULK1 antibody and analyzed by immunoblot with the indicated antibodies.

4.9 USP1 depletion impaires canonical autophagy

Since we showed that USP1 can modulate ULK1 compartmentalization and increases its K-63-linked ubiquitination, we next wanted to determine the effect of USP1 on the autophagic flux. For that, first we anayzed the localization of endogenous MAP1LC3A in U2-0S cells by immunofluorescence. MAP1LC3A is a ubiquitin-like molecule that is conjugated to phosphatidylethanolamine on induction of autophagy and undergoes lysosomal degradation. MAP1LC3A is a marker of autophagosomes and it is visualized by fluorescence microscopy either as a diffuse cytoplasmic pool or as punctate structures that represent autophagosomes. Therefore, autophagosomes formation was monitored by immunofluorescence analysis of MAP1LC3A following standard procedures, requiring the use of paraformaldehyde to fix cells and a mild detergent such as digitonin for permeabilization to protect autophagosomes structures. In parallel, the cells attached to the Petri dishes were lysed in sample buffer and the lysates utilized to check silencing efficiency and autophagy induction (Figure 4.12C). Rapamycin treatment clearly resulted in an increase of MAP1LC3A puncta in control cells. This effect was completely blocked by *USP1* siRNA treatment (Figure 4.12A and Figure 4.12B).

In parallel, we checked another autophagy marker, p62, a ubiquitin-binding scaffold protein that is degraded by autophagy and accumulates when autophagy is inhibited. p62 is incorporated into autophagosomes, thus under starvation conditions p62 puncta generated would represent autophagosomes[80,186]. Notably, in control cells, rapamycin treatment increased the rate of MAP1LC3A/p62 colocalization, as expected (Figure 4.13A and Figure 4.13B). Instead, in USP1 depleted cells MAP1LC3A/p62 already partially colocalized in basal conditions. Thus, this data suggests that, although important, MAP1LC3A is not essential for the recruitment of p62 to the

autophagosome, as was highlighted earlier by Mizushima's group[186]. Taken together these results suggest that without USP1, autophagy could be blocked at an early stage of the pathway. This last observation apparently contrasts with our previous results. Like Nazio et al, we reported a prominent rise in ULK1 activity upon ubiquitination

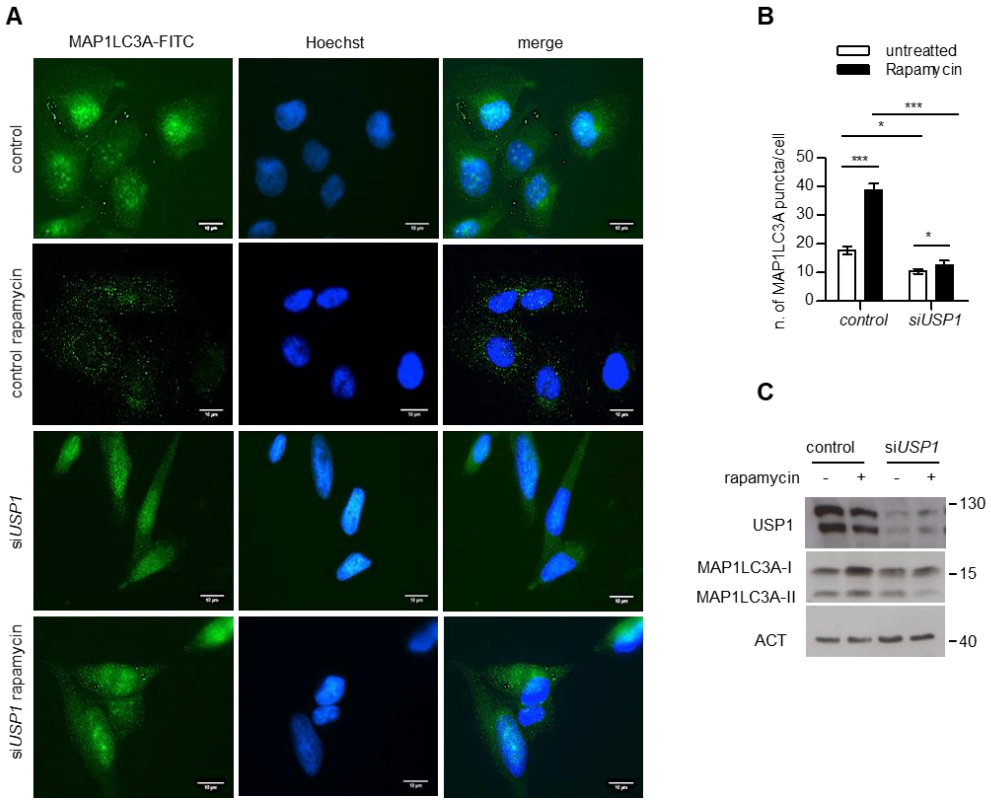

Figure 4.12 Canonical autophagy is impaired in USP1 depleted cells. (A-C) U2OS cells were transfected with scrambled control or *USP1* specific siRNA. 72 hours later, the cells were left untreated or treated with 0.5 µM rapamycin. After 3 hours, the cells were fixed with paraformaldehyde, permeabilized with digitonin and analized by immunofluorescence with anti-LC3 antibody. **(A)** Representative images. Scale bar represents 10 µm. **(B)** The graph reports the means +/-SD of the number of LC3 puncta per cell. At least 50 cells for each condition in each experiment were analyzed. N=3 independent experiments. *** =$P<$ 0.0001, *=$P<$ 0.05. **(C)** Control blot.

particularly in *USP1* depleted cells (Figure 4.10B). We assume that dynamic ubiquitination and deubiquitination of ULK1 is necessary for its function in

autophagy. Recently, a similar observation was also proposed for FANCD2, an USP1 substrates[187]. Indeed, the authors of this study provide two roles for the USP1-UAF1 complex in the FA pathway: USP1 is crucial to remove ubiquitin from ubiquitinated FANCD2 when FANCI has not been ubiquitinated and enables the formation of FANCD2/FANCI complex when both proteins are ubiquitinated. Secondly, USP1 removes ubiquitin from both FANCD2 and FANCI when DNA repair is ended. Similary, we hypothesize that USP1 cuts K63-linked ubiquitin from ULK1 when BECN1 is not ubiquitinated, promoting active complex formation only between ubiquitinated proteins. In addition, our data could suggest an additional role of ULK1, since ULK1 deubiquitination by USP1 coud work as an amplifier. In summary, our biochemical analysis of ubiquitinated ULK1, suggest that in USP1 depleted cells, ULK1 is maintained in an ubiquitinated form that need to be cyclically deubiquitinated by USP1 to ensure a dynamic role of ULK1 in the autophagic process.

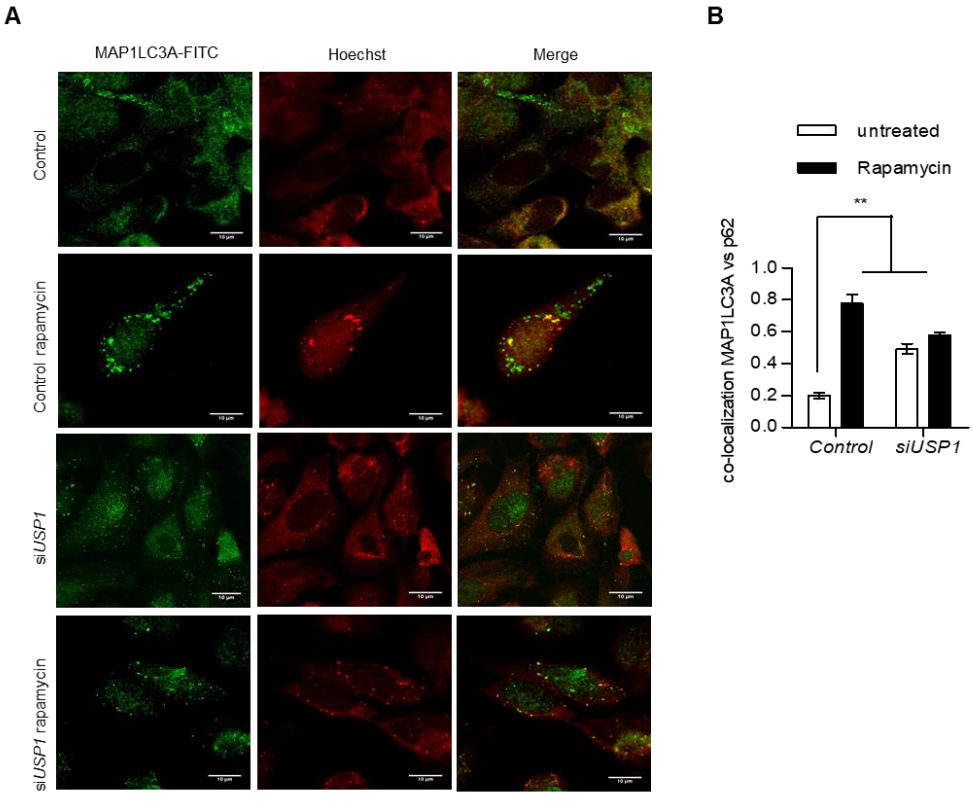

Figure 4.13. MAP1LC3A/p62 colocalization is altered in USP1 depleted cells. U2OS cells were transfected with scrambled control or *USP1* specific siRNA. 72 hours later, the cells were left untreated or treated with 0.5 μM rapamycin. After 3 hours, the cells were fixed with paraformaldehyde, permeabilized with digitonin and endogenous MAP1LC3A and p62 were analyzed by confocal laser scanning microscopy **(A)** Representative images. Scale bar represents 10 μm. **(B)** Quantification of MAP1LC3A/p62 colocalization. The graph reports the mean ± SD of 3 independent experiments; at least 50 cells per group per experiment were counted. **=P<0.001.

4.10 USP1 depletion inhibits the autophagic flux

As shown previously, the accumulation of autophagosomes may represent either an increment of the generation of autophagosomes and/or a block in autophagosomal maturation and the completion of the autophagy pathway[188]. To distinguish between these two possibilities, it is necessary to performe "autophagic flux" assays. Therefore, we analyzed MAP1LC3A turnover and p62 stability in U2-OS cells in response to rapamycin, in the presence or absence of a cathepsins inhibitor such as E64d and pepstatin A in both control and USP1 depleted cells. Since we found many autophagic markers in 5M urea soluble pellet, we analysed by immunoblotting both the Triton-X100 soluble fraction and the 5M urea-solubilized pellets. As shown in Figure 4.14A-C, in control cells, MAP1LC3A lipidation increased upon treatment with the cathepsin inhibitor cocktail. It also increased upon rapamycin treatment and was enhanced by the combined treatments, as expected for active induction of the autophagic flux. Likewise, p62 decreased upon rapamycin treatment and was rescued upon cathepsin inhibiiton. A similar result was observed for MAP1LC3A and p62 in the 5M urea solubilized pellet fraction extracted from USP1 depleted cells. This biochemical assay essentially confirmed the results obtained by immunofluorescence, indicating the requirement of USP1 for canonical autophagy.

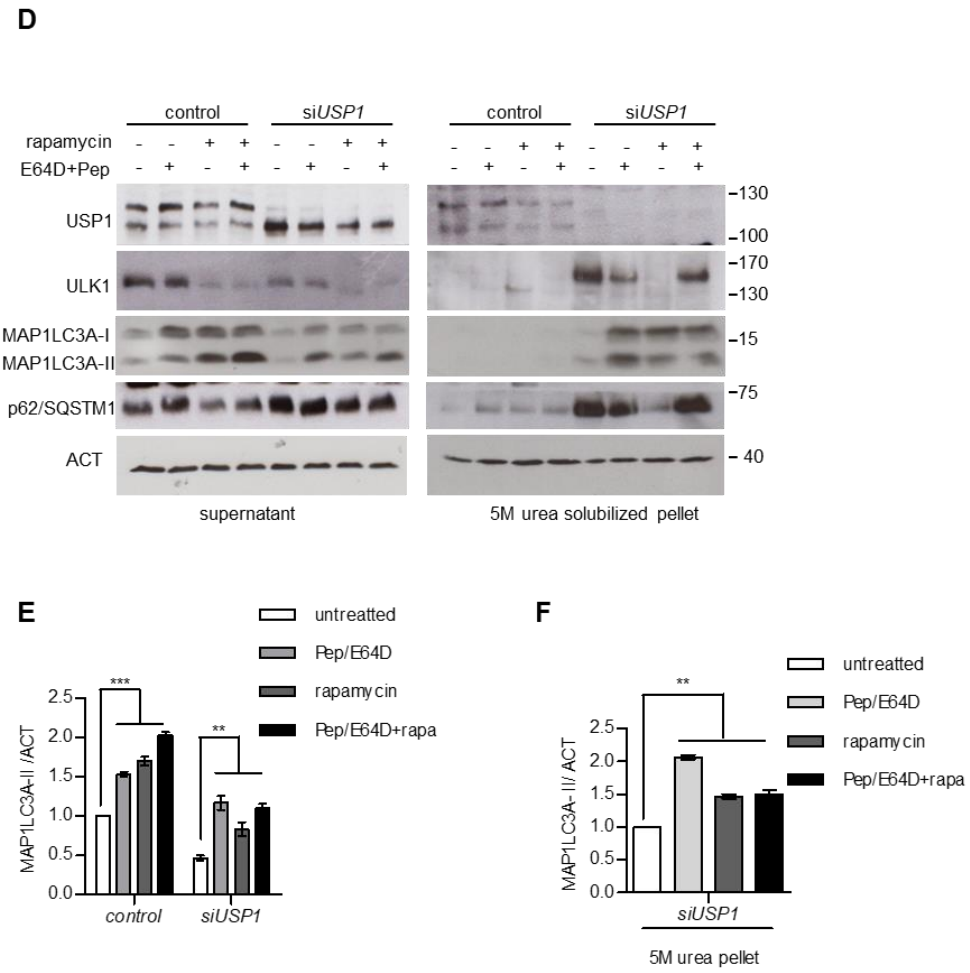

Figure 4.14 The autophagic flux is inhibited by USP1 siRNA treatment. (A) U2OS cells were transfected with control or *USP1* specific siRNA. 72 hours later, the cells were left untreated, or incubated with 0.5 μM rapamycin, or a cathepsin inhibitor cocktail (100 μM pepstatin A and 10 μg/ml E64D), or a combination of rapamycin and cathepsin inhibitors cocktail for 3 hours. Next, the detergent-soluble or insoluble fractions were prepared and analyzed by immunoblot analysis with the indicated antibodies. The relative amount of LC3-II was quantified using ImageJ and the ratio of p-LC3-II/ACT was calculated and indicated in the graphs **(B)** and **(C)**.

4.11 Targeting USP1 to kill autophagy competent cancer cells.

Aberrant overexpression of *USP1* mRNA and protein is often found in osteosarcoma and melanoma as well as in cervical and gastric cencer[114]. However, details of USP1 protein levels in breast cancer samples have not yet been published. In recently years, the role of autophagy in cancer development has been exstensively investigated. Given the emerging recognition that

autophagy maintains energy homeostasis by recycling cellular components, studies carried out in recent years have investigated the expression levels of autophagy-related proteins in a variety of cancers. For instance, the regulator of autophagy BECN1 has been identified as a tumor suppressor gene[75], while the expression of others autophagy-related (i.e SQSTM1/p62, MAP1LC3A, and MAP1LC3B) is elevated in several cancers, including lung[189], colon[190] and breast cancer[191,192]. Notably Lefort et al, provide evidence that the autophagic protein MAP1LC3A is upregulated in triple negative breast cancers and it represents a credible indicator of poor prognosis[114]. Based on these data, we selected a collection of 95 invasive breast tumor samples of four different molecular subtypes: 24 HER2 positive, 23 luminal A, 24 luminal B, and 24 triple negative samples (Table 4.1). De novo tumors, non-metastatic and non-pre-treated by neo-adjuvant regimen have been included. Among molecular groups, no significant differences in terms of age, whilst except for Luminal A tumors, the other three groups were characterized by an increased grade and stage. Tumor samples were analyzed by immunohistochemistry to assess USP1 (Figure 4.15A) and MAP1LC3A proteins (Figure 4.15B). Notably, all but one HER2 breast cancers were USP1 negative, possibly excluding its role in this molecular subtype. Conversely, about 40% of Luminal A, Luminal B and Triple Negative samples expressed this protein. Looking at the co-expression of USP1 and MAP1LC3A, the 30% of Luminal A and B samples, positively expressed both USP1 and MAP1LC3A, whereas in Triple Negative tumors the co-expression was about 90%. Spearman's Rho test was applied to the whole population of samples and to each group to measure the association between USP1 and MAP1LC3A and a significant correlation was found when considering the entire samples population, or only the group of triple negative tumor samples (Figure 4.15C). Simultaneously, Fisher's exact test was applied to the data and in this case a significant correlation was found when considering the entire population. Clearly, these data need to be confirmed on a larger cohort of patients. The high level of MAP1LC3A and USP1 expression observed in a subset of triple negative tumors, suggests that this subtype

display a high rate of basal autophagy and USP1 positively regulates this process. and USP1.

A

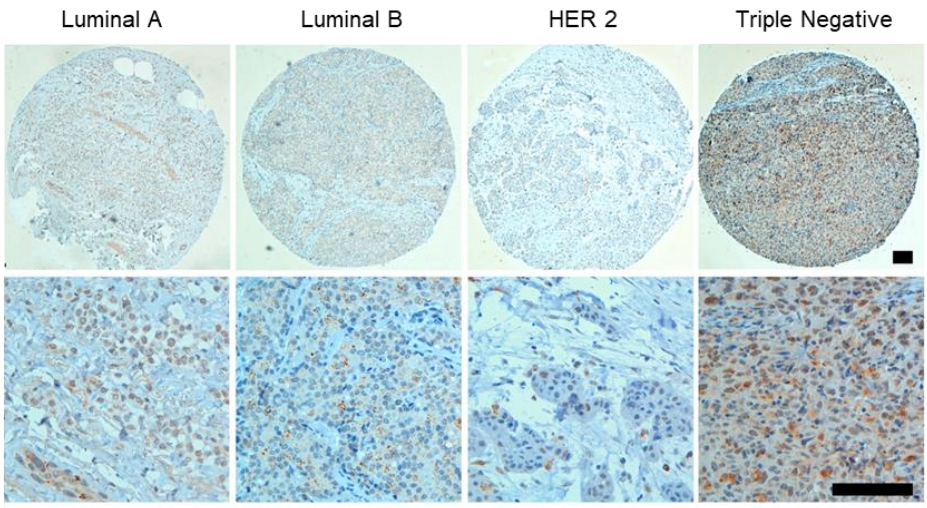

B

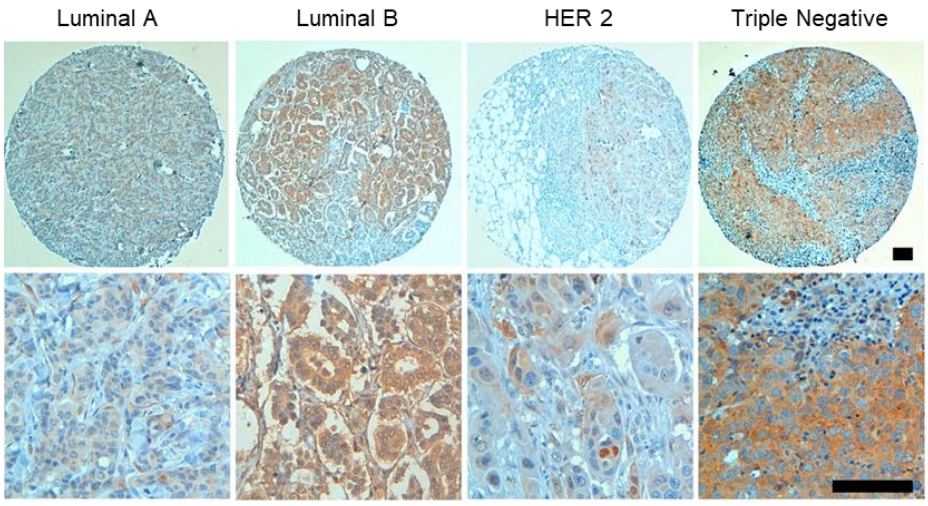

C

Molecular subtype	number of samples	USP1 positive LC3 positive	USP1 positive LC3 negative	USP1 negative LC3 positive	USP1 negative LC3 negative	Fisher's exact test p value	Spearman p value	correlation coefficient
HER2	24	1	0	6	17	n.s.	n.s.	
LUM-A	23	3	7	2	11	n.s.	n.s.	
LUM-B	24	3	7	1	13	n.s.	n.s.	
TRIP-NEG	24	7	1	7	9	n.s.	0,044	0,415
ALL SAMPLES	95	14	15	16	50	0,0304	0,012	0,255
%	100,0%	14,7%	15,8%	16,8%	52,7%			

Figure 4.15 USP1 and MAP1LC3A proteins are expressed and significantly correlate in a subset of mammary tumors. (A) and **(B)** Representative views of MAP1LC3A immunostaining from Luminal A and B, HER2 and Triple Negative subtype. **(C)** The table shows the number and percentage of USP1 and MAP1LC3A positive samples for each group. Fisher's exact test and Spearman's test were performed in order to verify the correlation between USP1 and MAP1LC3A expression. P values and statistics are indicated for each group.

Several studies showed that autophagy might exert a dual role in cancer development. In fact, although autophagy can prevent cancer initiation, it can also facilitate a survival mechanism for cancer cells to deal with low oxygen supply and chemotherapy[193]. Interestingly, some studies demonstrated a prosurvival autophagic pathway for breast cancer stem cells maintenance[194]. Therefore, several on going clinical trials are now testing autophagy inhibitors in combination with conventional chemotherapeutical drugs[193]. Notably, a latest publication describes an essential role for Fanconi anemia proteins in regulating autophagy[195]. In lighth of these published data and together with our observation that USP1 is overexpressed in tumors, we hypothesized that USP1 may provide a close cross-talks between autophagy and cancer. Hence, USP1 inhibition could be explored as a therapeutic approach by targeting autophagy in cancer. Former works, have identified a neuroleptic drug pimozide as a potent and highly selective reversible inhibitor of the enzymatic activity of USP1. Pimozide is also able to inhibit cellular proliferation of some breast cancer cell lines[196]. Based on these observations, we initially investigated whether pimozide had an anti-proliferative effect using ATPLite assay. Since the proteasome inhibitor Bortezomib has an anti-tumor activity in both solid and haematological malignancies[197], we decided to combine bortezomib and pimozide treatment to study their outcomes in cancer therapy. U2OS and MCF10AT cells were exposted to pimozide and bortezomib treatment for 24 and 48 hours. As expected, pimozide alone and in combination with bortezomib significantly affected cellular viability in both cell lines (Figure 4.16A and Figure 4.16B). Furthermore, we examined whether pimozide inhibited the ability of colony forming in U2-OS and MCF10AT cells. After treatment with 2,5 µM pimozide for two weeks, colony-forming efficiency was significantly reduced

in both cell lines (Figura 4.16C and Figure 4.16D). These results show that pimozide inhibited cell proliferation and the ability of colony forming in cancer cell lines, indicating that the antipsychotic agent pimozide may be a potential and novel therapeutic strategy for patients with cancer. Next, we tested whether the effect observed with pimozide treatment was USP1 dependent. Control and USP1 depleted cells were exposted to pimozide treatment for 24 and 48 hours and counted before and after pimozide addition. After 24 hours, pimozide induced an USP1 dependent decrease in cellular proliferation. USP1 depletion itself slowed cell growth, but this effect was not enhanced by pimozide treatment in fact, after 48 hours, the decrease in cellular growth was not dependent on USP1 (Figure 4.16E). This result was not surprising, since after 48 hours of pimozide treatment, USP1 protein level was sharply reduced (Figure 4.16F). A chemical screening has identified Pimozide as a Ca^{2+} channel blockers which triggers mTOR-independent autophagy[198]. Consequently, we examinated contribution of pimozide to autophagy in USP1 depleted cells, looking at levels of lipidated MAP1LC3A (i.e., LC3II) and p62 by immunoblot analysis. Notably, pimozide treatment did not enhance LC3 II in USP1 depleted cells (Figure 4.16F). Moreover after 48 hours of treatment autophagy was impaired in control cells; a comparable result was observed in USP1 depleted cells. An impairment of the autophagic pathway was also suggested by the accumulation of p62 level with pimozide treatment (Figure 4.16F). All these findings suggest that in U2-OS cells, pimozide did not stimulate authophagy and it occurs via an USP1-dependet mechanism.

Consistent with the inhibition of mTORC1 by ULK1, previuos studies have demostred that ULK1, ULK2 and ATG13 negatively regulate cell proliferation[199]. Therefore, we decided to investigate the relationship between autophagy and pimozide-induced cell growth in MEF *Ulk1*$^{-/-}$ and MEF *Atg13*$^{-/-}$ cells, using WST colorimetric assay. MEF *Ulk1*$^{+/+}$ and MEF *Ulk1*$^{-/-}$ cells were exposted to pimozide and bortezomib treatment for 24 and 48 hours. As expected, pimozide alone and in combination with bortezomib significantly inhibited cellular proliferation in both cell lines. Interestingly, we observed that

MEF *Ulk1*$^{-/-}$ were more sensible to pimozide then MEF *Ulk1*$^{+/+}$, in fact a greater reduction of cellular growth was observed in MEF *Ulk1*$^{-/-}$ (Figure 4.17A). Similar results were observed in MEF *Atg13*$^{-/-}$ cells (Figure 4.17B). Given the negative effect of pimozide on cellular growth, this data proposes that this drug is able to induce an USP1 dependent decrease in cellular proliferation not only in a conventional autophagy response under normal condition (MEF *Ulk1*$^{+/+}$), but also when mTOR-dependent autophagy is impaired, by enhancing the mTOR-independent autophagy. A similar thesis was proposed by Hau and colleagues. They provide insight into Coibamide A (an N-methyl-stabilized depsipeptide, isolated from a marine cyanobacterium) may be an invaluable tool for the study of both mTOR-independent autophagy and cell death signaling in apoptosis-resistant cancer cells[200]. Further work will be required to determine if pimozide acts via a known mTOR-independent pathway or via a new target. Altogether these data revealed a novel potential therapeutic strategy for USP1 positive tumors that rely on autophagy for survival.

To conclude, post-translational modifications are required for modulating autophagy and to adapt quikly to different environmental stress so as to prevent an excessive autophagy. During autophagy induction, MTOR dissociates from the ULK1 complex, leading to its activation. In addition, ULK1 TRAF6 ubiquitinates ULK1 by K63-linked ubiquitin chains and mediates its activation. In the enduring starvation, ULK1 is targeted by NEDD4L and the CUL3 for proteasome degradation. Moreover, in our model (Figure 4.18), USP1 removes K63-linked ubiquitin chains and facilitates its degradation. If USP1 is depleted, the activity of both NEDD4L and CUL3 is not enough to ULK1 proteasome degradation. In this framework, ULK1 is moved to the aggresome and gets frozen in an ubiquitinated form which although essential for full autophagy activity, must be cyclically deubiquitinated by USP1.

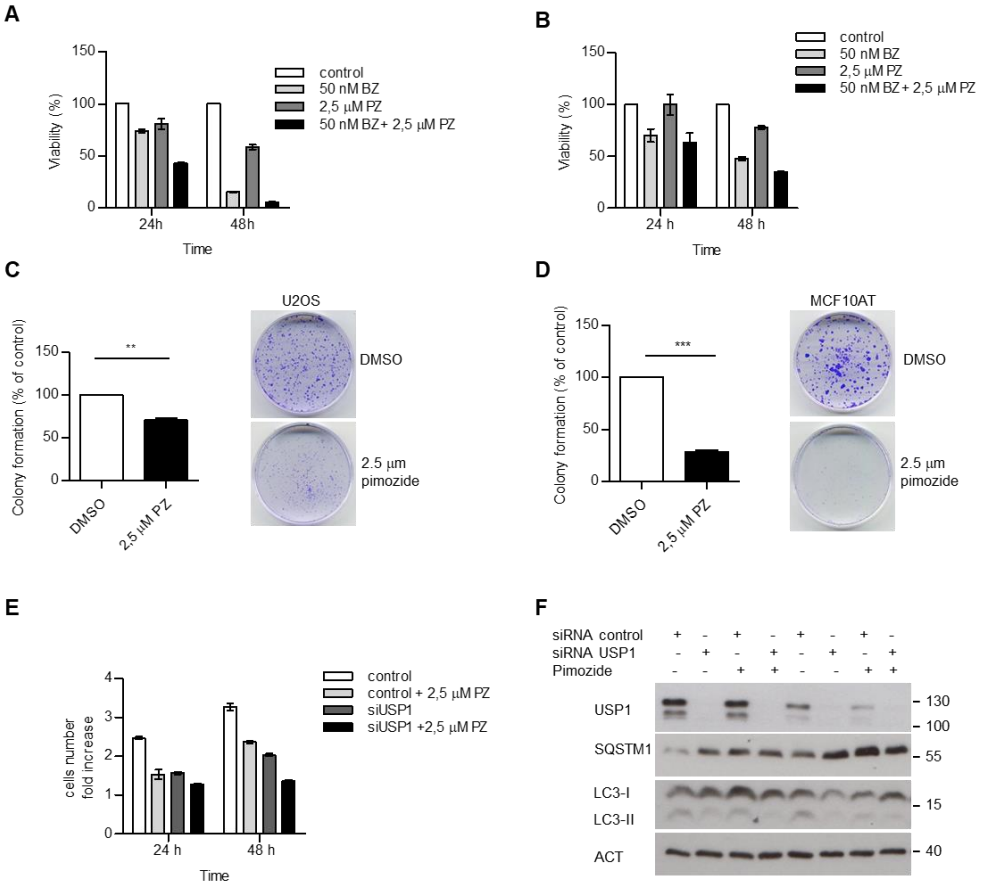

Figure 4.16 Pimozide affects cellular growth and colony forming efficiency. (A-B) U2OS **(A)** and MCF10AT **(B)** cells were left untreated, or treated with 50 nM bortezomib, 2,5 mM pimozide, or a combination of the two drugs. 24 and 48 hrs later, cell viability was measured by means of a fluorimeter after labeling with a commercial kit. The graph indicates the means +/-SD, n= 3 independent experiments. **(C)** and **(D)** Effect of pimozide on colony formation assay in U2OS cells **(C)** or MCF10AT cells **(D).** Cells were treated with 2.5 μM Pimozide for two weeks, before processing. The graphs report the average colony forming efficiency of 3 independent experiments. Colonies were counted using image J software; **=P< 0.001 and ***=P= 0.0001. Representative images are shown at the right side of each graph. **(E)** and **(F)** U2OS cells transfected with scrambled or USP1-specific siRNA. After 72 hours, the cells were either left untreated or grown in the presence of 2.5 μM pimozide. Cells were counted at time 0, 24 and 48 hours post drug addiction. **(E)** The graph indicates the means +/-SD of cell number increase after 24 and 48 hours respect to time 0. N= 3 independent experiments. **(F)** Western blot analysis after 24 and 48 hours of treatment for each condition. to monitor USP1, MAP1LC3A and p62 levels. ACT was used as loading control.

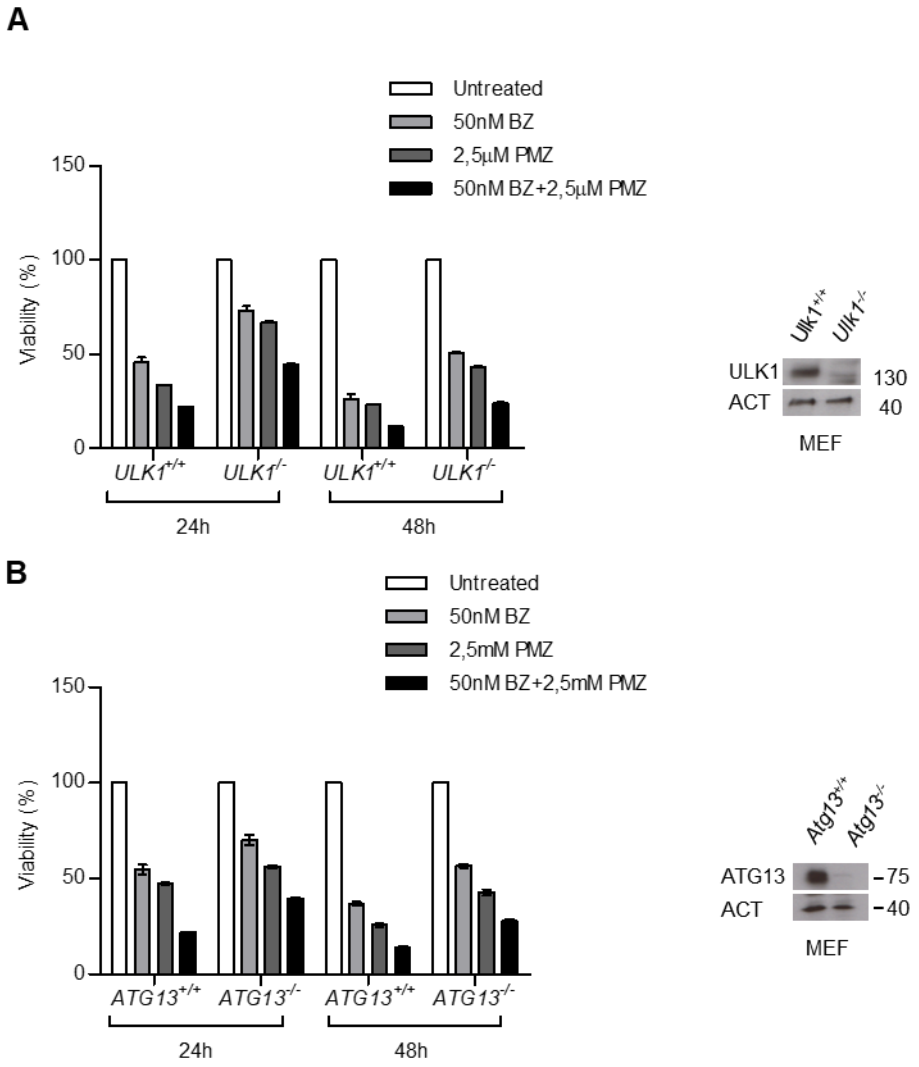

Figure 4.17 Pimozide affects cellular growth. (A-B) MEF *Ulk1*$^{+/+}$ and MEF *Ulk1*$^{-/-}$ **(A)** and MEF *Atg13*$^{+/+}$ and MEF *Atg13*$^{-/-}$ **(B)** cells were left untreated, or treated with 50 nM bortezomib, 2,5 mM pimozide, or a combination of the two drugs. 24 and 48 hrs later, cell viability was measured by means of a fluorimeter after labeling with a commercial kit. The graph indicates the means +/-SD, n= 3 independent experiments.

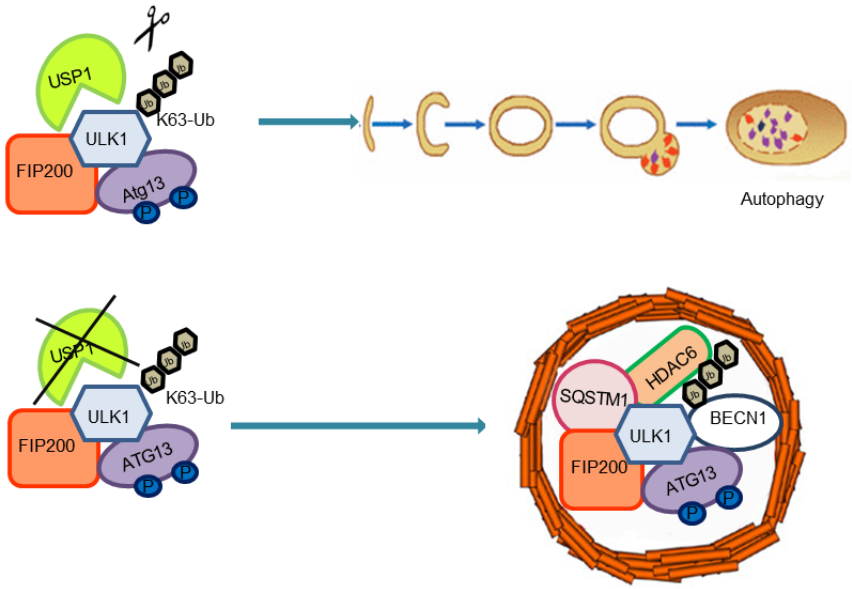

Figure 4.18 Schematic representation of a working model in which USP1 regulates the autophagic process.

Case N	Hystotype	Grade	pTN	molecular subtype	USP1 %	Int	USP1 Score	NEG	Int	LC3 Score
1	IDC	3	pT1cN0	HER2	NEG		0	NEG		0
2	IDC	3	pT1cN0	HER2	NEG		0	30	1	30
3	IDC	3	pT1cN0	HER2	NEG		0	NEG		0
4	IDC	3	pT1cN2a	HER2	NEG		0	NEG		0
5	IDC	3	pT1cN0	HER2	NEG		0	80	1	80
6	IDC	3	pT1cN0	HER2	NEG		0	NEG		0
7	IDC	3	pT2N0	HER2	NEG		0	NEG		0
8	IDC	2	pT2N1a	HER2	NEG		0	NEG		0
9	IDC	3	pT2N0	HER2	NEG		0	NEG		0
10	IDC	3	pT2N1a	HER2	NEG		0	NEG		0
11	IDC	1	pT1cN2a	HER2	NEG		0	NEG		0
12	IDC	3	pT1cN2a	HER2	NEG		0	NEG		0
13	IDC	3	pT1bN1a	HER2	NEG		0	NEG		0
14	IDC	3	pT2N0	HER2	NEG		0	NEG		0
15	IDC	3	pT2N2a	HER2	NEG		0	NEG		0
16	IDC	2	pT1cN2a	HER2	NEG		0	NEG		0
17	IDC	3	pT2N1a	HER2	NEG		0	20	1	20
18	IDC	3	pT1cN0	HER2	NEG		0	50	1	50
19	IDC	3	ypT2N0	HER2	NEG		0	70	2	140
20	IDC	3	pT2N2a	HER2	NEG		0	NEG		0
21	IDC	3	pT2N1a	HER2	10	1	10	30	1	30
22	IDC	3	pT3N1a	HER2	NEG		0	NEG		0
23	IDC	3	rpT2N0	HER2	NEG		0	40	1	40
24	IDC	3	pT2N3a	HER2	50	1	50	NEG		0
25	IDC	2	pT2N0	LUM-A	80	1	80	NEG		0
26	IDC	1	pT1cN0	LUM-A	NEG		0	NEG		0
27	IDC	1	pT1cN0	LUM-A	NEG		0	NEG		0

28	IDC	2	pT1cN0	LUM-A	80	1	80	NEG		0
29	IDC	2	pT1cN0	LUM-A	80	1	80	NEG		0
30	IDC	1	pT1bN0	LUM-A	60	1	60	NEG		0
31	IDC	2	pT1bN0	LUM-A	80	1	80	80	1	80
32	IDC	2	pT1cNx	LUM-A	NEG		0	NEG		0
33	IDC	1	pT1cN0	LUM-A	NEG		0	NEG		0
34	IDC	2	pT1bN0	LUM-A	NEG		0	30	1	30
35	IDC	2	pT2N0	LUM-A	NEG		0	NEG		0
36	IDC	2	pT1bN0	LUM-A	NEG		0	NEG		0
37	IDC	2	pT1cN0	LUM-A	50	1	50	NEG		0
38	IDC	1	pT1bN0	LUM-A	60	1	60	50	1	50
39	IDC	2	pT1cN1a	LUM-A	NEG		0	NEG		0
40	IDC	2	pT1bN0	LUM-A	60	1	60	NEG		0
41	IDC	2	pT1cN1mi	LUM-A	30	1	30	50	1	50
42	IDC	2	pT1bN0	LUM-A	NEG		0	NEG		0
43	IDC	1	pT1bN0	LUM-A	NEG		0	NEG		0
44	IDC	2	pT1bN1mi	LUM-A	NEG		0	NEG		0
45	IDC	1	pT1cN2a	LUM-A	NEG		0	80	1,5	120
46	IDC	2	pT4bN1a	LUM-A	NEG		0	NEG		0
47	IDC	1	pT1bN0	LUM-B	NEG		0	NEG		0
48	ILC	3	pT2N2a	LUM-B	30	1	30	NEG		0
49	ILC	2	pT2N2a	LUM-B	NEG		0	NEG		0
50	IDC	3	ypT2N0	LUM-B	30	1	30	NEG		0
51	IDC	3	pT2N0	LUM-B	NEG		0	NEG		0
52	IDC	2	pT1bN0	LUM-B	50	1	50	NEG		0
53	ILC	3	pT3N1a	LUM-B	NEG		0	NEG		0
54	IDC	1	pT1bNmi	LUM-B	NEG		0	NEG		0
55	IDC	3	pT1bN0	LUM-B	NEG		0	NEG		0
56	IDC	3	pT1cN1a	LUM-B	NEG		0	NEG		0
57	IDC	3	pT1bN0	LUM-B	NEG		0	NEG		0
58	IDC	3	pT1cN2a	LUM-B	60	1	60	NEG		0
59	IDC	3	pT1bN0	LUM-B	NEG		0	NEG		0
60	IDC	2	pT1cN1	LUM-B	80	1	80	30	1	30
61	IDC	2	pT1bN2	LUM-B	NEG		0	NEG		0
62	IDC	2	pT1cN0	LUM-B	30	1	30	NEG		0
63	IDC	2	pT2n1a	LUM-B	NEG		0	NEG		0
64	IDC	3	pT2N3a	LUM-B	30	1	30	NEG		0
65	ILC	2	pT1cN0	LUM-B	NEG		0	NEG		0
66	IDC	3	pT1cN0	LUM-B	NEG		0	100	1,5	150
67	IDC	2	pT2Nx	LUM-B	30	1	30	IN SITU		0
68	IDC	2	pT1bN0	LUM-B	NEG		0	NEG		0
69	IDC	2	pT1cN0	LUM-B	NEG		0	EG		0
70	IDC	2	pT1c	LUM-B	70	1	70	90	2	180
71	IDC	2	pT1cN0	LUM-B	30	2	60	NEG		0
72	IDC	3	pT4bN0	TRIP-NEG	90	1	90	70	1	70
73	IDC	3	pT1cN0	TRIP-NEG	NEG		0	NEG		0
74	IDC	3	pT1cNx	TRIP-NEG	NEG		0	60	1	60
75	IDC	3	pT2N1a	TRIP-NEG	NEG		0	NEG		0
76	IDC	3	pT1bN1mi	TRIP-NEG	NEG		0	NEG		0
77	IDC	2	pT2N0	TRIP-NEG	70	1	70	40	1	40
78	IDC	2	pT1bN0	TRIP-NEG	NEG		0	15	1	15
79	IDC	3	pT4bNx	TRIP-NEG	NEG		0	60	2	120
80	IDC	2	pT3N3a	TRIP-NEG	NEG		0	40	2	80
81	IDC	2	pT1cN1mi	TRIP-NEG	NEG		0	NEG		0
82	IDC	2	pT1cN0	TRIP-NEG	NEG		0	80	2	160
83	IDC	3	pT2Nx	TRIP-NEG	NEG		0	5	2	10
84	IDC	3	pT2N0	TRIP-NEG	NEG		0	NEG		0

85	IDC	3	pT1cN0	TRIP-NEG	60	2	120	60	2	120
86	IDC	3	pT2N0	TRIP-NEG	50	2	100	25	1	25
87	Medullary	3	pT2N1a	TRIP-NEG	60	1	60	60	1	60
88	IDC	2	pT1bN0	TRIP-NEG	NEG		0	NEG		0
89	IDC	3	pT1bN0	TRIP-NEG	60	1	60	70	2	140
90	IDC	2	pT1bN0	TRIP-NEG	NEG		0	50	1	50
91	ILC	3	pT2N0	TRIP-NEG	100	1	100	80	2	160
92	IDC	3	pT2N1a	TRIP-NEG	NEG		0	NEG		0
93	IDC	3	pT1cN1a	TRIP-NEG	NEG		0	NEG		0
94	IDC	3	pT2N0	TRIP-NEG	NEG		0	NEG		0
95	IDC	2	pT2N2a	TRIP-NEG	100	1	100	NEG		0

Table 4.1 Histopathological features of the 95 analyzed breast cancer samples and expression of USP1 and MAP1LC3A. IDC = Invasive ductal carcinoma; ILC = Invasive Lobular Carcinoma; G = Elston Ellis grade; pTN = tumor size (T) and lymph node involvement according to TNM classification; LUM-A = Luminal A; LUM-B = Luminal B; TRIP-NEG = Triple Negative; int = intensity.

5. CONCLUSION

The mammalian ULK complex is centrally involved in the initiating steps of autophagy. In recent years, the molecular regulation of this complex has been elucidated. Generally, upstream signals change the phosphorylation status of the components of this complex. However, several studies demonstrated the significance of other post-translational modifications, such as acetylation and ubiquitination, to control the ULK1-mediated autophagy. A latest work led by Stork' group, reported that the DUB inhibitor WP1130, increased ULK1 ubiquitination and relocated ULK1 to aggresome-like structures[166]. The work carried out for this thesis, permitted us to confirme that ULK1 deubiquitnation greatly affects its compartmentalization and to identify the deubiquitinating enzyme USP1 as a key regulator of this traffic. Contrary to what outlined for ID2, the reduced ULK1 protein level, in USP1 depleted U2-OS and MCF10AT cells, was not caused by proteasomal degradation. The observed USP1 effect might be due to proteasomal overload, which occurs, for example, when the autophagy/lysosome pathway is blocked. Consequently, ULK1 is accumulated into aggresome to be later re-used. However, ULK1 is moved to aggresome togheter with other autophagic protein including p62/SQSTM1 and BECN1, as shown by immunofluorescence analysis and immunoprecipitation experiments. Additionally, unlike Stork' group, we noted that the shift of ULK1 into aggresome did not have an impact upon the catalytic activity of ULK1, since p-ATG13 at Ser318 was present in the isoluble pellet togheter with ULK1. In order to further characterize USP1/ULK1 interaction, we confirmed in HEK293 cells extracts, the interaction between endogenous ULK1 and USP1 and consistently the interaction between endogenous ULK1 and ectopic UAF1 (which forms a complex with USP1). Further experiments are needed to investigate whether the interaction is direct or mediated by the other proteins of the ULK complex. Early data demostrated that ULK1 is located also in the nucleus[185]. By means of immunoblot and immunofluorescence analyses we identified a pool of ULK1 within the nucleus that interacts with USP1. Once established that the two proteins interact with each other and are present in

the same cellular compartment, we asked whether the ubiquitination status of ULK1 is affected by USP1. In 2013, Nazio and colleagues reported that AMBRA1-TRAF6 complex, promotes the activation and stability of the kinase ULK1 through its Lys-63-linked ubiquitylation[18]. In accordance with their data, we verified that USP1 depletion increases the TRAF6-dependent K63-linked ubiquitination of ULK1 triggered by rapamycin treatment, highlighting a specific involvement of USP1 in removing K-63-linked ubiquitin from ULK1. Furthermore, in line with Stork' group, USP1 siRNA treatment blocks the autophagic flux despite the requirement of K-63 ubiquitination of ULK1 for autophagy. We hypothesize that, similar to FANCD2 regulation[187], dynamic ubiquitination and deubiquitination of ULK1 is required to trigger the autophagic pathway.

Autophagy was shown to be required for breast cancer stem cells maintenance[194] and for growth of triple negative breast cancers[201]. Therefore, autophagy inhibitors in combination with conventional chemotherapeutical drugs might provide an approach to a future therapy. The findings reported in the present thesis reveal a significant relation between MAP1LC3A and USP1 proteins in breast cancer. Earlier works showed that USP1 inhibitor pimozide inhibits breast cancer growth[196]. Therefore, with our studies we assumed that pimozide induces an USP1 dependent decrease in cellular proliferation. Finally, we proposed that pimozide could trigger an USP1 dependent decrease in cellular proliferation also by enhancing mTOR-independent autophagy. This possibly reflects the different roles of autophagy within different stages of the disease. Further studies are required to evaluate this working hypothesis.

The new function of USP1 described in this thesis work, acquires more importance since we propose that USP1 modulates autophagy and helps survival and proliferation of cancer cells. A concomitant inhibition of the proteasome and USP1 may represent a novel therapeutic strategy for USP1 positive tumors that require autophagy for survival. This novel strategy could potentially lead to eradication of cancer cells also for osteosarcoma and other cancers that use USP1 autophagy axis for survival.

LIST OF PUBBLICATIONS

Raimondi M, Cesselli D, Di Loreto C, La Marra F, Schneider C and Demarchi F. Ubiquitin Specific Peptidase 1 targets ULK1 and regulates its cellular compartmentalization and autophagy. Manuscript submitted for publication.

Marcassa E, **Raimondi M**, Anwar T, Eskelinen EL, Myers MP, Triolo G, Schneider C, Demarchi F. Calpain mobilizes Atg9/Bif-1 vesicles from Golgi stacks upon autophagy induction by thapsigargin. Biol Open. 2017 May 15;6(5):551-562. doi: 10.1242/bio.022806.

Raimondi M, Marcassa E, Cataldo F, Arnandis T, Mendoza-Maldonado R, Bestagno M, Schneider C, Demarchi F. Calpain restrains the stem cells compartment in breast cancer. Cell Cycle. 2016;15(1):106-16. doi: 10.1080/15384101.2015.112132

REFERENCES

1. Yang, Z. & Klionsky, D. J. Eaten alive: a history of macroautophagy. *Nat. Cell Biol.* **12,** 814–822 (2010).
2. Mizushima, N. Autophagy: process and function. *Genes Dev.* **21,** 2861–2873 (2007).
3. Levine, B. & Klionsky, D. J. Development by self-digestion: molecular mechanisms and biological functions of autophagy. *Dev. Cell* **6,** 463–77 (2004).
4. Boya, P., Reggiori, F. & Codogno, P. Emerging regulation and functions of autophagy. *Nat. Cell Biol.* **15,** 713–720 (2013).
5. Levine, B. & Kroemer, G. Autophagy in the Pathogenesis of Disease. *Cell* **132,** 27–42 (2008).
6. Deretic, V. & Levine, B. Autophagy, Immunity, and Microbial Adaptations. *Cell Host Microbe* **5,** 527–549 (2009).
7. Mizushima, N. & Levine, B. Autophagy in mammalian development and differentiation. *Nat. Cell Biol.* **12,** 823–830 (2010).
8. Rubinsztein, D. C., Mariño, G. & Kroemer, G. Autophagy and aging. *Cell* **146,** 682–695 (2011).
9. Jiang, P. & Mizushima, N. Autophagy and human diseases. *Cell Res.* **24,** 69–79 (2014).
10. Mizushima, N. & Komatsu, M. Autophagy: Renovation of cells and tissues. *Cell* **147,** 728–741 (2011).
11. Mizushima, N., Yoshimori, T. & Ohsumi, Y. The Role of Atg Proteins in Autophagosome Formation. *Annu. Rev. Cell Dev. Biol.* **27,** 107–132 (2011).
12. He, C. & Klionsky, D. J. Regulation Mechanisms and Signalling Pathways of Autophagy. *Annu. Rev. Genet.* **43,** 67 (2009).
13. Longatti, A. & Tooze, S. A. Vesicular trafficking and autophagosome formation. *Cell Death Differ.* **16,** 956–965 (2009).
14. Xie, Y. *et al.* Posttranslational modification of autophagy-related proteins in macroautophagy. *Autophagy* **11,** 28–45 (2015).
15. Mercer, C. A., Kaliappan, A. & Dennis, P. B. A novel, human Atg13 binding protein, Atg101, interacts with ULK1 and is essential for macroautophagy. *Autophagy* **5,** 649–662 (2009).
16. Chan, E. Y. W., Longatti, A., McKnight, N. C. & Tooze, S. A. Kinase-Inactivated ULK Proteins Inhibit Autophagy via Their Conserved C-Terminal Domains Using an Atg13-Independent Mechanism. *Mol. Cell. Biol.* **29,** 157–171 (2009).
17. Hara, T. *et al.* FIP200, a ULK-interacting protein, is required for autophagosome formation in mammalian cells. *J. Cell Biol.* **181,** 497–510 (2008).
18. Nazio, F. *et al.* mTOR inhibits autophagy by controlling ULK1 ubiquitylation, self-association and function through AMBRA1 and TRAF6. *Nat. Cell Biol.* **15,** 406–416 (2013).

19. Russell, R. C., Yuan, H.-X. & Guan, K.-L. Autophagy regulation by nutrient signaling. *Cell Res.* **24,** 42–57 (2014).
20. Wesselborg, S. & Stork, B. Autophagy signal transduction by ATG proteins: From hierarchies to networks. *Cell. Mol. Life Sci.* **72,** 4721–4757 (2015).
21. Puente, C., Hendrickson, R. C. & Jiang, X. Nutrient-regulated phosphorylation of ATG13 inhibits starvation-induced autophagy. *J. Biol. Chem.* **291,** 6026–6035 (2016).
22. Cosker, K. E. *et al.* Regulation of PI3K signalling by the phosphatidylinositol transfer protein PITP during axonal extension in hippocampal neurons. *J. Cell Sci.* **121,** 796–803 (2008).
23. Sun, Q. *et al.* Identification of Barkor as a mammalian autophagy-specific factor for Beclin 1 and class III phosphatidylinositol 3-kinase. *Proc. Natl. Acad. Sci.* **105,** 19211–19216 (2008).
24. Di Bartolomeo, S. *et al.* The dynamic interaction of AMBRA1 with the dynein motor complex regulates mammalian autophagy. *J. Cell Biol.* **191,** 155–168 (2010).
25. Itakura, E. & Mizushima, N. Atg14 and UVRAG: Mutually exclusive subunits of mammalian Beclin 1-PI3K complexes. *Autophagy* **5,** 534–536 (2009).
26. Hamasaki, M. *et al.* Autophagosomes form at ER–mitochondria contact sites. *Nature* **495,** 389–393 (2013).
27. Carlsson, S. R. & Simonsen, A. Membrane dynamics in autophagosome biogenesis. *J. Cell Sci.* **128,** 193–205 (2015).
28. Rubinsztein, D. C., Shpilka, T. & Elazar, Z. Mechanisms of autophagosome biogenesis. *Curr. Biol.* **22,** R29–R34 (2012).
29. Nakatogawa, H. Two ubiquitin-like conjugation systems that mediate membrane formation during autophagy. *Essays Biochem.* **55,** 39–50 (2013).
30. Glick, D., Barth, S. & Macleod, K. F. Autophagy : cellular and molecular mechanisms. *J. Pathol.* **221,** 3–12 (2010).
31. Mizushima, N. Mouse Apg16L, a novel WD-repeat protein, targets to the autophagic isolation membrane with the Apg12-Apg5 conjugate. *J. Cell Sci.* **116,** 1679–1688 (2003).
32. Weidberg, H. *et al.* LC3 and GATE-16/GABARAP subfamilies are both essential yet act differently in autophagosome biogenesis. *EMBO J.* **29,** 1792–1802 (2010).
33. Kabeya, Y. LC3, a mammalian homologue of yeast Apg8p, is localized in autophagosome membranes after processing. *EMBO J.* **19,** 5720–5728 (2000).
34. Barth, S., Glick, D. & Macleod, K. F. Autophagy: Assays and artifacts. *J. Pathol.* **221,** 117–124 (2010).
35. Pankiv, S. *et al.* p62/SQSTM1 binds directly to Atg8/LC3 to facilitate degradation of ubiquitinated protein aggregates by autophagy*[S]. *J. Biol. Chem.* **282,** 24131–24145 (2007).
36. Kirkin, V. *et al.* A Role for NBR1 in Autophagosomal Degradation of Ubiquitinated Substrates. *Mol. Cell* **33,** 505–516 (2009).
37. Eskelinen, E. L. Roles of LAMP-1 and LAMP-2 in lysosome biogenesis and autophagy. *Mol.*

Aspects Med. **27,** 495–502 (2006).

38. Hyttinen, J. M. T., Niittykoski, M., Salminen, A. & Kaarniranta, K. Maturation of autophagosomes and endosomes: A key role for Rab7. *Biochim. Biophys. Acta - Mol. Cell Res.* **1833,** 503–510 (2013).
39. Efeyan, A., Zoncu, R. & Sabatini, D. M. Amino acids and mTORC1: From lysosomes to disease. *Trends Mol. Med.* **18,** 524–533 (2012).
40. Sancak, Y. *et al.* Ragulator-rag complex targets mTORC1 to the lysosomal surface and is necessary for its activation by amino acids. *Cell* **141,** 290–303 (2010).
41. Liu, E. Y. & Ryan, K. M. Autophagy and cancer - issues we need to digest. *J. Cell Sci.* **125,** 2349–2358 (2012).
42. Kim, J., Kundu, M., Viollet, B. & Guan, K.-L. AMPK and mTOR regulate autophagy through direct phosphorylation of Ulk1. *Nat. Cell Biol.* **13,** 132–141 (2011).
43. Singh, R. & Cuervo, A. M. Autophagy in the cellular energetic balance. *Cell Metab.* **13,** 495–504 (2011).
44. Ha, J., Guan, K. L. & Kim, J. AMPK and autophagy in glucose/glycogen metabolism. *Mol. Aspects Med.* **46,** 46–62 (2015).
45. Alers, S., Loffler, A. S., Wesselborg, S. & Stork, B. Role of AMPK-mTOR-Ulk1/2 in the Regulation of Autophagy: Cross Talk, Shortcuts, and Feedbacks. *Mol. Cell. Biol.* **32,** 2–11 (2012).
46. Agarwal, S., Bell, C. M., Rothbart, S. B. & Moran, R. G. AMP-activated Protein Kinase (AMPK) Control of mTORC1 Is p53- and TSC2-independent in Pemetrexed-treated Carcinoma Cells. *J. Biol. Chem.* **290,** 27476–27486 (2015).
47. Gwinn, D. M. *et al.* AMPK phosophorylation of raptor mediates a metabollic checkpoint. *Mol. Cell* **30,** 214–226 (2008).
48. Dibble, C. C. & Manning, B. D. Signal integration by mTORC1 coordinates nutrient input with biosynthetic output. *Nat. Cell Biol.* **15,** 555–564 (2013).
49. Bar-Peled, L., Schweitzer, L. D., Zoncu, R. & Sabatini, D. M. Ragulator is a GEF for the rag GTPases that signal amino acid levels to mTORC1. *Cell* **150,** 1196–1208 (2012).
50. Settembre, C. *et al.* A lysosome-to-nucleus signalling mechanism senses and regulates the lysosome via mTOR and TFEB. *EMBO J.* **31,** 1095–1108 (2012).
51. Gangaraju Vamsi K. Lin Haifan. NIH Public Access. *Nat Rev Mol Cell Biol.* **10 (2),** 116–125 (2009).
52. Filomeni, G., De Zio, D. & Cecconi, F. Oxidative stress and autophagy: the clash between damage and metabolic needs. *Cell Death Differ.* **22,** 377–388 (2015).
53. Roussy, I. G. *et al.* A dual role of p53 in the control of autophagy 1. *Autophagy* **8627,** 810–814 (2008).
54. Gao, W., Shen, Z., Shang, L. & Wang, X. Upregulation of human autophagy-initiation kinase ULK1 by tumor suppressor p53 contributes to DNA-damage-induced cell death. *Cell Death*

Differ. **18,** 1598–1607 (2011).

55. Duan, L. *et al.* P53-Regulated Autophagy Is Controlled By Glycolysis and Determines Cell Fate. *Oncotarget* **6,** 23135–56 (2015).
56. Bellot, G. *et al.* Hypoxia-Induced Autophagy Is Mediated through Hypoxia-Inducible Factor Induction of BNIP3 and BNIP3L via Their BH3 Domains. *Mol. Cell. Biol.* **29,** 2570–2581 (2009).
57. Sui, X. *et al.* Autophagy and chemotherapy resistance: a promising therapeutic target for cancer treatment. *Cell Death Dis.* **4,** e838 (2013).
58. Huang, J. & Brumell, J. H. Bacteria–autophagy interplay: a battle for survival. *Nat. Rev. Microbiol.* **12,** 101–114 (2014).
59. Choy, A. & Roy, C. R. Autophagy and bacterial infection: An evolving arms race. *Trends Microbiol.* **21,** 451–456 (2013).
60. Manuscript, A., Against, C. D. & Microbes, I. Autophagy in Immunity and Cell-Autonomous Defense Against Intracellular Microbes. **240,** 92–104 (2012).
61. Levine, B., Mizushima, N. & Virgin, H. W. Autophagy in immunity and inflammation. *Nature* **469,** 323–335 (2011).
62. Lee, I. H. *et al.* Atg7 Modulates p53 Activity to Regulate Cell Cycle and Survival During Metabolic Stress. *Science (80-.).* **336,** 225–228 (2012).
63. Wang, K. & Klionsky, D. J. Mitochondria removal by autophagy. *Autophagy* **7,** 297–300 (2011).
64. Mao, K., Liu, X., Feng, Y. & Klionsky, D. J. The progression of peroxisomal degradation through autophagy requires peroxisomal division. *Autophagy* **10,** 652–661 (2014).
65. Nixon, R. A. The role of autophagy in neurodegenerative disease. *Nat. Med.* **19,** 983–997 (2013).
66. Manuscript, A., Controls, M., Nucleostemin, R. & Between, P. NIH Public Access. **119,** 5124–5136 (2010).
67. Zare-shahabadi, A., Masliah, E., Johnson, G. V. W. & Rezaei, N. Autophagy in Alzheimer's Disease. **26,** 385–395 (2016).
68. Wang, B., Abraham, N., Gao, G. & Yang, Q. Dysregulation of autophagy and mitochondrial function in Parkinson's disease. *Transl. Neurodegener.* **5,** 19 (2016).
69. Shibata, M. *et al.* Regulation of intracellular accumulation of mutant huntingtin by beclin 1. *J. Biol. Chem.* **281,** 14474–14485 (2006).
70. Shintani, T. Autophagy in Health and Disease: A Double-Edged Sword. *Science (80-.).* **306,** 990–995 (2004).
71. Vellai, T., T??th, M. L. & Kov??cs, A. L. Janus-faced autophagy: A dual role of cellular self-eating in neurodegeneration? *Autophagy* **3,** 461–463 (2007).
72. White, E. the role for autophagy in cancer (White, 2015).pdf. *J. Clin. Invest.* **125,** 42–46 (2015).
73. Hanahan, D. & Weinberg, R. A. Hallmarks of cancer: The next generation. *Cell* **144,** 646–674 (2011).
74. Yang, X. *et al.* The role of autophagy induced by tumor microenvironment in different cells and

stages of cancer. *Cell Biosci.* **5,** 14 (2015).

75. Liang, X. H. *et al.* Induction of autophagy and inhibition of tumorigenesis by beclin 1. *Nature* **402,** 672–676 (1999).
76. Qu, X. *et al.* Promotion of tumorigenesis by heterozygous disruption of the beclin 1 autophagy gene. *J. Clin. Invest.* **112,** 1809–1820 (2003).
77. Han, Q. *et al.* Downregulation of ATG5-dependent macroautophagy by chaperone-mediated autophagy promotes breast cancer cell metastasis. *Sci. Rep.* **7,** 4759 (2017).
78. Moscat, J. & Diaz-Meco, M. T. p62 at the Crossroads of Autophagy, Apoptosis, and Cancer. *Cell* **137,** 1001–1004 (2009).
79. Ichimura, Y. *et al.* Structural basis for sorting mechanism of p62 in selective autophagy. *J. Biol. Chem.* **283,** 22847–22857 (2008).
80. Komatsu, M. *et al.* Homeostatic Levels of p62 Control Cytoplasmic Inclusion Body Formation in Autophagy-Deficient Mice. *Cell* **131,** 1149–1163 (2007).
81. Moon, E. J. & Giaccia, A. Dual roles of NRF2 in tumor prevention and progression: Possible implications in cancer treatment. *Free Radic. Biol. Med.* **79,** 292–299 (2015).
82. Deretic, V., Saitoh, T. & Akira, S. Autophagy in infection, inflammation and immunity. *Nat. Rev. Immunol.* **13,** 722–737 (2013).
83. Mah, L. Y. & Ryan, K. M. Autophagy and Cancer. 1–14 (2013). doi:10.1007/978-1-4614-6561-4
84. White, E. Deconvoluting the context-dependent role for autophagy in cancer. *Nat. Rev. Cancer* **12,** 401–410 (2012).
85. Wei, H., Wang, C., Croce, C. M. & Guan, J. Autophagy for Tumor Growth in Vivo. *Animals* 1204–1216 (2014). doi:10.1101/gad.237354.113.
86. Wei, H. *et al.* Suppression of autophagy by FIP200 deletion inhibits mammary tumorigenesis. *Genes Dev.* **25,** 1510–1527 (2011).
87. Takamura, A. *et al.* Autophagy-deficient mice develop multiple liver tumors. *Genes …* **5,** 795–800 (2011).
88. Kulathu, Y. & Komander, D. Atypical ubiquitylation — the unexplored world of polyubiquitin beyond Lys48 and Lys63 linkages. *Nat. Rev. Mol. Cell Biol.* **13,** 508–523 (2012).
89. Chen, Z. J. & Sun, L. J. Nonproteolytic Functions of Ubiquitin in Cell Signaling. *Mol. Cell* **33,** 275–286 (2009).
90. Bernassola, F., Karin, M., Ciechanover, A. & Melino, G. The HECT Family of E3 Ubiquitin Ligases: Multiple Players in Cancer Development. *Cancer Cell* **14,** 10–21 (2008).
91. Seirafi, M., Kozlov, G. & Gehring, K. Parkin structure and function. *FEBS J.* **282,** 2076–2088 (2015).
92. Sadowski, M. & Sarcevic, B. Mechanisms of mono- and poly-ubiquitination: Ubiquitination specificity depends on compatibility between the E2 catalytic core and amino acid residues proximal to the lysine. *Cell Div.* **5,** 19 (2010).

93. Chastagner, P., Israël, A. & Brou, C. Itch/AIP4 mediates Deltex degradation through the formation of K29-linked polyubiquitin chains. *EMBO Rep.* **7,** 1147–1153 (2006).

94. Meyer, H. J. & Rape, M. Enhanced protein degradation by branched ubiquitin chains. *Cell* **157,** 910–921 (2014).

95. Matsumoto, M. L. *et al.* K11-linked polyubiquitination in cell cycle control revealed by a K11 linkage-specific antibody. *Mol. Cell* **39,** 477–484 (2010).

96. Nishikawa, H. *et al.* Mass Spectrometric and Mutational Analyses Reveal Lys-6-linked Polyubiquitin Chains Catalyzed by BRCA1-BARD1 Ubiquitin Ligase. *J. Biol. Chem.* **279,** 3916–3924 (2004).

97. Ordureau, A. *et al.* Defining roles of PARKIN and ubiquitin phosphorylation by PINK1 in mitochondrial quality control using a ubiquitin replacement strategy. *Proc. Natl. Acad. Sci.* **112,** 6637–6642 (2015).

98. Lee, B. L., Singh, A., Mark Glover, J. N., Hendzel, M. J. & Spyracopoulos, L. Molecular Basis for K63-Linked Ubiquitination Processes in Double-Strand DNA Break Repair: A Focus on Kinetics and Dynamics. *J. Mol. Biol.* (2017). doi:10.1016/j.jmb.2017.05.029

99. Chen, J. & Chen, Z. J. Regulation of NF- κ B by Ubiquitination. *Curr. Opin. Immunol.* **25,** 4–12 (2013).

100. Erpapazoglou, Z., Walker, O. & Haguenauer-Tsapis, R. Versatile Roles of K63-Linked Ubiquitin Chains in Trafficking. *Cells* **3,** 1027–1088 (2014).

101. Nijman, S. M. B. *et al.* A genomic and functional inventory of deubiquitinating enzymes. *Cell* **123,** 773–786 (2005).

102. Reyes-Turcu, F. E., Ventii, K. H. & Wilkinson, K. D. Regulation and Cellular Roles of Ubiquitin-Specific Deubiquitinating Enzymes. *Annu. Rev. Biochem.* **78,** 363–397 (2009).

103. Komander, D., Clague, M. J. & Urbé, S. Breaking the chains: structure and function of the deubiquitinases. *Nat. Rev. Mol. Cell Biol.* **10,** 550–563 (2009).

104. Eletr, Z. M. & Wilkinson, K. D. Regulation of proteolysis by human deubiquitinating enzymes. *Biochim. Biophys. Acta - Mol. Cell Res.* **1843,** 114–128 (2014).

105. Ventii, K. H. & Wilkinson, K. D. Protein partners of deubiquitinating enzymes. *Biochem. J.* **414,** 161–175 (2008).

106. Song, L. & Rape, M. Reverse the curse-the role of deubiquitination in cell cycle control. *Curr. Opin. Cell Biol.* **20,** 156–163 (2008).

107. Hanpude, P., Bhattacharya, S., Dey, A. K. & Maiti, T. K. Deubiquitinating enzymes in cellular signaling and disease regulation. *IUBMB Life* **67,** 544–555 (2015).

108. Kimura, Y. & Tanaka, K. Regulatory mechanisms involved in the control of ubiquitin homeostasis. *J. Biochem.* **147,** 793–798 (2010).

109. Hymowitz, S. G. & Wertz, I. E. A20: from ubiquitin editing to tumour suppression. *Nat. Rev. Cancer* **10,** 332–341 (2010).

110. Popov, N. *et al.* The ubiquitin-specific protease USP28 is required for MYC stability. *Nat. Cell Biol.* **9,** 765–774 (2007).
111. Mungamuri, S. K. *et al.* USP7 Enforces Heterochromatinization of p53 Target Promoters by Protecting SUV39H1 from MDM2-Mediated Degradation. *Cell Rep.* **14,** 2528–2537 (2016).
112. Chen, D. *et al.* High-Resolution Crystal Structure and In Vivo Function of a Kinesin-2 Homologue in Giardia intestinalis. *Mol. Biol. Cell* **19,** 308–317 (2007).
113. Luna-Vargas, M. P. A. *et al.* Ubiquitin-specific protease 4 is inhibited by its ubiquitin-like domain. *EMBO Rep.* **12,** 365–372 (2011).
114. García-Santisteban, I., Peters, G. J., Giovannetti, E. & Rodríguez, J. A. USP1 deubiquitinase: cellular functions, regulatory mechanisms and emerging potential as target in cancer therapy. *Mol. Cancer* **12,** 91 (2013).
115. Huang, T. T. *et al.* Regulation of monoubiquitinated PCNA by DUB autocleavage. *Nat. Cell Biol.* **8,** 341–347 (2006).
116. López-Otín, C. & Hunter, T. The regulatory crosstalk between kinases and proteases in cell cancer. *Nat. Rev. Cancer* **10,** 278–292 (2010).
117. Hutti, J. E. *et al.* I □ B Kinase ␣ Phosphorylates the K63 Deubiquitinase A20 To Cause Feedback Inhibition of the NF- □ B Pathway □. **27,** 7451–7461 (2007).
118. Endo, A. *et al.* Nucleolar structure and function are regulated by the deubiquitylating enzyme USP36. *J. Cell Sci.* **122,** 678–686 (2009).
119. Roberta Verhoeft, K., Lam Ngan, H. & Wai Yan Lui, V. The cylindromatosis (CYLD) gene and head and neck tumorigenesis. *Cancers Head Neck* (2016). doi:10.1186/s41199-016-0012-y
120. Madan, B. *et al.* USP6 oncogene promotes Wnt signaling by deubiquitylating Frizzleds. *Proc. Natl. Acad. Sci.* **113,** E2945–E2954 (2016).
121. Fang, Y., Fu, D. & Shen, X. Z. The potential role of ubiquitin c-terminal hydrolases in oncogenesis. *Biochim. Biophys. Acta - Rev. Cancer* **1806,** 1–6 (2010).
122. Fraile, J. M., Quesada, V., Rodríguez, D., Freije, J. M. P. & López-Otín, C. Deubiquitinases in cancer: new functions and therapeutic options. *Oncogene* **31,** 2373–2388 (2012).
123. Bilguvar, K. *et al.* Recessive loss of function of the neuronal ubiquitin hydrolase UCHL1 leads to early-onset progressive neurodegeneration. *Proc. Natl. Acad. Sci.* **110,** 3489–3494 (2013).
124. Zhang, M., Cai, F., Zhang, S., Zhang, S. & Song, W. Overexpression of ubiquitin carboxyl-terminal hydrolase L1 (UCHL1) delays Alzheimer's progression in vivo. *Sci. Rep.* **4,** 7298 (2015).
125. Fujiwara, T. *et al.* Identification and chromosomal assignment of USP1, a novel gene encoding a human ubiquitin-specific protease. *Genomics* **54,** 155–8 (1998).
126. Williams, S. A. *et al.* USP1 deubiquitinates ID proteins to preserve a mesenchymal stem cell program in osteosarcoma. *Cell* **146,** 918–930 (2011).
127. Oestergaard, V. H. *et al.* Deubiquitination of FANCD2 Is Required for DNA Crosslink Repair.

Mol. Cell **28,** 798–809 (2007).

128. Cohn, M. A. *et al.* A UAF1-Containing Multisubunit Protein Complex Regulates the Fanconi Anemia Pathway. *Mol. Cell* **28,** 786–797 (2007).
129. Villamil, M. A., Chen, J., Liang, Q. & Zhuang, Z. A noncanonical cysteine protease USP1 is activated through active site modulation by USP1-associated factor 1. *Biochemistry* **51,** 2829–2839 (2012).
130. Cohn, M. A., Kee, Y., Haas, W., Gygi, S. P. & D'Andrea, A. D. UAF1 is a subunit of multiple deubiquitinating enzyme complexes. *J. Biol. Chem.* **284,** 5343–5351 (2009).
131. Cotto-Rios, X. M., Békés, M., Chapman, J., Ueberheide, B. & Huang, T. T. Deubiquitinases as a Signaling Target of Oxidative Stress. *Cell Rep.* **2,** 1475–1484 (2012).
132. Cotto-Rios, X. M., Jones, M. J. K. & Huang, T. T. Insights into phosphorylation-dependent mechanisms regulating USP1 protein stability during the cell cycle. *Cell Cycle* **10,** 4009–4016 (2011).
133. Villamil, M. A. *et al.* Serine Phosphorylation Is Critical for the Activation of Ubiquitin-Specific Protease 1 and Its Interaction with WD40-Repeat Protein UAF1. *Biochemistry* **51,** 9112–9123 (2012).
134. Garcia-Santisteban, I., Zorroza, K. & Rodriguez, J. A. Two nuclear localization signals in USP1 mediate nuclear import of the USP1/UAF1 complex. *PLoS One* **7,** (2012).
135. Cataldo, F. *et al.* CAPNS1 regulates USP1 stability and maintenance of genome integrity. *Mol. Cell. Biol.* **33,** 2485–96 (2013).
136. Jacq, X., Kemp, M., Martin, N. M. B. & Jackson, S. P. Deubiquitylating Enzymes and DNA Damage Response Pathways. *Cell Biochem. Biophys.* **67,** 25–43 (2013).
137. Fox, J. T., Lee, K. Y. & Myung, K. Dynamic regulation of PCNA ubiquitylation/deubiquitylation. *FEBS Lett.* **585,** 2780–2785 (2011).
138. Crossan, G. P. & Patel, K. J. The Fanconi anaemia pathway orchestrates incisions at sites of crosslinked DNA. *J. Pathol.* **226,** 326–337 (2012).
139. Taniguchi, T. *et al.* S-phase-specific interaction of the Fanconi anemia protein, FANCD2, with BRCA1 and RAD51. *Blood* **100,** 2414–2420 (2002).
140. Kee, Y. & D'Andrea, A. D. Expanded roles of the Fanconi anemia pathway in preserving genomic stability. *Genes Dev.* **24,** 1680–1694 (2010).
141. Nijman, S. M. B. *et al.* The deubiquitinating enzyme USP1 regulates the fanconi anemia pathway. *Mol. Cell* **17,** 331–339 (2005).
142. Kim, J. M. *et al.* Inactivation of Murine Usp1 Results in Genomic Instability and a Fanconi Anemia Phenotype. *Dev. Cell* **16,** 314–320 (2009).
143. Kirchmaier, A. L. Ub-family modifications at the replication fork: Regulating PCNA-interacting components. *FEBS Lett.* **585,** 2920–2928 (2011).
144. Pagès, V. & Fuchs, R. P. How DNA lesions are turned into mutations within cells? *Oncogene* **21,**

8957–8966 (2002).

145. Brun, J., Chiu, R. K., Wouters, B. G. & Gray, D. a. Regulation of PCNA polyubiquitination in human cells. *BMC Res. Notes* **3,** 85 (2010).
146. Kashiwaba, S. ichiro *et al.* USP7 Is a Suppressor of PCNA Ubiquitination and Oxidative-Stress-Induced Mutagenesis in Human Cells. *Cell Rep.* **13,** 2072–2080 (2015).
147. Lyden, D. *et al.* Id1 and Id3 are required for neurogenesis, angiogenesis and vascularization of tumour xenografts. *Nature* **401,** 670–677 (1999).
148. Yokota, Y. & Mori, S. Role of Id family proteins in growth control. *J. Cell. Physiol.* **190,** 21–28 (2002).
149. Perk, J., Iavarone, A. & Benezra, R. Id family of helix-loop-helix proteins in cancer. *Nat. Rev. Cancer* **5,** 603–614 (2005).
150. Lasorella, A., Uo, T. & Iavarone, A. Id proteins at the cross-road of development and cancer. *Oncogene* **20,** 8326–8333 (2001).
151. Linares, J. F. *et al.* K63 polyubiquitination and activation of mTOR by the p62-TRAF6 complex in nutrient-activated cells. *Mol. Cell* **51,** 283–296 (2013).
152. Antonioli, M. *et al.* AMBRA1 interplay with cullin E3 Ubiquitin ligases regulates autophagy dynamics. *Dev. Cell* **31,** 734–746 (2014).
153. McEwan, D. & Dikic, I. Cullins keep autophagy under control. *Dev. Cell* **31,** 675–676 (2014).
154. Shi, C. S. & Kehrl, J. H. TRAF6 and A20 Regulate Lysine 63-Linked Ubiquitination of Beclin-1 to Control TLR4-Induced Autophagy. *Sci. Signal.* **3,** ra42-ra42 (2010).
155. Platta, H. W., Abrahamsen, H., Thoresen, S. B. & Stenmark, H. Nedd4-dependent lysine-11-linked polyubiquitination of the tumour suppressor Beclin 1. *Biochem. J.* **441,** 399–406 (2012).
156. Liu, C. C. *et al.* Cul3-KLHL20 Ubiquitin Ligase Governs the Turnover of ULK1 and VPS34 Complexes to Control Autophagy Termination. *Mol. Cell* **61,** 84–97 (2016).
157. Shaid, S., Brandts, C. H., Serve, H. & Dikic, I. Ubiquitination and selective autophagy. *Cell Death Differ.* **20,** 21–30 (2013).
158. Liu, J. *et al.* Beclin1 controls the levels of p53 by regulating the deubiquitination activity of USP10 and USP13. *Cell* **147,** 223–234 (2011).
159. Tripathi, R., Ash, D. & Shaha, C. Beclin-1-p53 interaction is crucial for cell fate determination in embryonal carcinoma cells. *J. Cell. Mol. Med.* **18,** 2275–2286 (2014).
160. Jin, S. *et al.* USP19 modulates autophagy and antiviral immune responses by deubiquitinating Beclin-1. *EMBO J.* **35,** 866–880 (2016).
161. Geisler, S. *et al.* PINK1/Parkin-mediated mitophagy is dependent on VDAC1 and p62/SQSTM1. *Nat. Cell Biol.* **12,** 119–131 (2010).
162. Eiyama, A. & Okamoto, K. PINK1/Parkin-mediated mitophagy in mammalian cells. *Curr. Opin. Cell Biol.* **33,** 95–101 (2015).
163. Cornelissen, T. *et al.* The deubiquitinase USP15 antagonizes Parkin-mediated mitochondrial

ubiquitination and mitophagy. *Hum. Mol. Genet.* **23,** 5227–5242 (2014).

164. Cunningham, C. N. *et al.* USP30 and parkin homeostatically regulate atypical ubiquitin chains on mitochondria. *Nat. Cell Biol.* **17,** 160–169 (2015).
165. Taillebourg, E. *et al.* The deubiquitinating enzyme USP36 controls selective autophagy activation by ubiquitinated proteins. *Autophagy* **8,** 767–779 (2012).
166. Drießen, S. *et al.* Deubiquitinase inhibition by WP1130 leads to ULK1 aggregation and blockade of autophagy. *Autophagy* **11,** 1458–1470 (2015).
167. Nazio, F. *et al.* Fine-tuning of ULK1 mRNA and protein levels is required for autophagy oscillation. *J. Cell Biol.* **215,** 841–856 (2016).
168. Wesselborg, S. & Stork, B. Autophagy signal transduction by ATG proteins: from hierarchies to networks. *Cell. Mol. Life Sci.* **72,** 4721–57 (2015).
169. Wong, P.-M., Puente, C., Ganley, I. G. & Jiang, X. The ULK1 complex: sensing nutrient signals for autophagy activation. *Autophagy* **9,** 124–37 (2013).
170. Kim, J., Kundu, M., Viollet, B. & Guan, K.-L. AMPK and mTOR regulate autophagy through direct phosphorylation of Ulk1. *Nat. Cell Biol.* **13,** 132–141 (2011).
171. Kawaguchi, Y. *et al.* The Deacetylase HDAC6 Regulates Aggresome Formation and Cell Viability in Response to Misfolded Protein Stress. *Cell* **115,** 727–738 (2003).
172. Chen, J. *et al.* Selective and cell-active inhibitors of the USP1/ UAF1 deubiquitinase complex reverse cisplatin resistance in non-small cell lung cancer cells. *Chem. Biol.* **18,** 1390–1400 (2011).
173. Lee, J.-Y. *et al.* HDAC6 controls autophagosome maturation essential for ubiquitin-selective quality-control autophagy. *EMBO J.* **29,** 969–980 (2010).
174. Tan, Y. *et al.* Cullin 3 SPOP ubiquitin E3 ligase promotes the poly-ubiquitination and degradation of HDAC6. **8,** 47890–47901 (2017).
175. Russell, R. C. *et al.* ULK1 induces autophagy by phosphorylating Beclin-1 and activating VPS34 lipid kinase. *Nat. Cell Biol.* **15,** 741–750 (2013).
176. Takahashi, Y. *et al.* Bif-1 interacts with Beclin 1 through UVRAG and regulates autophagy and tumorigenesis. *Nat. Cell Biol.* **9,** 1142–1151 (2007).
177. Petherick, K. J. *et al.* Pharmacological inhibition of ULK1 kinase blocks mammalian target of rapamycin (mTOR)-dependent autophagy. *J. Biol. Chem.* **290,** 11376–11383 (2015).
178. Joo, J. H. *et al.* Hsp90-Cdc37 Chaperone Complex Regulates Ulk1- and Atg13-Mediated Mitophagy. *Mol. Cell* **43,** 572–585 (2011).
179. Hosokawa, N. *et al.* Nutrient-dependent mTORC1 association with the ULK1-Atg13-FIP200 complex required for autophagy. *Mol. Biol. Cell* **20,** 1981–91 (2009).
180. Ganley, I. G. *et al.* ULK1·ATG13·FIP200 complex mediates mTOR signaling and is essential for autophagy. *J. Biol. Chem.* **284,** 12297–12305 (2009).
181. Kim, J., Kundu, M., Viollet, B. & Guan, K.-L. AMPK and mTOR regulate autophagy through direct phosphorylation of Ulk1. *Nat. Cell Biol.* **13,** 132–141 (2011).

182. Dorsey, F. C. *et al.* Mapping the Phosphorylation Sites of Ulk1. *J. Proteome Res.* **8,** 5253–5263 (2009).

183. Shang, L. *et al.* Nutrient starvation elicits an acute autophagic response mediated by Ulk1 dephosphorylation and its subsequent dissociation from AMPK. *Proc. Natl. Acad. Sci.* **108,** 4788–4793 (2011).

184. Raimondi, M. *et al.* Calpain restrains the stem cells compartment in breast cancer. *Cell Cycle* **15,** 106–116 (2016).

185. Joshi, A. *et al.* Nuclear ULK1 promotes cell death in response to oxidative stress through PARP1. *Cell Death Differ.* **23,** 216–230 (2016).

186. Itakura, E. & Mizushima, N. p62 targeting to the autophagosome formation site requires self-oligomerization but not LC3 binding. *J. Cell Biol.* **192,** 17–27 (2011).

187. van Twest, S. *et al.* Mechanism of Ubiquitination and Deubiquitination in the Fanconi Anemia Pathway. *Mol. Cell* **65,** 247–259 (2017).

188. Mizushima, N., Yoshimori, T. & Levine, B. Methods in mammalian autophagy research. *Cell* **140,** 313–26 (2010).

189. Karpathiou, G. *et al.* Light-Chain 3A Autophagic Activity and Prognostic Significance in Non-small Cell Lung Carcinomas. *Chest* **140,** 127–134 (2011).

190. Miao, Y., Zhang, Y., Chen, Y., Chen, L. & Wang, F. GABARAP is overexpressed in colorectal carcinoma and correlates with shortened patient survival. *Hepatogastroenterology.* **57,** 257–61

191. Choi, J., Jung, W. & Koo, J. S. Expression of autophagy-related markers beclin-1, light chain 3A, light chain 3B and p62 according to the molecular subtype of breast cancer. *Histopathology* **62,** 275–286 (2013).

192. Lazova, R. *et al.* Punctate LC3B Expression Is a Common Feature of Solid Tumors and Associated with Proliferation, Metastasis, and Poor Outcome. *Clin. Cancer Res.* **18,** 370–379 (2012).

193. Jiang, P. & Mizushima, N. Autophagy and human diseases. *Cell Res.* **24,** 69–79 (2014).

194. Gong, C. *et al.* Beclin 1 and autophagy are required for the tumorigenicity of breast cancer stem-like/progenitor cells. *Oncogene* **32,** 2261–72, 2272–11 (2013).

195. Sumpter, R. *et al.* Fanconi Anemia Proteins Function in Mitophagy and Immunity. *Cell* **165,** 867–881 (2016).

196. Strobl, J. S. *et al.* Inhibition of human breast cancer cell proliferation in tissue culture by the neuroleptic agents pimozide and thioridazine. *Cancer Res.* **50,** 5399–405 (1990).

197. Roccaro, A. M., Vacca, A. & Ribatti, D. Bortezomib in the treatment of cancer. *Recent Pat. Anticancer. Drug Discov.* **1,** 397–403 (2006).

198. Renna, M., Jimenez-Sanchez, M., Sarkar, S. & Rubinsztein, D. C. Chemical inducers of autophagy that enhance the clearance of mutant proteins in neurodegenerative diseases. *J. Biol. Chem.* **285,** 11061–7 (2010).

199. Jung, C. H., Seo, M., Otto, N. M. & Kim, D.-H. ULK1 inhibits the kinase activity of mTORC1 and cell proliferation. *Autophagy* **7,** 1212–21 (2011).

200. Hau, A. M. *et al.* Coibamide A Induces mTOR-Independent Autophagy and Cell Death in Human Glioblastoma Cells. *PLoS One* **8,** e65250 (2013).

201. Lefort, S., Joffre, C., Kieffer, Y. & Givel, A. Inhibition of autophagy as a new means of improving chemotherapy efficiency in high- LC3B triple-negative breast cancers. *Autophagy* **10,** 2122–2142 (2014).